Patterns of drug-related behavior: role of VTA DA neurons and inhibitory GPCR-dependent signaling

A DISSERTATION
SUBMITTED TO THE FACULTY OF THE
UNIVERSITY OF MINNESOTA
BY

Margot Clara DeBaker

IN PARTIAL FULFILLMENT OF THE REQUIREMENTS
FOR THE DEGREE OF
DOCTOR OF PHILOSOPHY

Anna M. Lee, Advisor
Kevin D. Wickman, Co-Advisor

April 2022

Acknowledgements

First, I would like to thank my advisors Dr. Anna Lee and Dr. Kevin Wickman, who have been endlessly patient and supportive as we navigated the logistics of a co-mentorship and a global pandemic together. Each of you has provided me with a unique perspective on science, mentorship and life that has been vital to my growth as a scientist and a professional. Thank you for cultivating an environment that encourages curiosity, scientific rigor, and independence.

Second, I would like to thank Dr. Ezequiel Marron Fernandez de Velasco, who has been a mentor and friend in addition to being a lab mate to me over the years. Thank you for always being there for me to help troubleshoot equipment, bounce project ideas back and forth, discuss best scientific practice, and share recipes or treats.

I would also like to thank my thesis committee members, Dr. Lucy Vulchanova (Chair), Dr. Patrick Rothwell, and Dr. Jocelyn Richard, for the insights and encouragement they have provided me with over the years. I would like to especially thank Lucy, current DGS and whom I worked with as a teaching assistant. You inspire me with the care you show for each and every person, and your dedication to improving your classes to be as effective as possible for all students.

Thank you to the members of both the Wickman and Lee lab that I have had the great pleasure of working with over the years: Dr. Jill Touchette, Dr. Nora McCall, Dr. Baovi Vo, Dr. Allison Anderson, Dr. Janna Moen, Dr. Tim Rose, Sarah Mulloy, Shirley (Haichang) Luo, Eric Mitten, Bushra Haider, Amelia Schneider, Jenna Robinson, Ketki Pawaskar, Manini Mantri, Siddharth Sobti, Hannah Oberle, Melody Truong, Runbo Gao, Courtney Wright, Shaydel Engel, Fayzeh El Banna, Mehrsa Zahiremami, Morgainne Aback and numerous undergraduate students (especially Alyssa Wong, Greta Cutts, Anni Wickman, and Scott McElroy). Your friendship and support have brought immense joy to my daily

life throughout graduate school. They say it takes a village to raise a graduate student, but because I was lucky enough to have two villages, I feel I have become twice the graduate student.

I have also received tremendous amounts of support from the graduate students both in the Graduate Program in Neuroscience and the Molecular Pharmacology and Therapeutics program. I am so grateful for all of the warmth and support that come from being a part of these wonderful communities. I would like to give a special shoutout to my cohort, the entering class of 2017, who will forever be the best cohort.

I would also like to thank Dr. Sharolyn Kawakami-Schulz and Dr. Jenna Hicks from the Office of Professional Development for providing me with invaluable guidance as I formed my post-graduation plans. Your endless kindness and resources were instrumental in helping me find a career path that excites me.

Before coming to the University of Minnesota I had numerous mentors at Marquette University, without whom I probably never would have come to graduate school. Dr. John Mantsch and all the members of the Mantsch lab, thank you for being so supportive and encouraging, and believing in me even before I believed in myself. A special thank you to Dr. Elizabeth Doncheck, who dedicated significant time and effort to teaching and guiding me. Thank you for trusting me with your experiments and believing in me as a scientist. Thank you to my academic advisor, Dr. Khadijah Makky, whose advice led me to join a research lab in the first place, and who encouraged me to be a leader.

Thank you to all of my teachers and professors during my many years in school. You have put up with me talking outside of my turn, guided me through my quest for knowledge, encouraged me to share what I know, and taught me that science is exciting and fun.

Thank you to my mom and dad, Cheryl and Tim DeBaker, my first and continuous teachers. You have been there for me from day 1, teaching me about the world, making learning fun, and answering (or at least putting up with) my endless questions.

To all of my family and friends, thank you for supporting me and for always being interested in what I am doing, even if you still believe I just play with mice all day.

Lastly, I would like to thank my funding sources which supported this work. This includes grants from the National Institute of Health (NIH) to MD (DA007234 and AA028726), KW (DA034696 and AA027544), AML (AA026598), NMM (DA041767), and the University of Minnesota Viral Vector and Cloning Core (DA048742).

Abstract

Ventral tegmental area (VTA) dopamine (DA) neurons play an important role in modulating activity in the mesocorticolimbic system in response to reward. Output from VTA DA neurons is critical for mediating drug-related behaviors, as inhibition of these neurons blocks drug induced stimulation. Drugs of abuse act on a diverse set of molecular targets, but they share the ability to enhance DA levels throughout the mesocorticolimbic system. Enhanced DA levels engage negative feedback mechanisms on VTA DA neurons by activating inhibitory G protein-dependent signaling pathways, mediated by $GABA_B$ receptors ($GABA_BRs$) and D_2 DA receptors (D_2Rs). $GABA_BR$- and D_2R-dependent feedback in VTA DA neurons is further modulated by Regulator of G Protein Signaling (RGS) proteins, which act to enhance the deactivation of G protein signaling. The R7 family of RGS proteins, including RGS6, is known to modulate neuronal G protein signaling preferentially via $G\alpha_o$, and has been implicated in drug-related behaviors. One goal of the work in this thesis was to assess how changes in VTA DA neuron inhibition may alter drug-related behaviors.

In order to assess the relative influence of $GABA_BRs$ and D_2Rs on drug sensitivity, we characterized a neuron-specific CRISPR/Cas9 approach to ablate $GABA_BRs$ or D_2Rs in VTA DA neurons. Our ablation technique prevented VTA DA neuron somatodendritic responses to the $GABA_BR$ agonist baclofen or the D_2R agonist quinpirole in a receptor specific manner. Loss of VTA DA neuron D_2R-dependent signaling resulted in enhanced cocaine-induced motor stimulation in both male and female mice, whereas loss of VTA DA neuron $GABA_BR$-dependent signaling resulted in enhanced cocaine-induced motor stimulation only in males. Neither $GABA_BR$ nor D_2R ablation had an effect on morphine-induced motor stimulation. These data suggest that VTA DA neuron inhibitory G protein-dependent feedback modulates behaviors in a drug- and sex-specific way.

We also wanted to evaluate the role of RGS6 in modulating VTA DA neuron inhibitory feedback and drug-related behaviors. We showed that RGS6 and Gβ5, the binding partner of R7 RGS proteins, are expressed in the majority of VTA DA neurons. Additionally, both the $GABA_BR$ and D_2R can signal through $G\alpha_o$, the preferred substrate of RGS6, suggesting that RGS6 may modulate both $GABA_BR$- and D_2R-dependent signaling. Indeed, constitutive *RGS6*$^{-/-}$ mice exhibited enhanced amplitude of somatodendritic VTA DA neuron D_2R-dependent signaling and prolonged deactivation of $GABA_BR$-dependent signaling. Next, we utilized the CRISPR/Cas9 approach characterized previously to assess VTA DA neuron specific effects of *RGS6*$^{-/-}$. As with constitutive *RGS6*$^{-/-}$, VTA DA neuron specific RGS6 ablation enhanced D_2R-dependent current amplitude. Further, VTA DA neuron specific RGS6 overexpression reduced D_2R-dependent current amplitude. These data suggest a negative regulatory role for RGS6 in VTA DA neuron G protein-dependent signaling. We also report that both male and female constitutive *RGS6*$^{-/-}$ mice display decreased binge alcohol consumption, but that only female VTA DA neuron specific *RGS6*$^{-/-}$ display decreased binge alcohol consumption. Together these results suggest that RGS6 modulates VTA DA neuron G protein-dependent inhibition in a receptor-dependent manner, resulting in a sex-dependent influence on alcohol consumption.

Most humans using drugs of abuse have co-occurring substance use patterns, so in addition to assessing independent drug mechanisms it is also important to assess how drug-related behavior patterns change during drug co-consumption. As alcohol and nicotine are the most frequently co-used drugs of abuse, the second goal of this work was to assess how abstinence from either nicotine or alcohol, after weeks of concurrent consumption, affects intake of the remaining drug. We did this by utilizing a 3-bottle choice model of concurrent alcohol, nicotine, and water consumption. When we removed the

nicotine bottle after 3 weeks of concurrent consumption, we did not observe a change in levels of alcohol consumed, suggesting that mice do not compensate for the absence of nicotine by increasing alcohol consumption. When we instead added the aversive tastant quinine to the alcohol bottle, we saw an acute decrease in alcohol consumption in addition to an increase in the levels of nicotine consumed, suggesting that mice compensate for the absence of alcohol by increasing nicotine consumption. Further, chronically increasing quinine concentration in the alcohol bottle resulted in enhanced nicotine compensation in females but not in males. These results have important implications for treating patients with substance co-use disorders, as they suggest the order of drug abstinence may affect overall treatment outcomes.

Collectively, work presented in this thesis provides novel insights about how drug-related behavioral outcomes are affected by drug mechanism, underlying inhibitory architecture, sex of the subject, and drug availability. These insights highlight the importance of gaining a greater understanding of both individual and co-substance use disorders in order to inform patient-specific treatment strategies.

Table of Contents

List of Tables

List of Figures

List of Abbreviations

VTA	ventral tegmental area
DA	Dopamine
GPCRs	G protein coupled receptors
$GABA_BRs$	$GABA_B$ receptors
D_2R	dopamine D_2 receptor
RGS	Regulator of G protein Signaling protein
CRISPR	Clustered Regularly Interspaced Short Palindromic Repeats
gRNA	Guide RNA
SN	substantia nigra
CS	conditioned stimulus
NAc	nucleus accumbens
MSNs	medium spiny neurons
D_1R	dopamine D_1 receptors
SUD	substance use disorders
DSM-5	Diagnostic and Statistical Manual for Mental Disorders, 5th edition
ICD-11	International Statistical Classification of Diseases and Related Health Problems, 11th revision
NSDUH	National Survey of Drug Use and Health
iv	intravenous infusion
CPP	conditioned place preference model
CUD	Cocaine use disorder
DAT	dopamine transporter
SERT	serotonin transporter
NET	norepinephrine transporter
OUD	opiate use disorders
NMDA	N-methyl-D-aspartate
AUD	alcohol use disorder
GIRK	G protein-gated inwardly rectifying K^+
GAPs	GTPase activating proteins
GGL	G protein gamma-like domain
DEP/DHEX	Disheveled, Egl-10, Pleckstrin/Dep helical extension
R7BP	R7 binding protein

GPR158	G-protein coupled receptor 158
DREADDs	Designer Receptors Exclusively Activated by Designer Drugs
WT	C57BL/6J
CNO	Clozapine-N-Oxide
AAV	adeno-associated viruse
R_M	Input/membrane resistance
C_M	apparent capacitance
AP_{50}	Action potential half-width
I_h	hyperpolarization-induced current
bac	Baclofen
quin	Quinpirole
sulp	Sulpiride
CGP	CGP54626
ml	medial lemniscus
MT	medial terminal nucleus of the accessory optic tract
PBP	parabrachial pigmented nucleus of the VTA
SN_C	substantia nigra pars compacta
SN_R	substantia nigra pars reticulata
VTAR	rostral part of the VTA
$5HT_{1A}R$	5-hydroxytryptamine 1A receptor (Serotonin)
MOR	mu opioid receptor
ROI	region of interest

Chapter 1 : Introduction

1.1 Natural Reward System

Responding to natural rewards is evolutionarily critical to increase the likelihood of repeating events that promote survival, such as drinking, eating, reproduction, and social interactions (Delgado, 2007; McClure, York, & Montague, 2004; Schultz, 2010; Wise & Rompre, 1989). Reward processing takes place in the mesocorticolimbic system, which is made up of distinct brain regions that are interconnected to form a complex system of communication (Hikosaka, Bromberg-Martin, Hong, & Matsumoto, 2008; O'Doherty, 2004). Within the mesocorticolimbic system, limbic regions such as the nucleus accumbens, amygdala and hippocampus are implicated in predicting and reinforcing reward behaviors, while cortical regions such as the prefrontal cortex, orbitofrontal cortex and cingulate are implicated in integrating different aspects of reward processing and cognitive control (Hearing, Zink, & Wickman, 2012; Hikosaka et al., 2008). Human neuroimaging studies as well as animal studies show that activity in these brain regions is elevated during reward related activities (Delgado, 2007; Knutson & Cooper, 2005; McClure et al., 2004; Schultz, 2015; Wise, 2004).

One key modulator of activity in the mesocorticolimbic system is dopamine (DA). DA agonists increase activity in mesocorticolimbic structures, and pharmacological agents that block DA also attenuate behaviors in response to natural reward (Joseph & Hodges, 1990; Pfaus et al., 1990; Schultz, 2015; Wise & Rompre, 1989). DA signals are suggested to code reward prediction error, such that unexpected rewards increase DA output, expected rewards have no effect, and omissions of expected rewards decrease DA output (Hikosaka et al., 2008; Knutson & Cooper, 2005; Schultz, 2007). This DA signal reinforces the association of cues leading to the reward with positive outcomes to inform future

decision making (Schultz, 1998; Wise, 2002). DA signals in the mesocorticolimbic system originate from the substantia nigra (SN, A9) and ventral tegmental area (VTA, A10), two distinct populations of neurons located in the midbrain (Kalivas, Taylor, & Miller, 1985; Kelly, Seviour, & Iversen, 1975). DA neuron disfunction in VTA and SN is linked to psychiatric disease such as Parkinson's, schizophrenia, and depression (Nora D. Volkow et al., 1994; Walker, Ray, & Kuhn, 2006; Wise & Rompre, 1989). SN DA neurons tend to be more strongly linked to movement disorders, whereas VTA DA neurons are implicated in motivation and addiction-related behaviors (Nora D. Volkow, Wang, Fowler, Tomasi, & Telang, 2011; Wise, 2002). As the purpose of this thesis is to explore how pathological regulation of reward circuitry can lead to maladaptive responses to drugs of abuse, the remainder of the information will focus on VTA DA neurons and connecting regions.

1.1.1 Ventral Tegmental Area

The VTA is a critical node in the mesocorticolimbic system that is activated in response to rewards. The VTA contains DA, GABA, glutamate and co-transmitter releasing neurons, which form a complex circuit influencing each other as well as neurons in downstream brain regions (Lammel, Lim, & Malenka, 2014; Morales & Margolis, 2017). The vast majority of research on the VTA has focused on DA neurons due to their importance in mediating reward-related behaviors (Sanchez-Catalan, Kaufling, Georges, Veinante, & Barrot, 2014). VTA DA neuron output increases in response to natural reinforcers such as food or sex (Joseph & Hodges, 1990; Pleim, Matochik, Barfield, & Auerbach, 1990). Additionally, animals will work to receive direct stimulation of VTA DA neurons or associated ascending fibers, and will even forgo food in favor of direct stimulation (Wise, 2002; Wise & Rompre, 1989). This suggests that activation of VTA DA neurons is inherently rewarding.

VTA DA neurons have been implicated in associating cues with rewarding outcomes. When a natural reinforcer is repeatedly paired with a neutral cue such as a sound, often referred to as a conditioned stimulus (CS), VTA DA neurons begin to fire in response to the CS rather than the natural reinforcer (Schultz, 2015; Nora D. Volkow et al., 2011; Wise, 2002). Further, direct stimulation of VTA DA neurons can induce cue conditioning in the absence of a natural reinforcer, suggesting that VTA DA neurons play a critical role in driving this reward-learning process (Saunders, Richard, Margolis, & Janak, 2018). This learned response is evolutionarily important for making decisions by predicting signals or events in the world that tend to result in positive outcomes.

More recently, researchers have begun to parse out distinct groups of VTA DA neurons that communicate to specific downstream projection targets to coordinate different behavioral outputs (C. P. Ford, Mark, & Williams, 2006; Lammel et al., 2008; Margolis, Mitchell, Ishikawa, Hjelmstad, & Fields, 2008; Stefani & Moghaddam, 2006). These distinct neuron populations display diverse electrical and chemical properties (De Jong, Fraser, & Lammel, 2022; Lammel et al., 2014). The neurons with "classical" markers associated with DA neurons are described as possessing long action potential duration, large hyperpolarization-induced currents (I_h), slow baseline firing rates, and hyperpolarization by D_2 receptors; these neurons are enriched in the lateral VTA and project primarily to the lateral nucleus accumbens (NAc) shell (De Jong et al., 2022; Lammel et al., 2014). VTA DA neuron projections to the NAc are important for reward-related behaviors, as DA increases in the NAc after VTA DA neuron activation in response to reward (Delgado, 2007; Kelley, 2004; Nora D. Volkow et al., 2011). Additionally, DA levels in the NAc correlate with satiety, suggesting animals seek out stimuli that increase DA release in the NAc (Wise, 2002).

1.1.2 Nucleus Accumbens

The NAc lateral shell is the main target of lateral VTA DA neurons (Lammel et al., 2014). The NAc is part of the ventral striatum and is typically discussed as having two distinct regions, the core and the shell (Carlezon & Thomas, 2009; Kelley, 2004). The core and the shell have been shown to play distinct roles in reward-related behaviors, with the shell being critical for the motivational aspect of seeking rewards (Pontieri, Tanda, & Di Chiara, 1995). In support of this, injection of DA into the NAc increases locomotor exploration, a behavior typically associated with reward, but only DA in the shell, not the core, reinforces reward-seeking behaviors (Di Chiara & Imperato, 1988; Joyce & Iversen, 1979; Kalivas et al., 1985; Pijnenburg & van Rossum, 1973; Wise, 2002).

Similar to the VTA, there is a diversity of cell types within the NAc, with subsets of cells projecting to different regions (De Jong et al., 2022). The majority of cells within the NAc are GABA-releasing medium spiny neurons (MSNs), sometimes referred to as the "final common path" for reward circuitry, which can be categorized as D_1 or D_2 MSNs (Carlezon & Thomas, 2009; Wise, 2002). D_2 MSNs co-express the dopamine D_2 receptor (D_2R), which is inhibitory, and the endogenous opioid peptide enkephalin (Wise, 2002). D_2Rs have a higher affinity for DA compared to D_1R, and are thought to play a role in limiting reward signaling (Durieux et al., 2009; Koob & Volkow, 2016). D_1 MSNs co-express dopamine D_1 receptors (D_1R), which is stimulatory, substance P, and the endogenous opioid peptide dynorphin (Wise, 2002). D_1Rs require higher levels of DA in order to be activated due to their lower affinity for DA, but activation of these receptors is necessary for reward reinforcement (Caine et al., 2007; Koob & Volkow, 2016). In addition to mediating reward, a subset of D_1 MSNs project directly back to midbrain regions, and synapse onto DA neurons providing a critical source of bi-directional communication between the NAc and VTA (Edwards et al., 2017). This projection from NAc back to the

VTA is important for negative feedback regulation of DA neurons, as electrical stim of NAc depresses firing of VTA DA neurons (Carlezon & Thomas, 2009; Wang, 1981).

1.2 Substance Use Disorder

One frequently used method to study the natural reward circuit is by utilizing drugs of abuse, which are known to activate portions of the mesocorticolimbic system. Further, studying the actions of various drugs of abuse within the mesocorticolimbic system provides novel insights into how certain individuals develop substance use disorders (SUD). The current clinical definitions of SUD come from the Diagnostic and Statistical Manual for Mental Disorders, 5th edition (DSM-5) (American Psychiatry Association, 2013) and the International Statistical Classification of Diseases and Related Health Problems, 11th revision (ICD-11) (WHO, 2022). These resources have variations in diagnostic criteria, yet they both describe a loss of control, disruptions to daily life, and adverse health outcomes (Katie Witkiewitz, Pfund, & Tucker, 2022). Affected individuals, their family, and community members are substantially impacted by direct and indirect effects of SUD on healthcare costs, quality of life, crime and violence, among others (McLellan, 2017; Nelson, Bundoc-Baronia, Comiskey, & McGovern, 2017). This is problematic, as according to the 2020 National Survey of Drug Use and Health (NSDUH) over 80% of individuals report drug use in their lifetime, and at least 14% of those report an SUD. Therefore, studying drugs of abuse is important as understanding why individuals progress from drug use to drug abuse could reduce the burden on society by informing treatment and prevention strategies.

Substance use disorders have been described as having multiple stages: Binge/intoxication, withdrawal/negative affect, and preoccupation/anticipation (Becker & Koob, 2016; Koob & Le Moal, 1997; Nelson et al., 2017), which play a role in the

progression of SUD. The binge/intoxication stage involves the acute effects of drugs of abuse on the natural reward circuitry that lead to positive reinforcement. It focuses on rewarding aspects that drive motivation to seek and take drug, such as increases in DA in the mesocorticolimbic system (Koob, 2013). Indeed, drugs of abuse and related cues have been shown to increase activation of DA systems in the mesocorticolimbic system (N. D. Volkow, Fowler, Wang, Baler, & Telang, 2009; Nora D. Volkow et al., 2011). The withdrawal/negative affect stage, on the other hand, focuses on the presence of negative reinforcers during withdrawal due to neuroadaptations that arise from the continued supraphysiological surges in synaptic DA during continuous drug use (Kalivas & O'Brien, 2008). These negative reinforcers drive the motivation to use drugs in order to relieve this aversive state. People report feelings such as malaise, dysphoria, pain, sleep disturbances, and loss of motivation during withdrawal, which drive drug-seeking behaviors in an effort to reduce negative symptoms (Wise & Koob, 2014). The preoccupation/anticipation stage involves dysregulation of executive control systems, such as the prefrontal cortex (Koob, 2013). Impairments in prefrontal cortical signaling make it more difficult to make the executive decision to override habitual drug-seeking behaviors (Kalivas & O'Brien, 2008). In support of this, people with SUD show impairments in executive functions such as decision-making and behavioral inhibition, in addition to showing deficits in prefrontal cortical signaling (Nelson et al., 2017). All three stages involve the integration of reward-, stress- and homeostasis-related brain regions. Acknowledging the different aspects of disease progression is important for identifying individuals prone to or experiencing SUD.

The broad definition and multiple stages of SUD leads to a heterogeneous population of affected individuals, which can make treatment difficult and often only mildly effective (Longabaugh & Magill, 2011). Patients differ not only in their symptom presentation, but

also in their behavioral and biological risk factors (Sarvet & Hasin, 2016). It has been suggested that race, socioeconomic status, and age of first use may play a role in long term outcomes, but evidence is mixed (Nelson et al., 2017; Sarvet & Hasin, 2016). Co-morbid disorders have also been evaluated, as about half of the individuals experiencing SUD also have a co-occurring psychological disorder such as anxiety, depression, bipolar, or schizophrenia (National Institute of Mental Health, 2021). It is unclear whether one disease might lead to another, or if common risk factors underly both. Although many different variables have been identified, it is still unknown how these variables interact and why some individuals can regularly use drugs of abuse without developing SUD while others cannot. Recently the focus of research has shifted toward understanding what treatments are effective for specific patient populations and why, in order to offer personalized treatment strategies (Longabaugh & Magill, 2011; Nelson et al., 2017; Katie Witkiewitz et al., 2022). The heterogeneity of patient populations highlights the need for a deeper understanding of the neurobiology underlying the different aspects of SUD to develop more effective treatment strategies.

Animal Models of SUD

In order to elucidate neural mechanisms underlying SUD, many preclinical research studies utilize rodents. Rodents provide a relatively homologous underlying brain circuitry to humans and allow for the use of more invasive techniques in conjunction with assessment of fairly complex behaviors. Different behavioral models are used to assess various aspects of SUD, each with known strengths and weaknesses. Locomotor stimulation is a commonly used method to assess drug sensitivity, as the mesolimbic DA system plays an important role in initiating spontaneous motor activity (Di Chiara & Imperato, 1988; Joyce & Iversen, 1979; Kalivas et al., 1985). Therefore, this behavioral output provides a simple, high throughput readout of DA release from the VTA to the NAc.

Another method for assessing drug-related behaviors is by using self-administration studies. There are different forms of self-administration, including direct intravenous infusion (iv) and oral consumption, but they share the same advantage of allowing for animals to make a choice to consume the substance being tested. Animals tend to prefer consumption of substances that reinforce reward over neutral substances like water. A third commonly used method to assess drug reward is the conditioned place preference model (CPP). This paradigm consists of repeated pairing of drug or neutral substance in a particular context, followed by a test session where the animal is allowed to decide which context they prefer to spend their time in. Mice tend to prefer spending time in the drug-paired chamber, which indicates a motivation to seek positive reinforcement.

1.2.1 Psychostimulants – Cocaine

Cocaine use disorder (CUD) is one prevalent form of SUD that, like all SUDs, consists of a heterogeneous population of individuals. Cocaine is one of the most common illicit substances used in the United States, with over 1 million individuals reporting a CUD in the past year (Kampman, 2019). Men are more likely to use cocaine than women, but studies have reported that women who use cocaine progress from initial use to CUD faster and experience greater negative effects during withdrawal than men (Kosten, Gawin, Kosten, & Rounsaville, 1993; Nelson et al., 2017). It is important to consider the added factor of culture when discussing sex differences in human patients with SUD, as societal stigmas can play a large role in patterns of drug use (Brady & Randall, 1999). Similar to human literature, female rodents tend to acquire and escalate cocaine self-administration more quickly, show greater withdrawal symptoms, and relapse to cocaine seeking more frequently (Becker & Koob, 2016; Nelson et al., 2017). Identification and treatment of individuals prone to or experiencing CUD is critical for decreasing the negative impact that cocaine has on our society.

No medications to date have been approved for treatment of CUD, leaving psychosocial treatment as the only available strategy (Chan et al., 2019; Kampman, 2019; Nelson et al., 2017). Although psychosocial treatments have shown a lot of promise for some individuals, others show high rates of relapse, emphasizing the importance of focusing on individualized treatment for people suffering from CUD (Kampman, 2019). Heritability of CUD is high suggesting a large impact of biological factors and therefore potential for pharmacotherapy, but the exact biological mechanisms underlying CUD are still unclear (Jordan & Xi, 2022). Progress in the neurobiological understanding of CUD has led to new insights into promising targets for pharmacological treatments, but much is still unknown about the brain mechanisms driving CUD and therefore more research is necessary to inform patient treatment strategies.

Psychostimulants such as cocaine act by blocking the dopamine transporter (DAT), which increases levels of DA in synapses throughout the mesocorticolimbic system, enhancing attention and inducing euphoria (Nora D. Volkow et al., 2011; Wise, 2002). Human imaging studies show that administration of psychostimulants increases DA levels in the striatum (Nora D. Volkow et al., 1994). Additionally, acute administration of cocaine increases locomotor activity in rodents, indicating DA transmission from the midbrain to the striatum (Berke & Hyman, 2000). Within the striatum, the reinforcing aspects of cocaine administration are mediated by activation of D_1 MSNs in the NAc by large spikes of DA (Koob & Volkow, 2016). Indeed, D_1R deficient mice fail to acquire cocaine self-administration (Caine et al., 2007). In addition to blocking DAT, psychostimulants block the serotonin transporter (SERT) and norepinephrine transporter (NET), leading to accumulation of these neurotransmitters in the synapse which affect autonomic and emotional functions (Nelson et al., 2017). Accordingly, cocaine acutely reduces time spent sleeping, increases alertness and a sense of well-being, and increases learning rate in

rodents (Berke & Hyman, 2000). Overall, direct effects of cocaine on transporters in the brain are fairly well characterized, but a deeper understanding of how these interactions impact mesocorticolimbic communication and in turn lead to CUD will improve treatment potential.

1.2.2 Opiates – Morphine

Opiate use has increased significantly since the 90s, when a rapid surge of opioid prescriptions for pain relief initiated a chain of escalating opiate use and misuse (Nelson et al., 2017). Opiates account for a large portion of all drug-related deaths, a rapidly increasing phenomenon as the number of opiate-related overdoses has tripled in less than 4 years (Kampman, 2019). As with other drugs of abuse, men tend to use and become addicted to opiates more frequently than females (Becker & Koob, 2016; Brady & Randall, 1999; C. W. S. Lee & Ho, 2013). In rodents, on the other hand, females tend to display higher levels of reward and motivation, and learn to self-administer opiates more quickly than males (Becker & Koob, 2016; Karami & Zarrindast, 2008). This discrepancy again points to the importance of understanding the societal influences that play a role in human drug-use in addition to biological factors. Identifying individuals at risk for developing OUD and utilizing proper prevention or treatment strategies is crucial to forestall the rapidly increasing impact of OUD on society.

Pharmacotherapies to treat opiate use disorders (OUD) exist (methadone, buprenorphine, and naltrexone) but are not frequently taken advantage of. Most existing pharmacotherapies to treat OUD are controlled substances that must be dispensed by medical professionals, limiting access to treatment for many individuals. Methadone is a full μ-opioid receptor agonist and N-methyl-D-aspartate (NMDA) receptor antagonist, and buprenorphine is a partial μ-opioid receptor agonist and κ-opioid receptor antagonist (Y. K. Lee, Gold, & Fuehrlein, 2022). As both of these treatments are μ-opioid receptor

agonists, they have similar mechanistic actions to illicit opioid drugs and therefore effectively suppress opioid withdrawal symptoms reduce craving for illicit drugs, and reduce risk of overdose (Y. K. Lee et al., 2022). However, they also perpetuate dependence on opioid receptor activation and thus these drugs result in high rates of relapse after ceasing treatment (Bell & Strang, 2020). Because of this, these pharmacotherapies are typically only effective if used as a long-term treatment. Naltrexone acts as a μ- and κ-opioid receptor antagonist, and although it is very effective in blocking opioid receptor activation, it shows varying levels of promise in promoting abstinence (Y. K. Lee et al., 2022). More recent extended release formulations of naltrexone have improved the number of successful patient outcomes, but it can only be used for certain patient populations that are highly motivated as users must be opioid free before treatment can begin (Uhl, Koob, & Cable, 2019). Gaining a greater understanding of how neuronal opioid receptor activation leads to OUD could inform alternate targets for new pharmacological treatment strategies.

Opiates, such as morphine, are known to act on endogenous opioid receptors, and transgenic animal studies have been valuable in identifying individual genes and proteins that play an important role in OUD such as the μ-opioid receptor (Jordan & Xi, 2022). Although the drug targets are known, the exact mechanism leading to progressive opioid use and abuse is still unclear. It is suggested that opioid receptors may disinhibit VTA DA neurons via GABA interneuron inhibition as well as directly activating NAc neurons, both leading to changes in NAc output (Nelson et al., 2017; Nora D. Volkow et al., 2011). In rodents, administration of opioid receptor agonists increases firing of VTA DA neurons, and intra-VTA opioid receptor agonists produce a dose-dependent increase in locomotor activity suggesting enhanced DA output to the NAc (Johnson & North, 1992; Kalivas et al., 1985). Additionally, direct infusion of morphine in either the NAc or VTA produces an

increase in locomotor activity and conditioned place preference, suggesting the involvement of these brain regions in the reward-reinforcing mechanisms of morphine (W. C. Bunney, Massari, & Pert, 1984; Joyce & Iversen, 1979; Phillips & LePiane, 1980). Within the NAc, opioid use likely result in high levels of DA receptor stimulation on MSNs resulting in neuroadaptations that perpetuate OUD, as opioid-dependent subjects had lower levels of D_2R availability in the NAc compared to non-dependent individuals (Koob, 2020). More thorough mechanistic insights about how opioid use progresses to dependence are necessary to improve treatment and prevention of OUD.

1.2.3 Alcohol

Alcohol is the most commonly reported substance abused, with alcohol use disorder (AUD) accounting for 75% of all SUD (Nelson et al., 2017). Further, alcohol is among the leading causes of preventable deaths worldwide, with most of these deaths associated with AUD (K Witkiewitz, Litten, & Leggio, 2019). Men tend to drink more than women and are at higher risk for AUD, while women tend to progress from initial use to dependence faster (Becker & Koob, 2016; Brady & Randall, 1999; Keyes, Grant, & Hasin, 2008; Nelson et al., 2017). These reported sex differences in AUD seem to be changing with time, likely as societal norms also change. Similar to humans, studies in rodents describe faster acquisition of alcohol self-administration and higher levels of consumption in females compared to males (Becker & Koob, 2016; Cunningham & Shields, 2018; Li & Lumeng, 1984; Yoneyama, Crabbe, Ford, Murillo, & Finn, 2008). As alcohol use and abuse cause a significant amount of harm to both individuals and society, identification of factors leading to AUD and treatments for individuals experiencing AUD is of utmost importance.

Only 3 medications (disulfiram, acamprosate, and naltrexone) approved by the Food and Drug Administration exist for treatment of AUD (Crabbe et al., 2017). Disulfiram is an acetaldehyde dehydrogenase inhibitor, which is important in the breakdown of alcohol.

When alcohol is consumed after administration of disulfiram, the toxic agent acetaldehyde builds up resulting in nausea, headache, vomiting, and other unpleasant outcomes (K Witkiewitz et al., 2019). Although it is somewhat effective at decreasing alcohol consumption, this treatment has mixed efficacy as many patients forgo taking medication before consuming alcohol. Naltrexone, the opioid receptor antagonist, has shown promise for reducing alcohol craving and relapse to heavy drinking in certain patient populations, although the reasons for the efficacy are not fully understood (Domi, Domi, Adermark, Heilig, & Augier, 2021). Acamprosate is thought to act on the glutamate system to modulate neuronal excitability, and it has been somewhat beneficial in preventing relapse in patients that are already abstaining from alcohol (K Witkiewitz et al., 2019). The approved medications, even when used in conjunction with cognitive behavioral therapy and support groups, are only efficacious for some individuals (Crabbe et al., 2017; K Witkiewitz et al., 2019). In addition, the long-term success of current treatment strategies is low, emphasizing the need for new approaches to treat AUD (Uhl et al., 2019). One of the major reasons that pharmacological treatment of AUD is only mildly successful is that the neurobiology underlying this disorder is not well characterized, and therefore effective drug targets remain elusive. Of note, one drug that is approved for the treatment of AUD is baclofen, an agonist of the G protein-coupled receptor $GABA_B$. Clinical evidence suggests that it is able to reduce alcohol drinking, craving, withdrawal symptoms, and relapse, but it seems to only be effective in certain patient populations (Agabio & Colombo, 2014; De Beaurepaire, Heydtmann, & Agabio, 2019). Gaining a better understanding of how AUD develops will inform better, more individualized treatment strategies.

The exact mechanism by which alcohol acts to produce positive reinforcement is somewhat unclear, as alcohol tends to have many targets and affect many processes throughout the brain and body. One possible mechanism of alcohol action is via facilitated

GABAergic transmission onto GABA neurons, which would effectively serve to disinhibit VTA DA neurons (Nelson et al., 2017; Nora D. Volkow et al., 2011). Although the pathway is still uncertain, it is known that alcohol leads to activation of VTA DA neurons, resulting in increased levels of DA in the NAc and other downstream targets (Domi et al., 2021). This is supported by human imaging studies that show increased DA levels in the striatum after alcohol administration (Nora D. Volkow et al., 1994). In rodents, systemic or intra-VTA alcohol administration increases DA levels in the NAc, suggesting that alcohol increases output from VTA DA neurons to NAc (Di Chiara & Imperato, 1988; Ding, Ingraham, Rodd, & McBride, 2015). Additionally, inactivation of VTA DA neurons was able to reduce alcohol consumption and relapse behaviors, indicating that these neurons are at least partially necessary for mediating alcohol reinforcement (Liu et al., 2020). Within the NAc, prolonged alcohol exposure results in alteration in D_1R- and D_2R-dependent signaling, producing disruptions in excitatory/inhibitory balance and overall output of MSNs (Cheng et al., 2017). Additional insights about how alcohol may disrupt neuronal communication in the mesocorticolimbic system may inform novel targets for pharmacologic interventions and personalized treatment strategies for AUD.

1.2.4 Polysubstance Use

Although studying individual drugs provides a clearer mechanistic picture, it is important to note that over 50% of individuals that report drug use are polydrug abusers, meaning that they take more than one substance (SAMHSA, 2012). Additionally, reports suggest that individuals experiencing SUD may successfully decrease use of one substance while compensating with use of a different substance (Sarvet & Hasin, 2016). These insights highlight the importance of considering the additional adverse outcomes that arise due to polysubstance use, and how substance co-use may affect treatment strategies (Qato, Zhang, Gandhi, Simoni-Wastila, & Coleman-Cowger, 2020).

Alcohol is frequently cited as at least one of the drugs used in polysubstance abuse, and further, Alcohol and nicotine co-use is the most frequent co-use pattern reported (Qato et al., 2020). Alcohol and nicotine co-dependency leads to worse patient outcomes, with higher levels of consumption, more severe cravings and withdrawal signs, lower levels of achieving abstinence, and increased mortality (O'Malley et al., 2018; Verplaetse & McKee, 2017; Waeiss et al., 2019). Nicotine directly activates VTA DA neurons by stimulating nicotinic receptors, and also indirectly activates them by stimulating glutamatergic input onto VTA DA neurons (Nora D. Volkow et al., 2011). It is suggested that the underlying biological effects of alcohol and nicotine on the brain may coincide and even synergize, enhancing the rewarding effects and neurological changes (Grucza & Bierut, 2006; Waeiss et al., 2019). The exact mechanism underlying the effects seen with alcohol and nicotine co-consumption are still unknown, indicating more research is necessary to better understand and treat this and other combinations of SUD.

1.3 Regulation of VTA DA Neurons

Although there are significant differences in mechanisms and use patterns between drugs of abuse, they have in common that they increase DA levels throughout the mesocorticolimbic system (Arora et al., 2010; Di Chiara & Imperato, 1988; Nelson et al., 2017; Nora D. Volkow et al., 2011). Regulation of VTA DA neuron output, therefore, is a critical determinant of response to drugs of abuse. VTA DA neuron output is necessary for expression of drug-related behaviors (Liu et al., 2020; Solecki et al., 2020; Valyear et al., 2020), and it has been shown that administration of drugs of abuse can lead to changes in VTA DA neuron regulation (Arora et al., 2011; Brodie, 2002; Stewart et al., 2015). There are multiple mechanisms regulating VTA DA neuron output. One form of regulation is by autoinhibition via inhibitory D_2R activation. When VTA DA neurons are

activated, DA levels rise both in downstream brain regions and in the midbrain. DA in the midbrain binds to D_2Rs located on the DA cell bodies and inhibits further DA release, synthesis, and reuptake (Christopher P Ford, 2014). When DA levels rise in downstream targets of the VTA, such as the NAc, reciprocal GABAergic release from D_1 MSNs onto VTA DA neurons activates $GABA_B$ receptor ($GABA_B$R)-dependent signaling (Hearing et al., 2012) (Erhardt, Mathé, Chergui, Engberg, & Svensson, 2002; Morales & Margolis, 2017). This is often referred to as "long loop" feedback. Both the D_2R and the $GABA_B$R are inhibitory G protein-coupled receptors (GPCRs).

1.3.1 G Protein-Coupled Receptors

The classical actions of GPCRs are mediated by G protein subunits (Gα-GTP and G$\beta\gamma$). Ligand binding promotes the exchange of GTP for GDP on the Gα subunit, which leads to the dissociation of the G protein complex allowing the Gα and G$\beta\gamma$ subunits to independently interact with downstream effectors such as adenylyl cyclase or various ion channels (Bettler, Kaupmann, Mosbacher, & Gassmann, 2004; Hearing et al., 2012; Pinard, Seddik, & Bettler, 2010). Effector modulation ceases when the intrinsic GTPase activity of Gα hydrolyzes GTP to GDP, and the G$\alpha\beta\gamma$ complex re-forms (Gold, Ni, Dohlman, & Nestler, 1997). GPCRs are categorized based on the identity of G proteins that they couple to. The main distinctions arise from the Gα subunit family, which is broken down into Gα_s, G$\alpha_{i/o}$, Gα_q and Gα_{12}. These different families interact with effectors in distinct ways to modulate cell activity (Syrovatkina, Alegre, Dey, & Huang, 2016). The D_2R and $GABA_B$R are both G$\alpha_{i/o}$ coupled GPCRs, which act to inhibit cells. They are localized in the somatodendritic compartment and on axon terminals of VTA DA neurons; when activated at these locations, they hyperpolarize cells via G protein-gated inwardly rectifying K^+ (GIRK) channels and moderate neurotransmitter release via inhibition of voltage-gated Ca^{2+} channels and adenylyl cyclase (Bettler et al., 2004; Christopher P

Ford, 2014; Pinard et al., 2010). Importantly, both of these receptors have been implicated in drug-related behaviors.

GPCRs and Drugs of Abuse

The D_2R and $GABA_BR$ are important for tempering the effects of natural rewards and drugs of abuse in the brain, and expression levels and patterns are often affected by repeated drug use. Human brain imaging studies and post mortem tissue analyses have reported reductions in D_2R availability in subjects that use drugs of abuse (Tupala et al., 2001; Nora D. Volkow & Morales, 2015). In rodents, animals genetically lacking mesocorticolimbic D_2Rs show increased responding to the rewarding effects of alcohol and cocaine, and activation of D_2Rs decreases the reinforcing properties of psychostimulants (Bello et al., 2011; Bocarsly et al., 2019; Christopher P Ford, 2014). Similarly, the $GABA_BR$ agonist baclofen can reduce drug taking, craving, withdrawal symptoms, and relapse in clinical studies (Agabio & Colombo, 2014; Filip et al., 2015). In rodents, baclofen reduces drug consumption, reinstatement, and withdrawal symptoms. Further, the site of action for this effect has been localized to the VTA (Bechtholt & Cunningham, 2005; Brebner, Phelan, & Roberts, 2000; Filip et al., 2015; Lorrai, Maccioni, Gessa, & Colombo, 2016; Maccioni, Lorrai, Contini, Leite-Morris, & Colombo, 2018; Moore & Boehm, 2009; Vlachou & Markou, 2010). Together these data suggest that mesocorticolimbic D_2R- and $GABA_BR$-dependent signaling both play an important role in reward, motivation, and drug-related behaviors.

1.3.2 Regulation of G Protein-Coupled Receptors

GPCRs have further regulatory mechanisms and binding partners that can adjust the precise signaling pattern and duration. GTPase activating proteins (GAPs) accelerate the termination of G protein-dependent signaling (Lomazzi, Slesinger, & Lüscher, 2008). One important type of GAP that acts as a critical determinant of the strength and sensitivity of

G protein-dependent signaling is a Regulator of G protein Signaling (RGS) protein. At least 30 different subtypes of RGS proteins have been characterized and can be grouped into subfamilies based on structure and/or function (G. R. Anderson, Posokhova, & Martemyanov, 2009; Gold et al., 1997). The R7 subfamily of RGS proteins, which consists of RGS6, RGS7, RGS9, and RGS11, has been shown to play a negative regulatory role in D_2R- and $GABA_BR$-dependent signaling (Maity et al., 2012; Masuho, Xie, & Martemyanov, 2013; Ostrovskaya et al., 2014). R7 RGS proteins contain 3 distinct domains - a catalytic GAP domain, a G protein gamma-like domain (GGL), and a Disheveled, Egl-10, Pleckstrin/Dep helical extension (DEP/DHEX) domain. These domains are important for interacting with proteins that enhance stability and function. The GGL domain is critical for the formation of obligatory dimers with Gβ5, the atypical member of the Gβ subfamily. This dimerization is critical for stability and function of all R7 RGS family members. The DEP/DHEX domain is responsible for association with adaptor proteins including R7 binding protein (R7BP) and G protein-coupled receptor 158 (GPR158) that fine-tune functionality of the complex (G. R. Anderson et al., 2009; Hooks et al., 2003; Woodard, Jardín, Berna-Erro, Salido, & Rosado, 2015). Of note, R7 RGS proteins also play a key role in modulating the effects of drugs of abuse, as genetic manipulations altering relative levels of R7 RGS proteins influence drug responsivity (G. R. Anderson et al., 2010; Z. Rahman et al., 2003; Stewart et al., 2015; Zachariou et al., 2003). RGS6 levels were significantly associated with alcohol dependence symptom count, a quantitative measure of AUD, in a human Genome Wide Association Study (G. Chen et al., 2017). In addition, mice lacking R7 RGS proteins display altered consumption and reward of drugs of abuse including alcohol, morphine, and cocaine.

1.4 Purpose of Studies

The goal of this thesis work is to better understand drug-related behaviors both on the molecular and behavioral level. More specifically, to assess how changes in the regulation of VTA DA neuron output affect drug related behaviors, and to assess how access to multiple drugs of abuse affect consumption patterns. **Chapter 2** describes a novel CRISPR/Cas9 approach to selectively ablate inhibitory G protein-coupled receptors (GPCRs) in VTA DA neurons and utilizes this tool to demonstrate how loss of inhibitory GPCR-mediated currents differentially affects behavioral sensitivity to drugs of abuse based on receptor, sex, and drug. **Chapter 3** utilizes the same CRISPR/Cas9 tool to further demonstrate how loss of a regulatory element modulating VTA DA neuron GPCR-mediated inhibitory signaling affects drug consumption in a sex-dependent manner. Chapters 2 and 3 discuss drugs of abuse administered in isolation, whereas **Chapter 4** explores consumption patterns in a behavioral paradigm aimed to more closely mimic human drug co-consumption. All of these studies provide novel insights into the complex interplay of drug-related circuitry and behaviors.

Chapter 2 : Differential impact of inhibitory G protein signaling pathways in ventral tegmental area dopamine neurons on behavioral sensitivity to cocaine and morphine

Chapter 2 contains work previously published in eNeuro *2021 March; 8(2). "Differential impact of inhibitory G protein signaling pathways in ventral tegmental area dopamine neurons on behavioral sensitivity to cocaine and morphine."* ***Margot C. DeBaker****, Ezequiel Marron Fernandez de Velasco, Nora M. McCall, Anna M. Lee, Kevin Wickman.*

Author Contributions: KW, EMFdV, and MCD designed the project, planned experiments, and coordinated the work. NMC performed and analyzed initial DREADD electrophysiology and behavior. MCD performed and analyzed all other experiments. EMFdV assisted with production of all viral vectors associated with the study. AML provided co-mentorship support. MCD and KW wrote the manuscript, and all authors provided reviews.

2.1 Synopsis

Drugs of abuse engage overlapping but distinct molecular and cellular mechanisms to enhance dopamine (DA) signaling in the mesocorticolimbic circuitry. DA neurons of the ventral tegmental area (VTA) are key substrates of drugs of abuse and have been implicated in addiction-related behaviors. Enhanced VTA DA neurotransmission evoked by drugs of abuse can engage inhibitory G protein-dependent feedback pathways, mediated by $GABA_B$ receptors ($GABA_BRs$) and D_2 DA receptors (D_2Rs). Chemogenetic inhibition of VTA DA neurons potently suppressed baseline motor activity, as well as the motor-stimulatory effect of cocaine and morphine, confirming the critical influence of VTA DA neurons and inhibitory G protein signaling in these neurons on this addiction-related behavior. To resolve the relative influence of $GABA_BR$- and D_2R-dependent signaling pathways in VTA DA neurons on behavioral sensitivity to drugs of abuse, we developed a neuron-specific viral CRISPR/Cas9 approach to ablate D_2R and $GABA_BR$ in VTA DA neurons. Ablation of $GABA_BR$ or D_2R did not impact baseline physiological properties or excitability of VTA DA neurons, but it did preclude the direct somatodendritic inhibitory influence of $GABA_BR$ or D_2R activation. D_2R ablation potentiated the motor-stimulatory effect of cocaine in male and female mice, whereas $GABA_BR$ ablation selectively potentiated cocaine-induced activity in male subjects only. Neither D_2R nor $GABA_BR$ ablation impacted morphine-induced motor activity. Collectively, our data show that cocaine and morphine differ in the extent to which they engage inhibitory G protein-dependent feedback pathways in VTA DA neurons and highlight key sex differences that may impact susceptibility to various facets of addiction.

2.2 Significance Statement

Although inhibitory G protein-dependent signaling involving the $GABA_B$ ($GABA_BR$) and D_2 dopamine receptor (D_2R) in VTA DA neurons is thought to limit DA neurotransmission evoked by drugs of abuse, their relative impact on behavioral sensitivity to such drugs is unclear. Using a neuron-specific viral CRISPR/Cas9 approach, we show that that loss of D_2R in VTA DA neurons enhances behavioral sensitivity to systemic administration of cocaine in male and female mice, whereas loss of $GABA_BR$ enhances cocaine sensitivity only in males. Neither $GABA_BR$ nor D_2R ablation impacted behavioral sensitivity to morphine. Thus, differential engagement of inhibitory feedback pathways in VTA DA neurons likely contributes to drug-specific neurophysiological and behavioral effects and may underlie sex differences associated with some facets of addiction.

2.3 Introduction

Dopamine (DA) neurons of the ventral tegmental area (VTA) are an integral part of the mesocorticolimbic system, a network of brain regions that mediates responses to natural rewards and drugs of abuse (Juarez & Han, 2016; Lammel et al., 2014; Lüscher, 2016; Schultz, 2016; Nora D. Volkow & Morales, 2015). Drugs of abuse enhance DA neurotransmission in the mesocorticolimbic system via actions on distinct molecular targets (Di Chiara & Imperato, 1988; Lüscher & Ungless, 2006). Cocaine, for example, inhibits monoamine transporters, including the DA transporter (DAT) which recycles DA from the extracellular space, allowing DA levels to rise and persist in the VTA and its projection targets (Adell & Artigas, 2004; Adrover, Shin, & Alvarez, 2014; Beart, McDonald, & Gundlach, 1979; S. Y. Chen, Burger, & Reith, 1996; Di Chiara & Imperato, 1988; Groves, Wilson, Young, & Rebec, 1975; Iravani, Muscat, & Kruk, 1996; Kita, Kile, Parker, & Wightman, 2009). In contrast, morphine suppresses inhibitory GABAergic input,

enhancing VTA DA neuron activity via disinhibition (Jalabert et al., 2011; Jhou, Fields, Baxter, Saper, & Holland, 2009; Johnson & North, 1992).

While enhanced DA neurotransmission underlies addiction-related behaviors (Hyman, Malenka, & Nestler, 2006), it can also trigger negative feedback mediated by inhibitory G protein signaling pathways (Narayanan, Wallace, & Uretsky, 1996; S. Rahman & McBride, 2000; Steketee & Kalivas, 1990, 1991). For example, cocaine elevates DA levels in the VTA and terminal regions, provoking feedback inhibition of VTA DA neurons via activation of D2 DA receptors (D_2R) in the somatodendritic compartment and axon terminals (Beckstead, Grandy, Wickman, & Williams, 2004; Bradberry & Roth, 1989; Brodie & Dunwiddie, 1990; Einhorn, Johansen, & White, 1988; Christopher P Ford, 2014). Cocaine also provokes GABAergic feedback to VTA DA neurons indirectly, by stimulating D1R-expressing GABAergic medium spiny neurons in the NAc that project to the VTA (Edwards et al., 2017; Menegas et al., 2015; Pignatelli & Bonci, 2018; S. Rahman & McBride, 2001; Watabe-Uchida, Zhu, Ogawa, Vamanrao, & Uchida, 2012). This "long-loop" GABAergic feedback to VTA DA neurons is mediated primarily by activation of somatodendritic $GABA_BRs$ on VTA DA neurons (Edwards et al., 2017).

Pharmacological and genetic approaches have implicated $GABA_BR$ and D_2R-dependent signaling in the VTA in drug-induced behaviors. For example, pharmacological activation of D_2R in the VTA suppressed cocaine-induced activity (Koulchitsky et al., 2016) and cocaine-reinstated drugs seeking behavior (Xue, Steketee, Rebec, & Sun, 2011), while pharmacological inhibition of D_2R in the VTA increased psychostimulant-induced locomotor activity (N. H. Chen & Reith, 1994; Tanabe, Suto, Creekmore, Steinmiller, & Vezina, 2004). Similarly, intra-VTA infusion of the $GABA_BR$ agonist baclofen blocked the locomotor-stimulatory effect of psychostimulants and opioids (N. H. Chen & Reith, 1994; Kalivas, Duffy, & Eberhardt, 1990; Leite-Morris, Fukudome, & Kaplan, 2002; Leite-Morris,

Fukudome, Shoeb, & Kaplan, 2004; Steketee & Kalivas, 1991) and attenuated self-administration of cocaine, opioids, and other drugs of abuse (Backes & Hemby, 2008; Brebner et al., 2000; Leite-Morris et al., 2004; Xi & Stein, 1999). RNAi-mediated suppression of D_2R in the rat VTA (cell non-selective) enhanced cocaine-related behavior (R. Chen et al., 2018; De Jong et al., 2015), enhanced choice impulsivity (Bernosky-Smith et al., 2018), and increased functional brain activity (Martin, Smith, Luessen, Chen, & Porrino, 2020). Ablation of D_2R in DA neurons throughout the mouse brain correlated with enhanced cocaine-induced activity (Bello et al., 2011), as well as acquisition of cocaine self-administration and reactivity to drug-paired cues (Holroyd et al., 2015). Interestingly, partial suppression of $GABA_BR$ in VTA DA neurons unmasked cocaine-induced activity normally absent in BALB/c mice, but did not impact morphine-induced activity (Edwards et al., 2017).

Collectively, available data suggests that D_2R and $GABA_BR$-dependent signaling pathways in VTA DA neurons may exert a differential influence on behavioral sensitivity to drugs of abuse. Published studies investigating D_2R and $GABA_BR$ signaling in VTA DA neurons, however, have used approaches that provide either anatomic or cellular specificity, or do not completely suppress inhibitory signaling, or focus only on one signaling pathway or drug of abuse. Accordingly, the goal of this study was to compare the impact of D_2R or $GABA_BR$ ablation in VTA DA neurons on behavioral sensitivity to cocaine and morphine. To this end, we developed a neuron-specific viral CRISPR/Cas9 approach to ablate D_2R and $GABA_BR$ selectively in VTA DA neurons of adult mice. Our findings show that D_2R and $GABA_BR$-dependent signaling exert drug- and sex-specific influences on motor activity in mice.

2.4 Materials and Methods

2.4.1 Animals.

All studies were approved by the Institutional Animal Care and Use Committee at the University of Minnesota. The B6.SJL-*Slc6a3*$^{tm1.1(cre)Bkmn}$/J (stock #006660, The Jackson Laboratory; Bar Harbor, ME) knock-in line was used in this study; heterozygous subjects, referred to throughout as DATCre(+) mice, were generated by crossing with C57BL/6J subjects. DATCre(+) mice were also crossed in multiple rounds with a Cre-dependent Cas9GFP knock-in line (B6;129-Gt(ROSA)26Sor$^{tm1(CAG-cas9*,-EGFP)Fezh}$/J, The Jackson Laboratory, stock #026179), to generate DATCre(+) subjects homozygous for the Cas9GFP(+) mutation; these mice are referred to throughout as DATCre(+):Cas9GFP(+) mice. All mice used in experiments were bred in-house. Mice were group housed, maintained on a 14:10 h light/dark cycle and were provided *ad libitum* access to food and water.

2.4.2 Reagents.

Baclofen, quinpirole, and sulpiride were purchased from Sigma (St. Louis, MO), and CGP54626 and Clozapine-N-Oxide (CNO) were purchased from Tocris (Bristol, UK). Cocaine and morphine were obtained through Boynton Health Pharmacy at the University of Minnesota. All adeno-associated viruses (AAV) were packaged in AAV8 serotype by the University of Minnesota Viral Vector and Cloning Core (Minneapolis, MN) following standard packaging procedures (S. H. Chen et al., 2019); titers were between 0.2-4 x 10^{14} genocopies/mL. The packaging plasmids (pRC8 and pHelper) were obtained from the University of Pennsylvania Vector Core. The plasmids pAAV-hSyn-hM4Di(mCherry) and pAAV-hSyn-DIO-mCherry (Addgene plasmids #50475 and #50459, respectively) were gifts from Dr. Bryan Roth. To obtain the pAAV-hSyn-DIO-hM4Di(mCherry) plasmid, the mCherry from the pAAV-hSyn-DIO-mCherry was replaced by an hM4Di(mCherry)

cassette via subcloning. For the CRISPR/Cas9 experiments the pAAV-U6-gRNA-hSyn-NLSmCherry was generated using the backbone of the plasmid pAAV-U6-gRNA-hSyn-Cre-2A-EGFP-KASH (Platt et al., 2014) (Addgene plasmid #60231) that was a gift from Dr. Feng Zhang. The Genome Engineering and iPSC Center of Washington University designed and tested gRNA sequences targeting the Drd2 (D_2R) and Gabbr1 ($GABA_BR1$) genes. Sequences used were as follows: D_2R – CATGACAGTAACTCGGCGCT, $GABA_BR1$ – ACGGCGTGCAGTATACATCG, LacZ – TGCGAATACGCCCACGCGAT.

2.4.3 Intracranial manipulations.

Mice (>45 d) were placed in a stereotaxic frame (David Kopf Instruments; Tujunga, CA) under isoflurane anesthesia. Microinjectors, made by affixing a 33-gauge stainless steel hypodermic tube within a shorter 26-gauge stainless steel hypodermic tube, were attached to polyethylene-20 tubing affixed to 10 mL Hamilton syringes, and were lowered through burr holes in the skull to the VTA (from bregma: -2.75 mm A/P, ±0.55-0.7 mm M/L, -5 mm D/V); 300-500 nL of virus was injected per side at a rate of 100 nL/min. The optimized coordinates and viral load ensured full coverage of the VTA along anterior/posterior and rostral-caudal axes, with minimal spread into the adjacent substantia nigra pars compacta. Microinjectors were left in place for 10 min following infusion to reduce solution backflow along the infusion track. Slice electrophysiology and behavioral experiments were performed 3-4 wk and 5-6 wk after viral infusion for chemogenetic and CRISPR experiments, respectively.

2.4.4 Slice electrophysiology.

Electrophysiological properties of VTA DA neurons were evaluated in behaviorally naïve adult mice (66-93 d). Horizontal slices (225 mm) containing the VTA were prepared in ice-cold sucrose substituted ACSF, and allowed to recover at room temperature in ASCF containing (in mM): 125 NaCl, 2.5 KCl, 1.25 NaH_2PO_4, 25 $NaHCO_3$, 11 Glucose, 1

$MgCl_2$, and 2 $CaCl_2$, pH 7.4, for at least 1 h, as described (McCall et al., 2017). Neurons in the lateral VTA exhibiting appropriate fluorescence were targeted for analysis as this sub-region of the VTA receives prominent input from the NAc that mediates $GABA_BR$-dependent feedback (Edwards et al., 2017). Whole-cell data were acquired using a Multiclamp 700A amplifier and pCLAMPv.9.2 software (Molecular Devices, LLC; San Jose, CA), using recording conditions described in previous publications (McCall et al., 2017). Input/membrane resistance (R_M) and apparent capacitance (C_M) were determined using a 5 mV/10 ms voltage-step, with current responses filtered at 5 Hz. Immediately after establishing whole-cell access, I_h conductance was measured using a 200-ms voltage step to -120 mV; the difference in current from beginning to end of the -120 mV step was taken as I_h amplitude. Subsequently, spontaneous activity was measured in current-clamp mode (I=0) for 1 min. Neurons exhibiting no spontaneous activity were not evaluated. Action potential half-width (AP_{50}) was determined by averaging 5 AP_{50} values. For rheobase assessments, cells were held in current-clamp mode at -80 pA to prevent spontaneous activity, and then given 1-s current pulses, beginning at -100 pA and progressing in 20 pA increments. Rheobase was defined as the minimum current step that evoked one or more action potentials. In chemogenetic experiments, the change in rheobase measured before and after bath application of CNO application was determined. Somatodendritic holding currents were measured in voltage-clamp mode (V_{hold} = -60 mV) following bath application of CNO (10 mM), baclofen (200 mM), or quinpirole (10 mM). All command potentials factored in a junction potential of -15 mV predicted using JPCalc software (Molecular Devices, LLC). Series and input resistances were tracked throughout the experiment. If series resistance was unstable or exceeded 20 MOhm, the experiment was excluded from analysis.

2.4.5 Locomotor activity.

Locomotor activity was assessed in open-field activity chambers housed in sound-attenuating cubicles (Med-Associates, St. Albans, VT). Each cubicle was equipped with three 16-beam infrared arrays permitting automated measurements of distance traveled (Activity Monitor 5; Med-Associates). Animals were habituated to the testing room for at least 30 min before testing. Subjects were acclimated over 3 d; on day 1, animals were handled and placed in the open field for 60 min. On day 2 and 3, animals were given an IP injection of saline and placed in the open field for 60 min. For DREADD experiments, mice were injected with CNO (2 mg/Kg IP) 30 min prior to either saline, cocaine (15 mg/Kg IP), or morphine (10 mg/Kg IP) injection on Day 4. Distance traveled during the 60-min period following saline or drug injection was measured; separate cohorts of mice received saline, cocaine and morphine injections. For CRISPR/Cas9 experiments, mice were placed in the open field for 30 min before injection each day to acclimate to the chamber. Activity was measured on day 3 following saline injection, and again on day 4 following injection of cocaine (15 mg/Kg IP) or morphine (10 mg/Kg IP); separate cohorts of mice were used for cocaine and morphine studies. Thigmotaxis was quantified by dividing the distance traveled in the periphery by the total distance traveled, as described (Pravetoni & Wickman, 2008). After behavioral testing, the scope and accuracy of viral targeting was assessed by fluorescence microscopy; 225 mm horizontal slices of the midbrain were obtained using a vibratome and images were acquired on an Olympus IX-80 microscope using MetaMorph Advanced Acquisition v.7.7.7.0 software (Molecular Devices, LLC). Only data from animals with bilateral viral-driven fluorescence, where the majority of fluorescence was confined to VTA (with minimal spread to the adjacent substantia nigra), were included in the final analysis.

2.4.6 Statistical analysis.

Data are presented throughout as the mean±SEM. Statistical analyses were performed using Prism v.9 software (GraphPad Software, La Jolla, CA). All studies included balanced numbers of male and female mice, and data were analyzed first for sex effects. If no sex differences were observed, data from male and female subjects were pooled. If any data point fell outside the range of 2 standard deviations from the mean, it was excluded as an outlier. Across the entire study, this outlier detection approach led to the removal of 1 point from the hM4Di/morphine activity dataset and 1 point from the hM4Di control/morphine activity dataset. Differences were considered significant if $P < 0.05$.

2.5 Results

2.5.1 G protein-dependent inhibition of VTA DA neurons suppresses motor activity

Motor activation is an unconditioned DA-dependent response in mice to systemic administration of cocaine and morphine (Delfs, Schreiber, & Kelley, 1990; Kalivas & Duffy, 1993; van Rossum, van der Schoot, & Hurkmans, 1962) that can be recapitulated by direct chemogenetic or optogenetic stimulation of VTA DA neurons (Boender et al., 2014; Guo et al., 2014; Kim et al., 2012; Tye et al., 2013). To test whether inhibitory G protein-dependent signaling in VTA DA neurons can suppress the locomotor stimulatory effect of systemic cocaine and morphine, we used DATCre(+) mice and a Cre-dependent viral inhibitory chemogenetic approach. Cre-dependent AAV vectors harboring either hM4Di(mCherry) or mCherry control were infused into the VTA of adult male and female DATCre(+) mice to permit selective chemogenetic inhibition of VTA DA neurons (**Fig. 2.1A**).

In acutely isolated midbrain slices from virally treated DATCre(+) mice, bath application of clozapine-N-oxide (CNO) decreased the excitability (increased the rheobase) of hM4Di-expressing, but not mCherry control, DA neurons (**Fig. 2.1B,C**). CNO also evoked a somatodendritic inhibitory current (V_{hold} = -60 mV) reversed by 0.3 mM Ba^{2+} in hM4Di(mCherry)-expressing but not control VTA DA neurons (**Fig. 2.1D,E**). Thus, chemogenetic inhibition of VTA DA neurons, like the direct somatodendritic inhibition evoked by D_2R and $GABA_BR$ activation, is likely mediated by activation of G protein-gated inwardly rectifying K^+ (GIRK/Kir3) channels (Arora et al., 2010; Beckstead et al., 2004; Cruz et al., 2004; Labouèbe et al., 2007). Consistent with a previous report (Runegaard et al., 2018), chemogenetic inhibition of VTA DA neurons suppressed motor activity evoked by injection of saline, as well as cocaine and morphine (**Fig. 2.1F**). These results confirm that VTA DA neurons are key regulators of motor activity in mice and show that activation of inhibitory G protein signaling in these neurons can potently suppress baseline activity and the motor-stimulatory effects of cocaine and morphine.

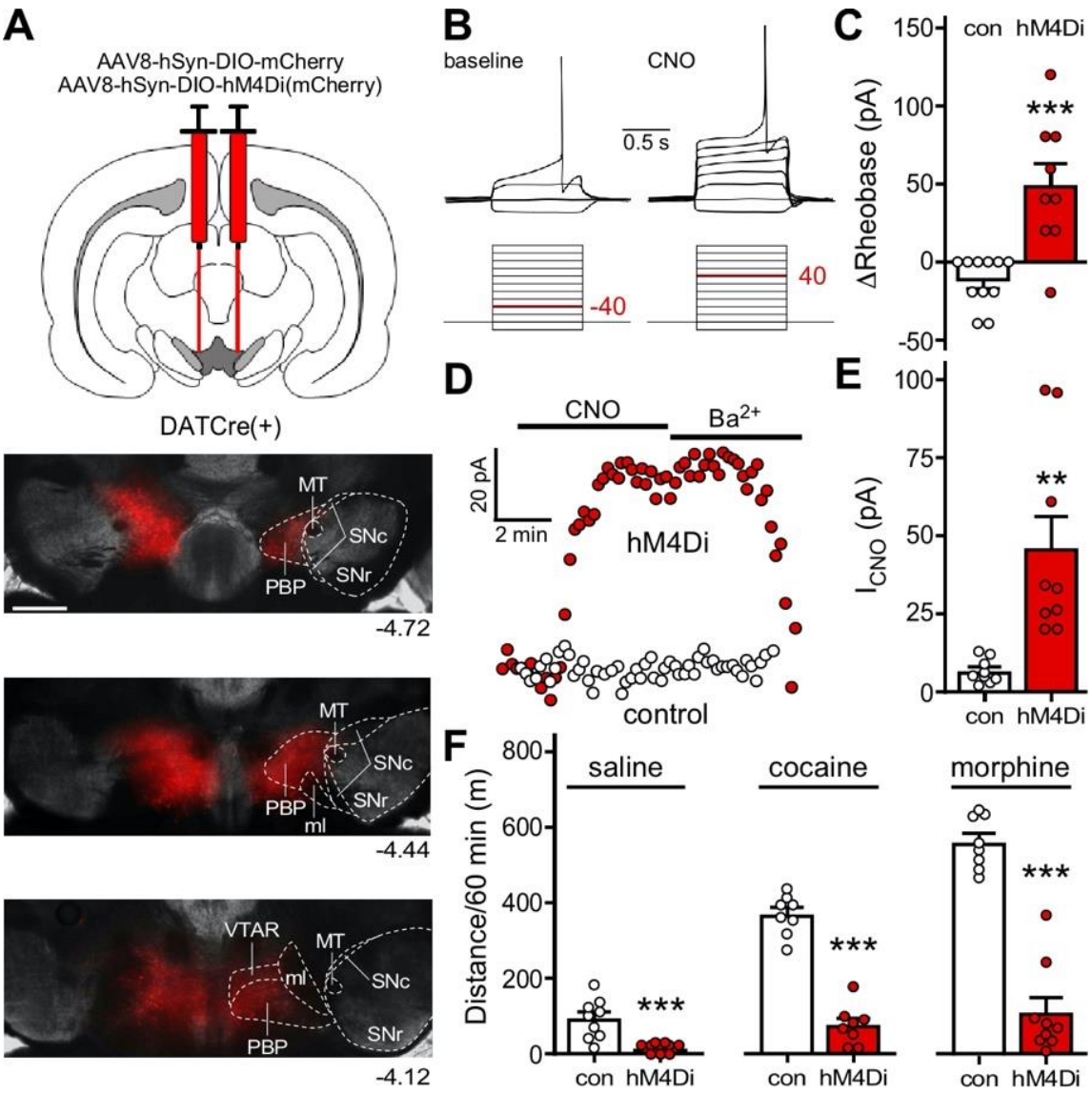

Figure 2.1. Inhibitory G protein signaling in VTA DA neurons suppresses baseline and drug-induced motor activity cocaine and morphine

(A) Viral targeting in a DATCre(+) mouse treated intra-VTA AAV8-hSyn-DIO-mCherry, with rostro-caudal tiling of panels highlighting viral spread (mCherry fluorescence). Abbreviations: ml - medial lemniscus, MT - medial terminal nucleus of the accessory optic tract, PBP - parabrachial pigmented nucleus of the VTA, SNc - substantia nigra pars compacta, SNr - substantia nigra pars reticulata, VTAR - rostral part of the VTA. Scale bar: 500 mm.

(B) Example of rheobase measurement in a VTA DA neuron expressing hM4Di, prior to and after bath perfusion of CNO (10 mM). The traces shown were the first to display spiking and were recorded following injection of the current indicated in red below.

(C) Change in rheobase induced by CNO (10 mM) in VTA DA neurons from DATCre(+) mice treated with AAV8-hSyn-DIO-hM4Di(mCherry) or AAV8-hSyn-DIO-mCherry control (t_{18}=4.555; ***P=0.0002; unpaired student's t test; n=9-11/group).

(D) Somatodendritic inhibitory currents (V_{hold} =-60 mV) evoked by CNO (10 mM) in VTA DA neurons from DATCre(+) mice treated with AAV8-hSyn-DIO-hM4Di(mCherry) or AAV8-hSyn-DIO-mCherry control.

(E) Summary of CNO-induced somatodendritic currents in VTA DA neurons from DATCre(+) treated with AAV8-hSyn-DIO-hM4Di(mCherry) or AAV8-hSyn-DIO-mCherry control (t_{16}=3.732; **P=0.0018; unpaired student's t test; n=9/group).

(F) Total distance traveled in an open field during the 60-min interval following injection of saline (t_{16}=4.385, ***P=0.0005), 15 mg/Kg cocaine (t_{14}=11.20, ***P<0.0001), and 10 mg/Kg morphine (t_{15}=9.401, ***P<0.0001) in DATCre(+) mice treated with intra-VTA AAV8-hSyn-DIO-hM4Di(mCherry) or AAV8-hSyn-DIO-mCherry control (n=8-9 mice/group). CNO (2 mg/Kg IP) was administered to all subjects 30-min prior to saline or drug challenge.

2.5.2 CRISPR/Cas9 ablation of D_2R and $GABA_BR$ in VTA DA neurons

To assess the impact of D_2R and $GABA_BR$-dependent signaling pathways in VTA DA neurons on behavioral sensitivity to cocaine and morphine, we developed a DA neuron-specific, viral CRISPR/Cas9 ablation approach. DATCre(+) mice were crossed with a Cre-dependent Cas9GFP line to generate DATCre(+):Cas9GFP(+) mice. AAV vectors harboring guide RNAs (gRNAs) targeting LacZ (control), D_2R, or $GABA_BR1$ were generated and infused into the VTA of male and female DATCre(+):Cas9GFP(+) mice (**Fig. 2.2A**).

To assess the efficacy and selectivity of the viral vectors, somatodendritic currents evoked by bath application of the $D_{2/3}R$ agonist quinpirole and the $GABA_BR$ agonist baclofen were measured in VTA DA neurons 5-6 wk after viral infusion. In slices from LacZ gRNA-treated subjects, somatodendritic outward inhibitory currents were reliably evoked by quinpirole and baclofen (**Fig. 2.2B**), consistent with previous studies (Arora et al., 2010; Beckstead et al., 2004; Cruz et al., 2004; Labouèbe et al., 2007; McCall et al., 2017). In VTA DA neurons from mice treated with D_2R gRNA, quinpirole-induced currents were completely absent (**Fig. 2.2B,C**), while baclofen (applied after quinpirole) evoked normal responses (**Fig. 2.2B,D**). Interestingly, a sex difference in the amplitude of quinpirole-induced responses was observed, with currents in VTA DA neurons from female subjects larger than those in males (**Fig. 2.2C**). No sex differences were observed in the amplitude of baclofen-induced currents.

In VTA DA neurons from mice treated with $GABA_BR1$ gRNA, somatodendritic responses to baclofen were completely absent (**Fig. 2.2E,F**). Responses to quinpirole (applied after baclofen application) were larger than those seen in VTA DA neurons from LacZ-treated controls (**Fig. 2.2G**). As this difference may reflect the impact of prior activation by $GABA_BR$ of a shared effector in control cells, we conducted a separate study

where only quinpirole was applied to the slice. In these experiments, quinpirole-induced somatodendritic currents were not significantly different between $GABA_BR$-lacking and control VTA DA neurons (**Fig. 2.2H**).

We also examined the impact of D_2R and $GABA_BR$ ablation on VTA DA neuron excitability, as measured by spontaneous activity and rheobase. No sex differences were observed with respect to either excitability measure and, as such, data from male and female subjects were pooled to increase the power of the study. Ablation of D_2R or $GABA_BR$ did not impact spontaneous activity of VTA DA neurons (**Fig. 2.2I**) or rheobase (**Fig. 2.2J**). Similarly, no impact of D_2R or $GABA_BR$ ablation was detected on I_h current amplitude, cell capacitance, action potential half-width, or input resistance (**Table 2.1**). Collectively, these data show that we can selectively ablate $GABA_BR$ or D_2R-dependent signaling in VTA DA neurons, and that loss of these signaling pathways does not impact baseline electrophysiological characteristics of VTA DA neurons

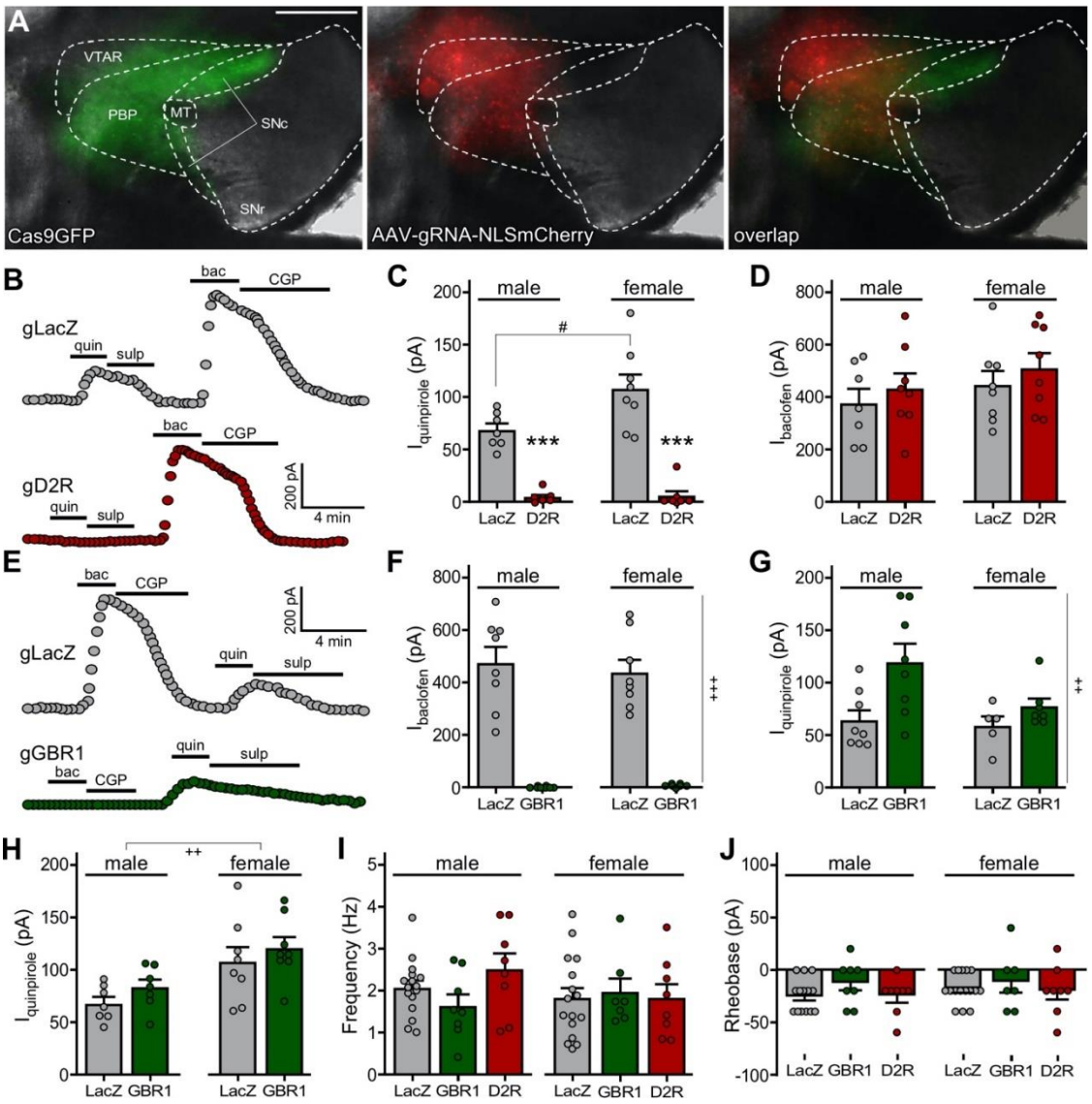

Figure 2.2. Viral CRISPR/Cas9 ablation of $GABA_BR$ and D_2R in VTA DA neurons

(A) Viral targeting in a DATCre(+):Cas9GFP(+) mouse treated with intra-VTA AAV8-U6-gRNA-hSyn-NLSmCherry; nucleus-localized mCherry fluorescence highlights the anatomic scope of viral targeting, and GFP fluorescence denotes the Cre-dependent expression of Cas9GFP in midbrain DA neurons of the VTA and substantia nigra. Abbreviations: MT - medial terminal nucleus of the accessory optic tract, PBP - parabrachial pigmented nucleus of the VTA, SNc - substantia nigra pars compacta, SNr - substantia nigra pars reticulata, VTAR - rostral part of the VTA. Scale bar: 500 mm.

(B) Somatodendritic inhibitory currents (V_{hold} =-60 mV) evoked by sequential bath application of quinpirole (quin, 20 mM) and then baclofen (bac, 200 mM) in VTA DA neurons from DATCre(+):Cas9GFP(+) mice treated with AAV8-U6-gD2R-hSyn-NLSmCherry or AAV8-U6-gLacZ-hSyn-NLSmCherry control. Currents were reversed by the $D_{2/3}R$ antagonist sulpiride (sulp, 5 mM) and CGP54626 (CGP, 2 mM).

(C) Summary of currents evoked by quinpirole (applied first) in VTA DA neurons from DATCre(+):Cas9GFP(+) mice treated with AAV8-U6-gD2R-hSyn-NLSmCherry or AAV8-U6-gLacZ-hSyn-NLSmCherry control. Main effects of sex ($F_{1,27}$=6.391, *P*=0.0176) and viral treatment ($F_{1,27}$=104.6, *P*<0.0001) were detected, along with an interaction between sex and viral treatment ($F_{1,27}$=5.590, *P*=0.0255). Symbols: $^{\#}P$<0.05; ***P<0.001 vs LacZ (within sex).

(D) Summary of currents evoked by baclofen, measured after quinpirole/sulpiride application (C), in VTA DA neurons from DATCre(+):Cas9GFP(+) mice treated with AAV8-U6-gD2R-hSyn-NLSmCherry or AAV8-U6-gLacZ-hSyn-NLSmCherry control. There was no main effect of sex ($F_{1,27}$=1.741, *P*=0.1981) or viral treatment ($F_{1,27}$=1.183, *P*=0.2864), nor was there an interaction between sex and viral treatment ($F_{1,27}$=0.0047, *P*=0.9461).

(E) Somatodendritic inhibitory currents (V_{hold}= -60 mV) evoked by sequential bath application of baclofen (bac, 200 mM) and then quinpirole (quin, 20 mM) in VTA DA neurons from DATCre(+):Cas9GFP(+) mice treated with AAV8-U6-gGBR1-hSyn-NLSmCherry or AAV8-U6-gLacZ-hSyn-NLSmCherry control. Currents were reversed by CGP54626 (CGP, 2 mM) and sulpiride (sulp, 5 mM).

(F) Summary of currents evoked by baclofen (applied first) in VTA DA neurons from DATCre(+):Cas9GFP(+) mice treated with AAV8-U6-gGBR1-hSyn-NLSmCherry or AAV8-U6-gLacZ-hSyn-NLSmCherry control. A main effect of viral treatment was observed ($F_{1,27}$=120.9, *P*<0.0001), but there was no main effect of sex ($F_{1,27}$=0.1910, *P*=0.6655) or interaction between sex and viral treatment ($F_{1,27}$=0.2216, *P*=0.6416). Symbol: ^{+++}P<0.001 (main effect of viral treatment).

(G) Summary of currents evoked by quinpirole, measured after baclofen/CGP54626 application (F) in VTA DA neurons from DATCre(+):Cas9GFP(+) mice treated with AAV8-U6-gGBR1-hSyn-NLSmCherry or AAV8-U6-gLacZ-hSyn-NLSmCherry control. A main effect of viral treatment was observed ($F_{1,24}$=8.182, *P*=0.0086), but there was no main effect of sex ($F_{1,24}$=3.429, *P*=0.0764) or interaction between sex and viral treatment ($F_{1,24}$=1.970, *P*=0.1733). Symbol: ^{++}P<0.001 (main effect of viral treatment).

(H) Summary of currents evoked by quinpirole in VTA DA neurons from a separate cohort of DATCre(+):Cas9GFP(+) mice treated with AAV8-U6-gGBR1-hSyn-NLSmCherry or AAV8-U6-gLacZ-hSyn-NLSmCherry control. A main effect of sex was observed ($F_{1,26}$=13.41, *P*=0.0011), but there was no main effect of viral treatment ($F_{1,26}$=1.766, *P*=0.1954) or interaction between sex and viral treatment ($F_{1,26}$=0.0129, *P*=0.9105). Symbol: ^{++}P<0.01 (main effect of sex).

(I) Impact of D_2R or $GABA_BR$ ablation on spontaneous activity in VTA DA neurons. No main effect of sex ($F_{1,56}$=0.7079, *P*=0.4037) or viral treatment ($F_{2,56}$=0.6571, *P*=0.5223) was detected, nor was there an interaction between sex and viral treatment ($F_{2,56}$=1.276, *P*=0.2870).

(J) Impact of D_2R or $GABA_BR$ ablation on rheobase in VTA DA neurons. No main effect of sex ($F_{1,56}$=0.8080, *P*=0.3725) or viral treatment ($F_{2,56}$=1.495, *P*=0.2332) was detected, nor was there an interaction between sex and viral treatment ($F_{2,56}$=0.1573, *P*=0.8548).

Sex	gRNA	N/n	C_M (pF)	R_M (MW)	I_h (pA)	AP_{50} (ms)
Male	LacZ	8/15	60 ± 2	200 ± 10	313 ± 49	0.83 ± 0.04
	$GABA_BR1$	3/8	56 ± 3	194 ± 11	240 ± 66	0.92 ± 0.07
	D_2R	3/8	62 ± 4	207 ± 34	246 ± 45	0.92 ± 0.04
			$F_{2,28}$=0.8299	$F_{2,28}$=0.1024	$F_{2,28}$=0.6179	$F_{2,28}$=1.154
			P=0.4465	*P*=0.9030	*P*=0.5463	*P*=0.3301
Female	LacZ	9/16	62 ± 2	186 ± 11	274 ± 39	0.85 ± 0.04
	$GABA_BR1$	3/7	60 ± 4	203 ± 21	225 ± 70	0.89 ± 0.06
	D_2R	4/8	62 ± 3	174 ± 22	338 ± 71	0.99 ± 0.05
			$F_{2,28}$=0.2026	$F_{2,28}$=0.6060	$F_{2,28}$=0.7869	$F_{2,28}$=2.431
			P=0.8178	*P*=0.5525	*P*=0.4651	*P*=0.1063

Table 2.1. Electrophysiological properties of VTA DA neurons.

Data extracted from whole-cell recordings of VTA DA neurons from male and female DATCre(+):Cas9GFP(+) mice treated with intra-VTA control (LacZ), D_2R, or $GABA_BR1$ gRNA vectors. Abbreviations: N/n - number of mice and individual experiments, C_M – apparent capacitance, R_M – input/membrane resistance, I_h – hyperpolarization-activated current, AP_{50} – action-potential half-width.

2.5.3 Impact of D_2R and $GABA_BR$ in VTA DA neurons on baseline and cocaine-induced activity

We next examined the impact of D_2R or $GABA_BR$ ablation on open-field motor activity measured after injection of saline or cocaine. Given the observed sex difference in the strength of D_2R-dependent signaling in VTA DA neurons, and our prior report of a sex difference in cocaine-induced motor activity in mice (McCall et al., 2017), we analyzed data from male and female subjects separately. In support of this approach, we found that while male and female LacZ control mice showed no difference in total distance traveled after cocaine injection, the temporal profile of cocaine-induced activity was notably different for male and female subjects (Extended Data **Fig. 2.4**); female subjects showed sharper time-to-peak and decay phases relative to male subjects.

In females, we observed main effects of drug and viral treatment, as well as a significant interaction between drug and viral treatment, on total distance traveled in the post-injection interval. D_2R or $GABA_BR$ ablation did not impact saline-induced activity in females (**Fig. 2.3A, left**). Loss of D_2R, but not $GABA_BR$, yielded enhanced cocaine-induced activity (**Fig. 2.3A, right**). Although the temporal profile of motor activity during the post-injection interval was qualitatively similar across the groups, loss of D_2R and $GABA_BR$ in VTA DA neurons correlated with elevated activity levels at all time points following injection (**Fig. 2.3B**). Cocaine also enhanced thigmotaxis, as assessed by calculating the ratio of distance traveled in the field periphery to total distance traveled (**Fig. 2.3C**). There was, however, no impact of D_2R or $GABA_BR$ ablation in VTA DA neurons on thigmotaxis index (**Fig. 2.3C**).

In males as in females, we observed main effects of drug and viral treatment, and a significant interaction between drug and viral treatment on total distance traveled. Loss of D_2R or $GABA_BR$ did not impact saline-induced activity (**Fig. 2.3D, left**). In contrast to

our observations in females, however, ablation of D_2R or $GABA_BR$ in males yielded comparably enhanced cocaine-induced activity over the 60-min post-injection interval (**Fig. 2.3D, right**). Interestingly, loss of D_2R in males correlated with higher levels of activity seen shortly after cocaine injection (**Fig. 2.3E**), yielding a temporal profile that was qualitatively similar to that observed in females (Extended Data **Fig. 2.4**). As was the case with female subjects, thigmotaxis was significantly impacted by drug but not viral treatment (**Fig. 2.3C**). Thus, D_2R-dependent signaling in VTA DA neurons tempers behavioral sensitivity to cocaine in male and female mice, whereas $GABA_BR$-dependent signaling exerts an influence on behavioral sensitivity to cocaine in male mice only.

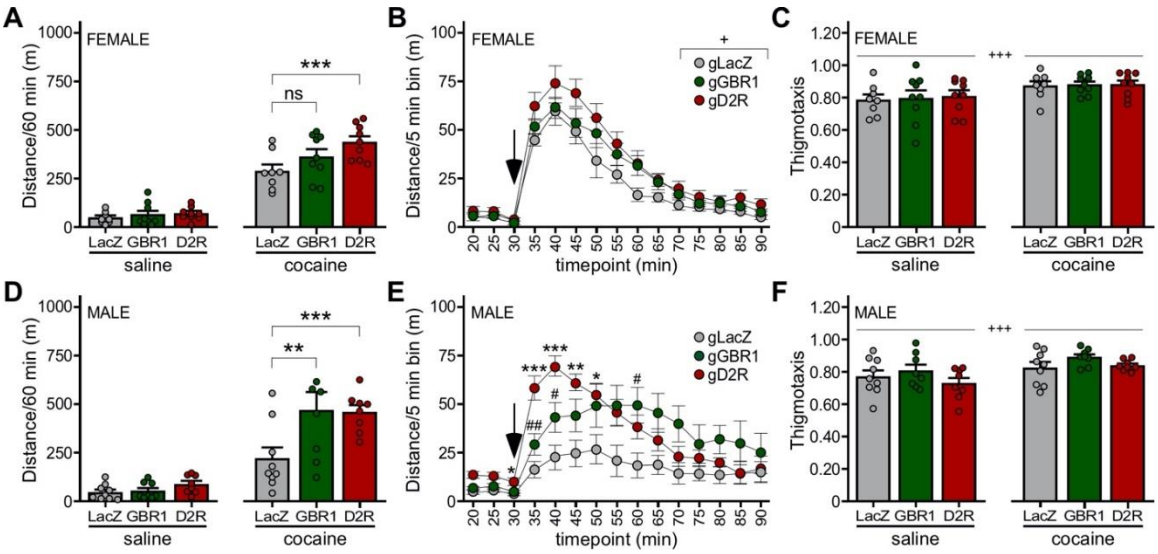

Figure 2.3. Impact of $GABA_BR$ and D_2R ablation on the motor-stimulatory effect of cocaine

(A) Total distance traveled during the 60-min period after injection of saline (left) or cocaine (15 mg/Kg IP, right) in female DATCre(+):Cas9GFP(+) mice treated with AAV8-U6-gGBR1-hSyn-NLSmCherry (n=9), AAV8-U6-gD2R-hSyn-NLSmCherry (n=9), or AAV8-U6-gLacZ-hSyn-NLSmCherry control (n=8). Two-way repeated measures ANOVA revealed main effects of drug ($F_{1,23}$=328.2, *P*<0.0001) and viral treatment ($F_{2,23}$=3.778, *P*=0.0381), and an interaction between drug and viral treatment ($F_{2,23}$=4.600, *P*=0.0209). Symbols: ***P<0.001; ns = not significant (*P*=0.1209).

(B) Distance traveled for female subjects prior to and after cocaine injection (denoted by arrow), evaluated in 5-min bins. Two-way repeated measures ANOVA revealed a main effect of bin ($F_{3.055,70.26}$=82.89, *P*<0.0001; Geisser-Greenhouse correction for sphericity) and viral treatment ($F_{2,23}$=4.613, *P*=0.0207), but there was no interaction between bin and viral treatment ($F_{24, 276}$=0.9807, *P*=0.4919). Symbol: *P<0.05 (main effect of viral treatment).

(C) Thigmotaxis index for female subjects following saline or cocaine injection. Two-way repeated measures ANOVA revealed a main effect of drug ($F_{1,23}$=16.40, *P*=0.0005) but not viral treatment ($F_{2,23}$=0.07351, *P*=0.9293), and there was no interaction between drug and viral treatment ($F_{2,23}$=0.03955, *P*=0.9613). Symbol: ^{+++}P<0.001 (main effect of drug).

(D) Total distance traveled during the 60-min period after injection of saline (left) or cocaine (15 mg/Kg IP, right) in male DATCre(+):Cas9GFP(+) mice treated with AAV8-U6-gGBR1-hSyn-NLSmCherry (n=8), AAV8-U6-gD2R-hSyn-NLSmCherry (n=8), or AAV8-U6-gLacZ-hSyn-NLSmCherry control (n=9). Two-way repeated measures ANOVA revealed main effects of drug ($F_{1,22}$=91.27, *P*=0.0157) and viral treatment ($F_{2,22}$=4.173, *P*=0.0291), and an interaction between drug and viral treatment ($F_{2,22}$=5.050, *P*=0.0157). Symbols: **,***P<0.01 and 0.001, respectively.

(E) Distance traveled for male subjects prior to and after cocaine injection (denoted by arrow), evaluated in 5-min bins. Two-way repeated measures ANOVA revealed a main effect of bin ($F_{3.131, 68.88}$=21.10, *P*<0.0001) and viral treatment ($F_{2, 22}$=4.747, *P*=0.0193), and an interaction between bin and viral treatment ($F_{24, 264}$=4.743, *P*<0.0001). Symbols: *,**,*** - *P*<0.05, 0.01, and 0.001, respectively (gD2R vs. LacZ); $^{\#}$, $^{\#\#}$ - *P*<0.05 and 0.01, respectively (gGBR1 vs. LacZ).

(F) Thigmotaxis index for male subjects following saline or cocaine injection. Two-way repeated measures ANOVA revealed a main effect of drug ($F_{1,22}$=21.75, *P*=0.0001), but no main effect of viral treatment ($F_{2,22}$=1.534, *P*=0.2380) or interaction between drug and viral treatment ($F_{2,22}$=0.9989, *P*=0.3844). Symbol: $^{+++}$*P*<0.001 (main effect of drug).

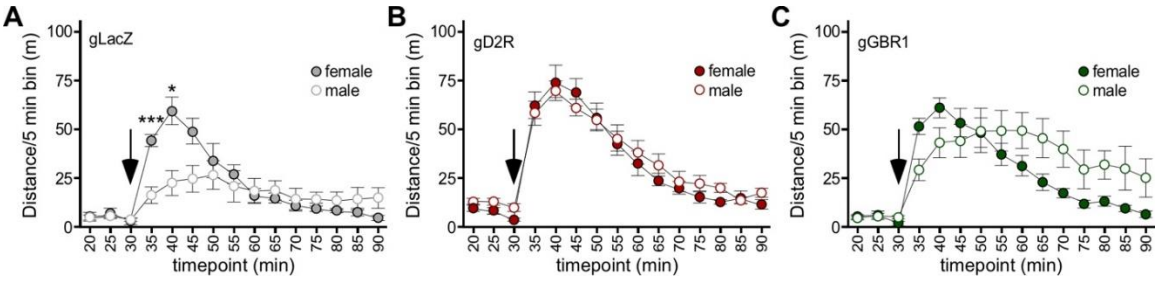

Extended Data (**Figure 2.4)** shows comparisons of male and female subjects for distance traveled following cocaine administration, within viral treatment groups.

Figure 2.4. Sex differences in the temporal profile of cocaine-induced motor activity

(A) Distance traveled for male and female AAV8-U6-gLacZ-hSyn-NLSmCherry control-treated subjects prior to and after cocaine injection (denoted by arrow), evaluated in 5-min bins. Two-way repeated measures ANOVA revealed no main effect of sex ($F_{1,15}$=0.9539, *P*=0.3442) but there was a main effect of bin ($F_{2.812,42.17}$=21.50, *P*<0.0001) and an interaction between bin and sex ($F_{12,180}$=9.073, *P*<0.0001). *,*** *P*<0.05 and 0.001, respectively, vs. male. Symbols: *, *** - *P*<0.05 and 0.001, respectively.

(B) Distance traveled for male and female AAV8-U6-gD2R-hSyn-NLSmCherry-treated male and female subjects prior to and after cocaine injection (denoted by arrow), evaluated in 5-min bins. Two-way repeated measures ANOVA revealed a main effect of bin ($F_{3.058,45.88}$=48.48, *P*<0.0001), but no main effect of sex ($F_{1,15}$=0.3164, *P*=0.5821) or interaction between bin and sex ($F_{12,180}$=0.6755, *P*=0.7735).

(C) Distance traveled for male and female AAV8-U6-gGBR1-hSyn-NLSmCherry treated subjects prior to and after cocaine injection (denoted by arrow), evaluated in 5-min bins. Two-way repeated measures ANOVA revealed no main effect of sex ($F_{1,15}$=1.159, *P*=0.2987), but a main effect of bin ($F_{3.059,45.88}$=21.96, *P*<0.0001) and an interaction between bin and sex ($F_{12,180}$=6.077, *P*<0.0001). Pairwise comparisons, however, revealed no significant differences between male and female subjects at any timepoint.

2.5.4 Impact of D_2R and $GABA_BR$ in VTA DA neurons on baseline and morphine-induced activity

As we previously reported that the loss of GIRK channel activity in DA neurons in mice correlated with enhance motor stimulation in response to systemic administration of 10 mg/Kg morphine (Kotecki et al., 2015), we next compared the relative contribution of D_2R and $GABA_BR$ to this morphine-induced behavior. In female subjects, we observed a main effect of drug on motor activity, but no main effect of viral treatment or interaction between drug and viral treatment. Notably, no significant impact of D_2R or $GABA_BR$ ablation on morphine-induced activity was observed in females (**Fig. 2.5A, right**). Although D_2R ablation correlated with elevated activity levels at all time points following morphine injection, activity levels were not significantly different from controls (**Fig. 2.5B**). Consistent with prior reports (Mickley, Mulvihill, & Postler, 1990), we observed a marked increase in thigmotaxis in all subjects after morphine injection, but there was no difference between viral treatment groups (**Fig. 2.5C**).

In males, we also observed a main effect of drug, but no main effect of viral treatment or interaction between drug and viral treatment. As was the case in females, loss of either D_2R or $GABA_BR$ in males had no significant impact on morphine-induced activity during the 60-min interval (**Fig. 2.5D, right**) or on the temporal activity profile following morphine injection (**Fig. 2.5E**). We also observed a similar increase in thigmotaxis after injection of morphine as seen in females, with no difference between viral treatment groups (**Fig. 2.5F**). Thus, neither D_2R nor $GABA_BR$ ablation in VTA DA neurons exerts a significant impact on morphine-induced motor activity in mice.

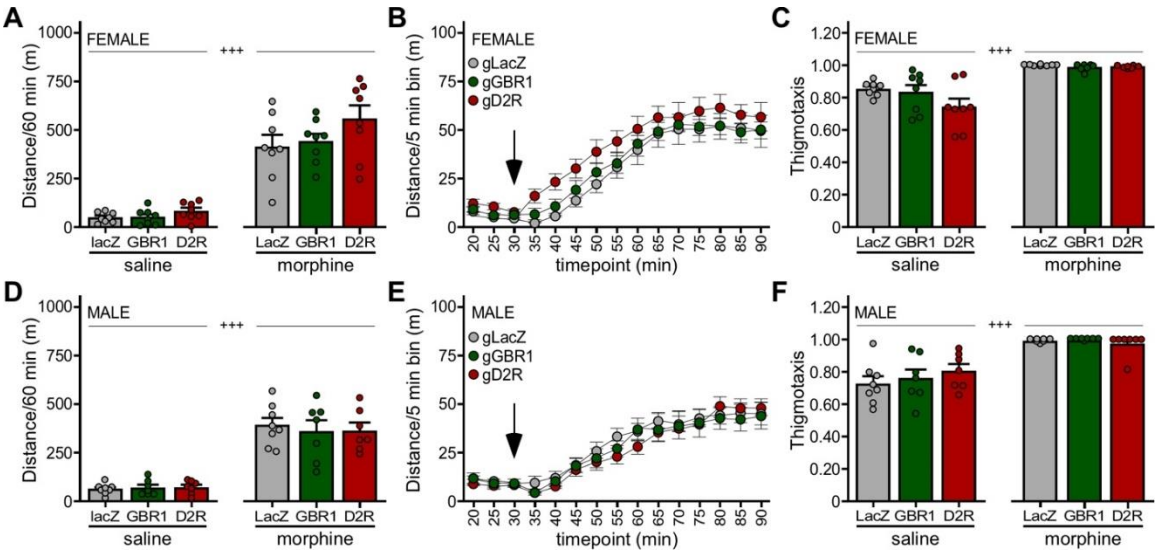

Figure 2.5. Impact of $GABA_BR$ and D_2R ablation on the motor-stimulatory effect of morphine

(A) Total distance traveled during the 60-min period after injection of saline (left) or morphine (10 mg/Kg IP, right) in female DATCre(+):Cas9GFP(+) mice treated with AAV8-U6-gGBR1-hSyn-NLSmCherry (n=8), AAV8-U6-gD2R-hSyn-NLSmCherry (n=8), or AAV8-U6-gLacZ-hSyn-NLSmCherry control (n=8). Two-way repeated measures ANOVA revealed a main effect of drug ($F_{1,21}$=185.3, *P*<0.0001), but no main effect of viral treatment ($F_{2,21}$=2.145, *P*=0.1420) or interaction between drug and viral treatment ($F_{2,21}$=1.183, *P*=0.3260). Symbol: ^{+++}P<0.001 (main effect of drug).

(B) Distance traveled for female subjects prior to and after morphine injection (denoted by arrow), evaluated in 5-min bins. Two-way repeated measures ANOVA revealed a main effect of bin ($F_{3.057,67.26}$=97.73, *P*<0.0001), but no effect of viral treatment ($F_{2,22}$=1.920, *P*=0.1704) or interaction between bin and viral treatment ($F_{24,264}$=0.5380, *P*=0.9640).

(C) Thigmotaxis index for female subjects following saline or morphine injection. Two-way repeated measures ANOVA revealed a main effect of drug ($F_{1,21}$=59.23, *P*<0.0001), but no significant difference with viral treatment ($F_{2,21}$=2.462, *P*=0.1095), and no interaction between drug and viral treatment ($F_{2,21}$=1.995, *P*=0.1609). Symbol: ^{+++}P<0.001 (main effect of drug).

(D) Total distance traveled during the 60 min period after injection of saline (left) or morphine (10 mg/Kg IP, right) in male DATCre(+):Cas9GFP(+) mice treated with AAV8-U6-gGBR1-hSyn-NLSmCherry (n=7), AAV8-U6-gD2R-hSyn-NLSmCherry (n=7), or AAV8-U6-gLacZ-hSyn-NLSmCherry control (n=8). Two-way repeated measures ANOVA revealed main effects of drug ($F_{1,19}$=176.1, *P*<0.0001), but no main effect of viral treatment ($F_{2,19}$=0.05804, *P*=0.9438) or interaction between drug and viral treatment ($F_{2,19}$=0.3193, *P*=0.7305). Symbol: ^{+++}P<0.001 (main effect of drug).

(E) Distance traveled for male subjects prior to and after morphine injection (denoted by arrow), evaluated in 5-min bins. Two-way repeated measures ANOVA revealed a main effect of bin ($F_{2.264,43.02}$=80.68, *P*<0.0001), but no main effect of viral treatment

($F_{2,19}$=0.1417, *P*=0.8688) or interaction between drug and viral treatment ($F_{24,228}$=0.9227, *P*=0.5711).

(F) Thigmotaxis index for male subjects following saline or morphine injection. Two-way repeated measures ANOVA revealed a main effect of drug ($F_{1,19}$=68.91, *P*<0.0001), but no significant difference with viral treatment ($F_{2,19}$=0.3907, *P*=0.6819), and no interaction between drug and viral treatment ($F_{2,19}$=1.195, *P*=0.3244). Symbol: ^{+++}P<0.001 (main effect of drug).

2.6 Discussion

Here, we utilized a neuron-specific viral CRISPR/Cas9 approach to compare the impact of D_2R or $GABA_BR$ ablation in VTA DA neurons on baseline activity and behavioral sensitivity to cocaine and morphine. Loss of $GABA_BR$ or D_2R in VTA DA neurons had no significant impact on baseline activity, paralleling the lack of effect of these manipulations on excitability and other electrophysiological properties of VTA DA neurons. These behavioral findings are consistent with studies involving genetic suppression or ablation of D_2R or $GABA_BR$ in the rodent VTA (De Jong et al., 2015; Edwards et al., 2017). Thus, D_2R and $GABA_BR$-dependent signaling pathways in VTA DA neurons exert minimal influence on baseline DA neuron excitability. Notably, mice lacking D_2R in DA neurons displayed hyperlocomotion (Bello et al., 2011), indicating that D_2R-dependent signaling in DA neuron populations outside of the VTA may regulate baseline motor activity.

D_2R ablation in VTA DA neurons potentiated cocaine-induced activity in male and female mice, consistent with studies involving DA neuron-specific ablation of D_2R in mice (Bello et al., 2011), and an RNAi-based approach targeting D_2R in the rat VTA (De Jong et al., 2015). $GABA_BR$ ablation also potentiated cocaine-induced activity, but the influence of this signaling pathway was restricted to males. Enhanced D_2R-dependent signaling in VTA DA neurons from female mice may compensate for the loss of $GABA_BR$-signaling, explaining the weak influence of $GABA_BR$ on cocaine-induced activity in females. Alternatively, there may be reduced GABAergic feedback to VTA DA neurons in females, rendering the loss of $GABA_BR$ less effective (Zachry et al., 2021).

Behavioral sensitivity to morphine was unaffected by the loss of D_2R and/or $GABA_BR$ in VTA DA neurons, consistent with previous reports (Edwards et al., 2017; Maldonado et al., 1997; Steketee & Kalivas, 1991). The lack of impact of D_2R ablation in VTA DA neurons is surprising given that opioids, like cocaine, increase VTA DA levels (V

I Chefer, Denoroy, Zapata, & Shippenberg, 2009). Cocaine and opioids differ, however, in their influence on VTA DA neurons. While cocaine hyperpolarizes VTA DA neurons in a D_2R-dependent manner (Beckstead et al., 2004), opioids increase VTA DA neuron firing by suppressing GABAergic input from local GABA neurons and/or RMTg GABA neurons (Jalabert et al., 2011; Jhou et al., 2009; Johnson & North, 1992), as well as disinhibiting glutamatergic input to VTA DA neurons (Yang et al., 2020). Thus, any inhibitory influence of somatodendritic D_2R activation triggered by the opioid-induced rise in VTA DA is likely offset by the excitatory influence of disinhibition.

Since morphine increases NAc DA levels (Vladimir I. Chefer, Kieffer, & Shippenberg, 2003; Spielewoy et al., 2000; Vander Weele et al., 2014), and DA neurotransmission in the NAc drives $GABA_B$R-dependent feedback to VTA DA neurons (Edwards et al., 2017), it is also surprising that $GABA_B$R ablation does not impact behavioral sensitivity to morphine. This outcome might reflect differences in the amplitude of the DA increase evoked by cocaine and morphine. Indeed, NAc DA levels in freely moving rats increased more in response to intravenous cocaine than morphine (Pontieri et al., 1995). The spatio-temporal pattern of DA increases in the NAc may also differ for cocaine and morphine. Consistent with this premise, cocaine elicited a more pronounced increase in DA in the NAc shell as compared to core (B. J. Aragona et al., 2008; Brandon J Aragona et al., 2009), whereas morphine evoked similar DA increases in NAc core and shell (Vander Weele et al., 2014). Moreover, the morphine-induced increase in NAc DA was relatively transient, a phenomenon potentially linked to a simultaneous increase in NAc GABA levels evoked by morphine (Vander Weele et al., 2014).

The differential apparent engagement of $GABA_B$R- and D_2R-dependent signaling pathways by cocaine and morphine may also reflect differential molecular target location. Morphine can act on opioid receptors in other brain regions to regulate motor activity,

bypassing VTA DA neurons. For example, locomotor activity decreased initially following intra-NAc injection of morphine in rats (Costall, Fortune, & Naylor, 1978). In addition, NAc lesions failed to eliminate morphine-induced motor activation, suggesting a potential role of other brain regions in this effect (Stevens, Mickley, & McDermott, 1986). Also, intra-NAc infusion of morphine abolished the motor stimulatory effect of intra-NAc DA, showing that opioid and dopaminergic pathways in the NAc exert competing influence on locomotion (Layer, Uretsky, & Wallace, 1991).

The direct inhibitory influence of $GABA_BR$ and D_2R activation on VTA DA neurons is mediated primarily by activation of GIRK channels (Ackerman, Johansen, Clark, & White, 1993; Beckstead et al., 2004; Brodie & Dunwiddie, 1990; E. B. Bunney, Appel, & Brodie, 2001; N. N. H. Chen & Pan, 2000; Cruz et al., 2004; Christopher P Ford, 2014; Mercuri et al., 1997), though other effectors are modulated as well (Philippart & Khaliq, 2018; Su et al., 2019). Genetic ablation of Girk2 globally or selectively in DA neurons correlated with increased motor-stimulatory effect of cocaine (Kotecki et al., 2015; McCall et al., 2017; McCall, Marron Fernandez De Velasco, & Wickman, 2019; Pravetoni & Wickman, 2008) and morphine (Kotecki et al., 2015). The contribution of GIRK channels to cocaine-induced activity was further localized to VTA DA neurons (McCall et al., 2019). Given that GIRK channels mediate the D_2R- and $GABA_BR$-dependent inhibition of VTA DA neurons and that DA neuron-specific loss of GIRK channels enhances the motor-stimulatory effect of cocaine and morphine, the lack of impact of D_2R or $GABA_BR$ ablation on morphine-induced activity was unexpected. It is possible that $GABA_BR$- and D_2R-dependent signaling pathways are functionally redundant and that both need to be eliminated to see an influence on morphine-induced activity. GIRK channels in non-VTA DA neurons, perhaps in the adjacent substantia nigra pars compacta (Koyrakh et al., 2005), may also explain the impact of GIRK channel ablation on morphine.

Females are more susceptible to various facets of addiction (Anker & Carroll, 2011; Becker & Koob, 2016; Fattore, Altea, & Fratta, 2008), fueling interest in identifying relevant sex differences at molecular and cellular levels. Here, we found multiple sex differences related to inhibitory G protein signaling in VTA DA neurons. Loss of $GABA_BR$, for example, had minimal impact on behavioral sensitivity to cocaine in females, but significantly enhanced the motor-stimulatory effect of cocaine in males. D_2R-dependent somatodendritic inhibitory currents were also larger in VTA DA neurons from females. This difference could reflect elevated D_2R expression and/or function in VTA DA neurons from females and is predicted to decrease cocaine sensitivity. Indeed, females exhibit elevated D_2R-dependent signaling at baseline as compared to males (Walker et al., 2006; Zachry et al., 2021).

Cocaine-induced activity was characterized by a more rapid and sharp peak in females as compared to males, which could be explained by a tighter regulation of synaptic dopamine by DAT in females compared to males (Zachry et al., 2021). D_2R ablation in VTA DA neurons in male mice yielded a temporal profile comparable to that seen in female mice. While this suggests that D_2R-dependent signaling in VTA DA neurons is critical in tempering the early behavioral response to cocaine, the shift in the temporal profile observed in males is somewhat counterintuitive given that somatodendritic D_2R-dependent signaling is weaker in VTA DA neurons from males. This apparent discrepancy is perhaps explained by sex differences in the influence of presynaptic/terminal D_2R (which should also be eliminated by the CRISPR/Cas9 ablation approach) on DA dynamics in the NAc. Presynaptic D_2R-dependent signaling in VTA DA neurons in males may be stronger than that seen in females. Alternatively, while D_2R-dependent somatodendritic response amplitudes are larger in VTA DA neurons from

female mice, VTA DA neurons in males may be more sensitive to D_2R-dependent inhibition.

While D_2R- and $GABA_B$R-dependent signaling pathways in the VTA can suppress behavioral sensitivity to cocaine, psychostimulant exposure can weaken these inhibitory feedback pathways. For example, a transient decrease in D_2R influence on VTA DA neuron firing has been reported after repeated cocaine treatment or self-administration (Ackerman & White, 1990; Henry, Greene, & White, 1989). This adaptation, and corresponding potentiation of cocaine-induced motor activity, was reproduced by repeated quinpirole treatment (Henry, Hu, & White, 1998). Cocaine self-administration in rats also increased firing rate and burst activity of midbrain DA neurons, paralleled by decreased ability of quinpirole to inhibit DA neuron firing rate (Marinelli, Cooper, Baker, & White, 2003). Self-administration of amphetamine in rats reduced the ability of D_2R to suppress evoked DA release in the NAc, an effect mediated in part by an RGS2-dependent disruption of $D_{2/3}R/G\alpha_{i2}$ functional coupling (Calipari et al., 2014; Sun, Calipari, Beveridge, Jones, & Chen, 2015). Repeated cocaine in male rats also decreased $GABA_B$R/G protein coupling (Kushner & Unterwald, 2001). Finally, cocaine suppressed $GABA_B$R-dependent somatodendritic signaling in putative VTA DA neurons (Arora et al., 2011), and methamphetamine self-administration suppressed D_2R and $GABA_B$R-dependent somatodendritic responses in VTA DA neurons (Sharpe, Varela, Bettinger, & Beckstead, 2015).

Notably, D_2R activation appears critical for many of these forms of plasticity, which likely contribute to the hyperexcitability of meso-accumbens DA pathway following psychostimulant exposure (Francis, Gantz, Moussawi, & Bonci, 2019; Henry et al., 1998). The reciprocal relationship between psychostimulants and inhibitory G protein-dependent feedback pathways in VTA DA neurons may be dependent on age and/or species, or

methodological variables. Indeed, repeated methamphetamine injections correlated with enhanced D_2R-dependent hyperpolarization in young (8-10 d) rats (Amano, Matsubayashi, Seki, Sasa, & Sakai, 2003). In mice, repeated methamphetamine injections suppressed somatodendritic $GABA_B$R-dependent (but not D_2R-dependent) signaling in VTA DA neurons, but only when methamphetamine was given in novel environment (Munoz et al., 2016).

Our work highlights innate signaling mechanisms that regulate behavioral sensitivity to cocaine. Knowledge of the molecular players and neuron populations regulating behavioral sensitivity to cocaine and other drugs of abuse may help in identifying individuals at risk for developing addiction. Further investigation of mechanisms regulating the strength and sensitivity of inhibitory G protein signaling pathways in VTA DA neurons may suggest opportunities for selective therapeutic interventions tailored to specific drugs of abuse.

2.7 Acknowledgements

The authors would like to thank Hannah Oberle, Mehrsa Zahiremami, and Courtney Wright for exceptional care of the mouse colony, and the Genome Engineering and iPSC Center of Washington University for designing and validating gRNA sequences used in this study.

2.8 Funding and Disclosures

This work was supported by NIH grants to KW (DA034696, AA027544), MD (DA007234), NMM (DA041767), AML (AA026598), and the University of Minnesota Viral Vector and Cloning Core (DA048742). The authors declare no competing interests.

Chapter 3 : RGS6 regulation of inhibitory G protein signaling in ventral tegmental area dopamine neurons and binge alcohol consumption

Chapter 3 contains work to be submitted for publication. "RGS6 regulation of inhibitory G protein signaling in ventral tegmental area dopamine neurons and binge alcohol consumption." ***Margot C DeBaker****, Eric H Mitten, Timothy R Rose, Ezequiel Marron Fernandez de Velasco, Runbo Gao, Anna M Lee and Kevin Wickman.*

Author Contributions: KW, EMFdV, and MCD designed the project, planned experiments, and coordinated the work. EHM performed surgeries, electrophysiology, and analysis of optogenetic studies assessing $GABA_BR$-dependent current kinetics. TRR prepared and processed tissue for fluorescent *in situ* hybridization studies. RG wrote the code used to analyze fluorescent *in situ* hybridization studies. MCD performed and analyzed all other experiments. EMFdV also assisted with production of viral vectors associated with the study. AML provided co-mentorship support. MCD and KW wrote the manuscript, and all authors provided reviews.

3.1 Synopsis

Dopamine (DA) neurons in the ventral tegmental area (VTA) are critical for mediating behavioral responses to drugs of abuse, including alcohol. Alcohol increases DA levels in the VTA throughout the mesocorticolimbic system. Increased DA neurotransmission engages negative feedback mechanisms in VTA DA neurons mediated by inhibitory G protein signaling pathways. Inhibitory G protein signaling pathways are subject to modulation by Regulator of G protein Signaling proteins (RGS), which accelerate G protein deactivation. Members of the R7 family of RGS proteins, including RGS6, have been implicated in drug-related behaviors. Here, we show that RGS6 and its cognate partner Gβ5 is expressed in the majority of VTA DA neurons in the adult mouse. As RGS6/Gβ5 complexes selectively regulate signaling mediated by $G\alpha_o$, we assessed the contribution of $G\alpha_o$ to inhibitory G protein signaling in VTA DA neurons. CRISPR/Cas9-mediate ablation of $G\alpha_o$ in VTA DA neurons yielded a significant reduction in somatodendritic currents evoked by activation of D2 DA (D_2R)- and $GABA_B$ ($GABA_BR$) receptors, suggesting that D_2R and $GABA_BR$-dependent signaling pathways may be subject to negative regulation by RGS6. Indeed, VTA DA neurons from *RGS6*$^{-/-}$ mice exhibited larger D_2R-dependent somatodendritic currents, and prolonged deactivation of synaptically evoked $GABA_BR$-dependent currents. Further, selective ablation of RGS6 in VTA DA neurons enhanced D_2R-dependent currents, whereas RGS6 overexpression in these neurons reduced D_2R-dependent currents. *RGS6*$^{-/-}$ mice show lower binge alcohol consumption than wild-type counterparts, a phenotype recapitulated in female (but not male) mice lacking RGS6 in VTA DA neurons. Thus, RGS6 in VTA DA neurons exerts receptor- and sex-dependent influence on inhibitory G protein signaling and voluntary alcohol consumption in adult mice.

3.2 Introduction

The mesocorticolimbic system mediates responses to natural rewards, as well as to drugs of abuse and associated cues (Hearing et al., 2012; Wise & Rompre, 1989). This system includes the ventral tegmental area (VTA), which projects to limbic (*e.g.*, nucleus accumbens, amygdala, hippocampus) and cortical (*e.g.*, prefrontal cortex, orbitofrontal cortex, cingulate) regions that subserve different aspects of reward processing (Hikosaka et al., 2008; Kalivas & Volkow, 2005; Koob & Nestler, 1997). The VTA harbors neurons that release dopamine (DA), GABA, glutamate, or combinations of neurotransmitters (Morales & Margolis, 2017). Drugs of abuse share an ability to enhance DA neurotransmission in the mesocorticolimbic system, via engagement with various molecular and cellular targets (Uhl et al., 2019; Nora D. Volkow et al., 2011). Alterations in VTA DA transmission have been linked to a variety of neuropsychological diseases and disorders such as addiction, depression, schizophrenia, and Parkinson's Disease (Kalivas & Volkow, 2005; Wise & Rompre, 1989).

VTA DA neurotransmission is negatively regulated by inhibitory G protein signaling pathways (Hearing et al., 2012; Marron Fernandez de Velasco, McCall, & Wickman, 2015; Steketee, Striplin, Murray, & Kalivas, 1992), including pathways controlled by D_2 dopamine (D_2R) and $GABA_B$ ($GABA_BR$) receptors (Erhardt et al., 2002; Christopher P Ford, 2014; Mercuri et al., 1997). Activation of these signaling pathways in VTA DA neurons limits acute behavioral responses to drugs of abuse (Liu et al., 2020; Solecki et al., 2020; Valyear et al., 2020). Moreover, in vivo exposure to psychostimulants can transiently suppress these inhibitory G protein signaling pathways, suggesting that plasticity of inhibitory G protein signaling in VTA DA neurons contributes to some of the physiological and behavioral consequences associated with drug experience (Arora et al., 2011; Munoz et al., 2016).

D_2R and $GABA_BR$-dependent signaling is mediated by the inhibitory ($G\alpha_{i/o}$) subclass of heterotrimeric G proteins (Steketee et al., 1992). The kinetics of G protein signaling are controlled largely by the GTPase activity of $G\alpha$, which hydrolyzes GTP to GDP, allowing the inactive heterotrimeric G protein complex to re-form (Gold et al., 1997). Regulator of G protein Signaling (RGS) proteins exert catalytic influence on this process, enhancing the GTPase activity of $G\alpha$ subunits and, consequently, accelerating the termination of G protein-dependent signaling (Lomazzi et al., 2008). At least 30 different subtypes of RGS proteins have been characterized and they can be grouped into subfamilies based on structural and/or functional distinctions (G. R. Anderson et al., 2009; Gold et al., 1997). The R7 subfamily of RGS proteins, which exhibits a strong substrate preference for $G\alpha_o$ G proteins (Hooks et al., 2003; Masuho et al., 2020), negatively regulates inhibitory G protein signaling pathways in multiple neuron populations (G. R. Anderson et al., 2010; Z. Rahman et al., 2003; Stewart et al., 2015; Zachariou et al., 2003), as well as the heart (A. Anderson et al., 2020; Wydeven, Posokhova, Xia, Martemyanov, & Wickman, 2014). The R7 RGS sub-family consists of 4 members (RGS6, RGS7, RGS9, RGS11), each containing an RGS catalytic domain and a module analogous to the G protein Gγ subunit (G-gamma-like or GGL domain) (Woodard et al., 2015). The GGL domain promotes stable association with the atypical member of the G protein $G\beta$ family ($G\beta5$), and this interaction is critical to the stability and function of R7 RGS proteins (G. R. Anderson et al., 2009; C. K. Chen et al., 2003).

RGS6 has been implicated in inhibitory G protein-dependent signaling involving $GABA_BR$, 5-hydroxytryptamine 1A receptor ($5HT_{1A}R$), and the mu opioid receptor (MOR) in multiple brain regions (Garzón, López-Fando, & Sánchez-Blázquez, 2003; Maity et al., 2012; Stewart et al., 2014). Interestingly, constitutive *RGS6*$^{-/-}$ mice exhibit decreased alcohol consumption and reward, phenotypes partially restored by systemic administration

of $GABA_BR$ or D_2R antagonists. While the anatomic and cellular basis for the influence of RGS6 on alcohol consumption is unclear, voluntary alcohol consumption increased RGS6 expression in the VTA (Stewart et al., 2015). Moreover, RGS6 expressed in midbrain DA neurons, including DA neurons in the VTA, has been documented in both newborn and adult mice (Bifsha, Yang, Fisher, & Drouin, 2014; Stewart et al., 2015). At present, the anatomic and cellular basis underpinning the influence of RGS6 in alcohol consumption is unknown, and the functional and behavioral relevance of RGS6 in VTA DA neurons is unclear. The goal of this study was to address whether inhibitory G protein-dependent signaling pathways in VTA DA neurons are negatively regulated by RGS6, and whether this regulatory mode impacts voluntary alcohol consumption. Our findings reveal that RGS6 modulates the dynamics of $GABA_BR$- and D_2R-dependent signaling in VTA DA neurons, in discrete GPCR-dependent fashion, and that loss of this regulatory influence in VTA DA neurons suppresses binge alcohol consumption in female but not male mice.

3.3 Materials and Methods

3.3.1 Animals.

All studies were approved by the Institutional Animal Care and Use Committee at the University of Minnesota. The generation of *RGS6*$^{-/-}$ mice was described previously (Posokhova, Wydeven, Allen, Wickman, & Martemyanov, 2010). C57BL/6J mice, bred on site or purchased from The Jackson Laboratory, were used as wild-type (WT) controls for studies when noted; all other mice were bred in-house. B6.SJL-*Slc6a3*$^{tm1.1(cre)Bkmn}$/J mice (stock #006660, The Jackson Laboratory; Bar Harbor, ME), hereafter referred to as DATCre(+) mice, were used in viral overexpression electrophysiological assessments. DATCre(+) mice were also crossed with a Cre-dependent Cas9GFP knock-in line (B6;129-Gt(ROSA)26Sor$^{tm1(CAG-cas9*,-EGFP)Fezh}$/J, The Jackson Laboratory, stock #026179),

to generate DATCre(+) subjects homozygous for the Cas9GFP(+) mutation; these mice are referred to throughout as DATCre(+):Cas9GFP(+) mice and were used in all CRISPR/Cas9 ablation studies (DeBaker, Marron Fernandez de Velasco, McCall, Lee, & Wickman, 2021). All mice were group-housed until the start of behavioral experiments, after which they were individually housed to monitor drinking. Mice were maintained on a 14:10 h light/dark cycle and were provided *ad libitum* access to food and water.

3.3.2 Reagents & Viral Vectors

Baclofen, quinpirole, sulpiride, kynurenic acid, and picrotoxin were purchased from Sigma (St. Louis, MO), and CGP54626 was purchased from Tocris (Bristol, UK). Adeno-associated viruses (AAVs) used in this study were packaged in AAV8 serotype unless noted; the University of Minnesota Viral Vector and Cloning Core provided all but one vector used in this study, at titers ranging from 0.7-4 x 10^{13} genocopies/mL. AAV9-CaMKIIa-hChR2(H134R)-mCherry was a gift from Karl Deisseroth (Addgene viral prep # 26975-AAV9), for use in ex vivo optogenetic experiments. Packaging plasmids (pRC8 and pHelper) were obtained from the University of Pennsylvania Vector Core. For CRISPR/Cas9 experiments, the pAAV-U6-gRNA-hSyn-NLSmCherry was generated using the backbone of the plasmid pAAV-U6-gRNA-hSyn-Cre-2A-EGFP-KASH (Platt et al., 2014) (Addgene plasmid #60231) that was a gift from Dr. Feng Zhang. Guide RNA (gRNA) sequences targeting RGS6, $G\alpha_o$, and LacZ were as follows: RGS6 – TGTAGCCCTGGGCGGCAATA, $G\alpha_o$ – GTCGCCCCAGAGTCGCATCA, LacZ – TGCGAATACGCCCACGCGAT. For RGS6 overexpression experiments, AAV8-hSyn-DIO-RGS6-IRES-GFP was used to overexpress RGS6 in a Cre-dependent manner, and AAV8-hSyn-DIO-hSyn-GFP served as control.

3.3.3 Fluorescent in situ hybridization.

To examine expression of RGS6 in the VTA, adult male and female WT mice were sacrificed and brains were removed, snap frozen in isopentane, and sectioned by cryostat (16 μm). Sections were adhered to Superfrost® Plus slides, kept at −20 C for 60 min to dry, and stored at −80 C until use. Sections were fixed with 4% paraformaldehyde for 1 h and processed for multichannel fluorescent *in situ* hybridization (RNAScope) according to manufacturer instructions (Advanced Cell Diagnostics/ACD; Newark, CA). Sections were counterstained with DAPI for 20 s at room temperature, cover-slipped with Prolong Gold Antifade (ThermoFisher Scientific), and stored at 4 C. Probes for detection of specific targets (DAT, Gβ5, and RGS6) were purchased from ACD, and fluorescent Opal dyes (Opal 520, 620, 690) for detection of specific probes were purchased from Akoya Biosciences (Marlborough, MA). Sections containing the VTA were imaged on a Keyence BZ-X810 epifluorescent microscope at 20x magnification (Keyence; Itasca, IL). Images for each channel were obtained from multiple focus planes and stitched using Keyence BZ-X800 analysis software; all images were acquired and processed in the same manner. Multichannel images, including DAPI, were overlaid.

3-4 mice per group per sex were analyzed, with 2-4 images analyzed independently from each mouse. For each image, the region of interest (ROI) was selected using the Computer Vision Toolbox in MATLAB (MathWorks; Natick, MA). The ROIs for the VTA consisted of a rectangle capturing the medial and lateral VTA. ROI images were exported from MATLAB to CellProfiler (Carpenter et al., 2006; Kamentsky et al., 2011; McQuin et al., 2018; Stirling et al., 2021) (www.cellprofiler.org). Background fluorescence was subtracted, intensity information was removed, and images were converted to grayscale. CellProfiler was used to identify the cell area and the probe puncta within the cell. The background probe expression in areas defined as non-cell was

calculated and compared with probe expression within each defined cell using MATLAB. Cells were considered positive for that probe if the puncta expression was statistically different from background expression using a binomial distribution test with a Bonferroni correction for the number of cells. The percent of cells per ROI that were positive for the target probe(s) was calculated.

3.3.4 Slice electrophysiology.

Electrophysiological properties of VTA DA neurons were evaluated in behaviorally naïve mice (35-93 d). Horizontal slices (225 mm) containing the VTA were prepared in ice-cold sucrose substituted ACSF and allowed to recover at room temperature in ASCF containing (in mM): 125 NaCl, 2.5 KCl, 1.25 NaH_2PO_4, 25 $NaHCO_3$, 11 Glucose, 1 $MgCl_2$, and 2 $CaCl_2$, pH 7.4, for at least 1 h, as described (DeBaker et al., 2021; McCall et al., 2017). Neurons in the lateral VTA were targeted for analysis as this sub-region of the VTA receives prominent $GABA_BR$-dependent feedback (Edwards et al., 2017) and correlates well with traditional DA neuron markers including DAT, I_h and D_2R-dependent inhibition (Arora et al., 2010; Lammel et al., 2014). In studies involving *RGS6*$^{-/-}$ or WT mice, putative dopaminergic neurons were selected based on morphology, size (apparent capacitance >40 pF), I_h current (>80 pA), and spontaneous activity (<5 Hz) (**Table 1**).

Whole-cell data were acquired using a Multiclamp 700A amplifier and pCLAMPv.9.2 software (Molecular Devices, LLC; San Jose, CA), using recording conditions described in previous publications (McCall et al., 2017). Input/membrane resistance (R_M) and apparent capacitance (C_M) were determined using a 5 mV/10 ms voltage-step, with current responses filtered at 5 Hz. Immediately after establishing whole-cell access, I_h conductance was measured using a 200-ms voltage step to -120 mV; the difference in current from beginning to end of the -120-mV step was taken as I_h amplitude. Subsequently, spontaneous activity was measured in current-clamp mode (I=0) for 1 min.

Neurons exhibiting no spontaneous activity were not evaluated. For rheobase assessments, cells were held in current-clamp mode at -80 pA to prevent spontaneous activity, and then given 1-s current pulses, beginning at -100 pA, and progressing in 20 pA increments. Rheobase was defined as the minimum current step that evoked one or more action potentials. Somatodendritic outward currents evoked by an EC_{50} dose of baclofen (10 µM baclofen; (Cruz et al., 2004; Labouèbe et al., 2007)) or quinpirole (60 nM quinpirole; (Bowery, Rothwell, & Seabrook, 1994)) and a saturating concentration of baclofen (200 µM) or quinpirole (20 µM) were measured within the same cell for each drug. Response to the saturating concentration of drug was considered the maximal current amplitude. Changes in agonist sensitivity were assessed using the ratio of EC_{50} dose response divided by the maximal response to the same drug in the same cell times 100% (EC_{50}% of total). Series and input resistances were tracked throughout the experiment. If series resistance was unstable or exceeded 20 MΩ, the experiment was excluded from analysis.

For optogenetic experiments, hChR2(H134R)-mCherry expression was assessed in the NAc, the injection site, prior to recording from VTA containing slices. The superfusion medium contained kynurenic acid (2 mM) and picrotoxin (100 µM) to block responses mediated by glutamate and $GABA_A$ receptors, respectively. Optical stimulation was provided via a 200 µm fiber aimed above the entire slice through a 4x objective. Optically evoked $GABA_BR$-dependent responses were obtained with a 1-s stimulation protocol containing 20 pulses of 473-nm wavelength light (2-5 mW, 3 ms pulse width) as this protocol has been shown to induce $GABA_BR$-dependent inhibitory postsynaptic currents in VTA DA neurons (Edwards et al., 2017). The $GABA_BR$ antagonist CGP54626 (2 µM) was applied to assess the $GABA_BR$-dependence of optically evoked responses. All command potentials factored in a junction potential of -15 mV predicted using JPCalc

software (Molecular Devices, LLC). Separate single-term exponential fits were assigned to the activation and deactivation phases of the optically evoked $GABA_BR$ responses in ClampFit (Molecular Devices, LLC; San Jose, CA).

3.3.5 Intracranial manipulations.

Mice (≥45 d) were placed in a stereotaxic frame (David Kopf Instruments; Tujunga, CA) under isoflurane anesthesia. Microinjectors, made by affixing a 33-gauge stainless steel hypodermic tube within a shorter 26-gauge stainless steel hypodermic tube, were attached to polyethylene-20 tubing affixed to 10 µL Hamilton syringes, and were lowered through burr holes in the skull to the VTA (from bregma: -2.75 mm A/P, ±0.55 mm M/L, -5 mm D/V); 400 nL of virus per side was injected at a rate of 100 nL/min. The optimized coordinates and viral load ensured full coverage of the VTA along anterior/posterior and rostral-caudal axes, with minimal spread into the adjacent substantia nigra pars compacta. For slice electrophysiological experiments utilizing optogenetics, microinjectors were lowered to the NAc (from bregma: +1.7 mm A/P, ± 1.7 M/L, -4.65 mm D/V); 400 nL of virus per side was injected at a rate of 100 nL/min. Microinjectors were left in place for 10 min following infusion to reduce solution backflow along the infusion track. Slice electrophysiology and behavioral experiments were performed 5-6 wk after viral infusion for CRISPR experiments, and 3-4 wk after viral infusion for all others.

3.3.6 Behavior.

Mice (≥53 d) were singly housed before the start of the procedure to facilitate measurement of individual intake. Unsweetened alcohol (ethanol) (Decon Labs, King of Prussia, PA) was mixed with tap water to 20% (v/v) for each experiment. The water bottle was replaced with an alcohol bottle for 2 h on Days 1 to 3, and 4 h on Day 4, beginning 2 h after the start of the dark cycle. Consumption was measured by bottle weights before and after each drinking session, with drippage and evaporation accounted for using control

bottles in an empty cage. Mice had free access to water at all other times. In studies involving intracranial viral manipulations, the scope and accuracy of viral targeting was assessed by fluorescence microscopy after behavioral testing; 225 mm horizontal slices of the midbrain were obtained using a vibratome and images were acquired on a Keyence microscope. Only data from animals with bilateral viral-driven fluorescence, where the majority of fluorescence was confined to VTA (with minimal spread to the adjacent substantia nigra), were included in the final analysis.

3.3.7 Statistical analysis.

Data are presented throughout as the mean±SEM. Statistical analyses were performed using Prism v.9 (GraphPad Software, La Jolla, CA). All studies involved balanced groups of male and female mice, and data were analyzed first for sex effects. If no sex differences were observed, data from male and female subjects were pooled. If any data point fell outside the range of 2 standard deviations from the mean, it was excluded as an outlier. Differences were considered significant if $p < 0.05$.

3.4 Results

3.4.1 VTA DA neurons in adult mice express Gβ5 and RGS6

We used fluorescent *in situ* hybridization to determine if RGS6 is expressed in adult mouse VTA cells expressing the dopamine transporter (DAT), a commonly used DA neuron-specific marker (Bäckman et al., 2006; Morales & Margolis, 2017). As RGS6 and other R7 RGS proteins form stable complexes with Gβ5, we also evaluated the expression of Gβ5 in the VTA. Analysis of sections from adult male and female C57BL/6J mice revealed that RGS6 and Gβ5 were expressed throughout the VTA, in both DAT-positive and DAT-negative cells. Notably, RGS6 and Gβ5 expression was detected in the vast majority (>95%) of DAT-positive cells (**Fig. 3.1A-C**). These data are consistent with prior

reports that RGS6 is expressed in midbrain DA neurons (Bifsha et al., 2014; Stewart et al., 2015) and suggest that RGS6 might regulate inhibitory G protein signaling in VTA DA neurons.

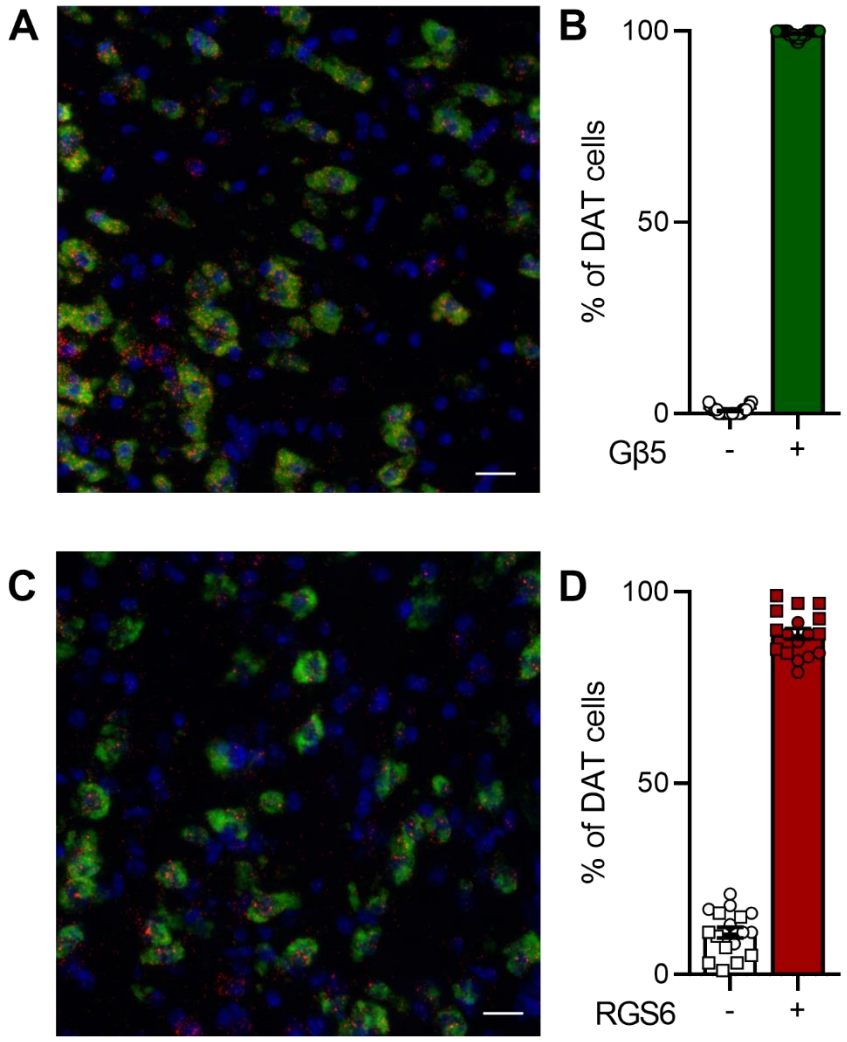

Figure 3.1. Expression of Gβ5 and RGS6 in VTA DA neurons

(A) Example image of fluorescent in situ hybridization used to detect Gβ5 (red) transcript in cells of the VTA that express the dopamine transporter (DAT, green) in WT mice; 20x magnification, scale bar: 20 µm.

(B) Summary of coded analysis of images indicating that 99% of DAT expressing cells also expressed Gβ5.

(C) Example image of fluorescent in situ hybridization used to detect RGS6 (red) transcript in cells of the VTA that express the dopamine transporter (DAT, green) in WT mice; 20x magnification, scale bar: 20 µm.

(D) Summary of coded analysis of images indicating that 95% of DAT expressing cells also expressed RGS6.

3.4.2 Impact of Gαo in VTA DA neurons on GPCR-dependent signaling

R7 RGS/Gβ5 complexes exhibit a strong substrate preference for $G\alpha_o$ over $G\alpha_i$ (A. Anderson et al., 2020; Hooks et al., 2003; Masuho et al., 2020) and as such, are predicted to exert stronger negative regulatory influence on signaling pathways mediated by $G\alpha_o$. Little is known regarding the specific Gα isoforms used by $GABA_BR$ and D_2R to regulate intracellular signaling pathways in neurons. To establish whether the inhibitory influence of $GABA_BR$ and D_2R in VTA DA neurons is mediated by $G\alpha_o$, we employed a VTA DA neuron-specific viral CRISPR/Cas9 ablation approach (**Fig. 3.2A**), as described previously (DeBaker et al., 2021). DATCre(+):Cas9GFP(+) mice received intra-VTA infusions of AAV vectors harboring a $G\alpha_o$-specific or control (LacZ) guide RNA (gRNA). Subsequently (5-6 wk later), we used slice electrophysiological methods to extract baseline neuronal excitability measures (spontaneous activity and rheobase), and to measure D_2R- and $GABA_BR$-dependent somatodendritic currents, in VTA DA neurons (**Fig. 3.2B**).

VTA DA neurons from control or $G\alpha_o$ gRNA-treated mice did not differ in terms of spontaneous activity or rheobase, nor were differences detected in other physiological properties (**Table 3.1**). In VTA DA neurons from mice treated with $G\alpha_o$ gRNA, however, somatodendritic currents evoked by the $D_{2/3}R$ agonist quinpirole were lower than those measured in LacZ control-treated mice (**Fig. 3.2E;** unpaired Welch's t test; $t_{19.61}$=3.010; P=0.0070; n=13-14/group). Similarly, somatodendritic currents evoked by the $GABA_BR$ agonist baclofen were lower in VTA DA neurons from Ga_o gRNA-treated mice (**Fig. 3.2D;** unpaired Welch's t test; $t_{20.22}$=6.845; P<0.0001; n=13-14/group). Thus, $G\alpha_o$ contributes to the somatodendritic inhibitory influence of D_2R and $GABA_BR$ activation on VTA DA neurons.

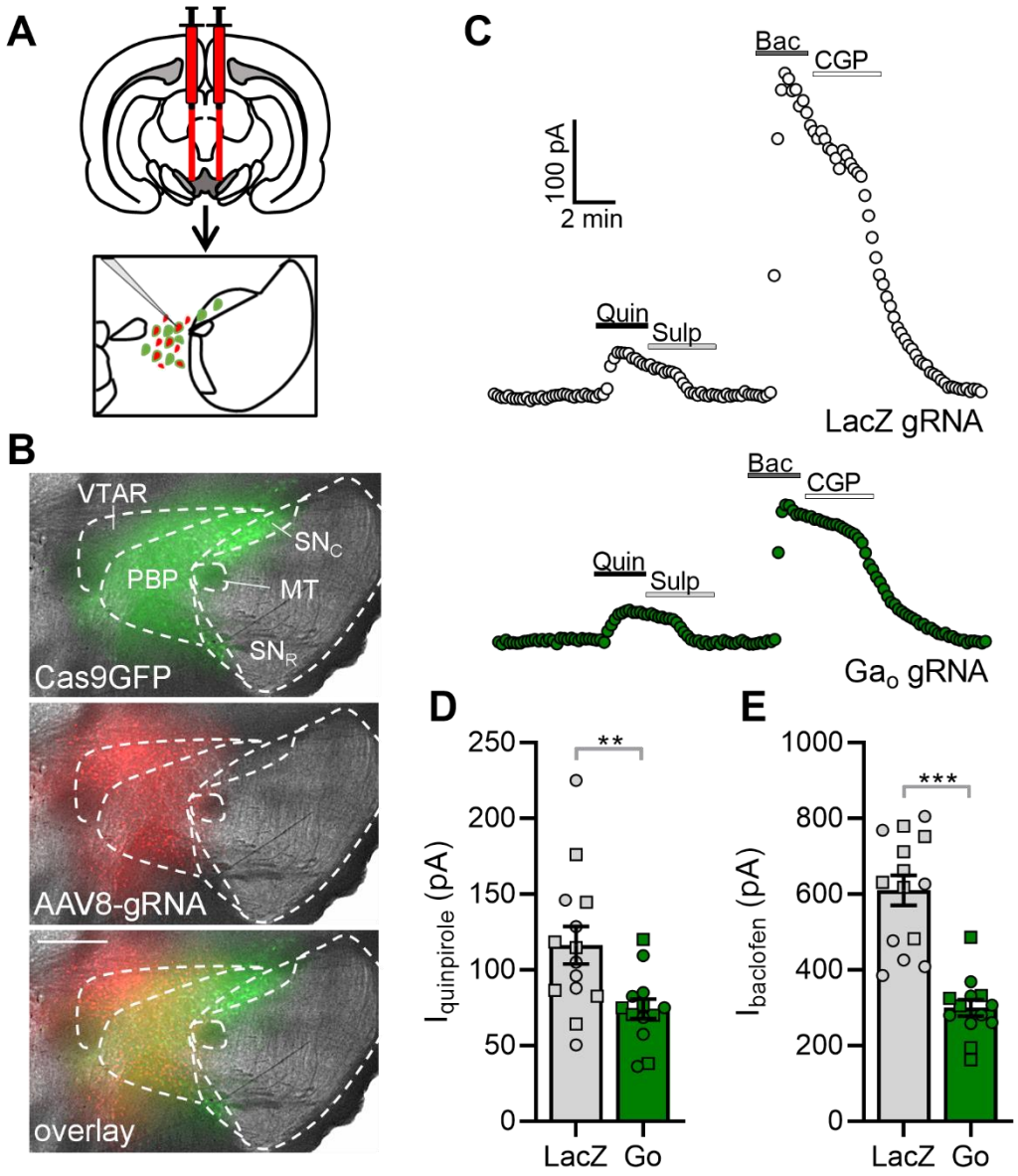

Figure 3.2. G protein isoform dependence of $GABA_BR$ and D_2R

(A) DATCre(+):Cas9GFP(+) mice were treated with intra-VTA AAV8-U6-gRNA-hSyn-NLSmCherry. Following viral injection (5 w), mice were processed for slice electrophysiology.

(B) Example of viral targeting in a DATCre(+):Cas9GFP(+) mouse; GFP fluorescence (green) denotes the Cre-dependent expression of Cas9GFP in midbrain DA neurons of the VTA and substantia nigra, and nucleus-localized mCherry fluorescence (red) highlights the anatomic scope of viral targeting. Abbreviations: MT - medial terminal nucleus of the accessory optic tract, PBP - parabrachial pigmented nucleus of the

VTA, SN_C - substantia nigra pars compacta, SN_R - substantia nigra pars reticulata, VTAR - rostral part of the VTA. Scale bar: 400 µm.

(C) Somatodendritic inhibitory currents (V_{hold} =-60 mV) evoked by sequential bath application of quinpirole (quin, 20 µM) and then baclofen (bac, 200 µM) in VTA DA neurons from DATCre(+):Cas9GFP(+) mice treated with AAV8-U6-gLacZ-hSyn-NLSmCherry control or AAV8-U6-gGa_o-hSyn-NLSmCherry. Currents were reversed by sulpiride (sulp, 5 µM) and CGP54626 (CGP, 2 µM).

(D) Summary of currents evoked by quinpirole (applied first) in VTA DA neurons from DATCre(+):Cas9GFP(+) mice treated with AAV8-U6- gGa_o -hSyn-NLSmCherry or AAV8-U6-gLacZ-hSyn-NLSmCherry control ($t_{19.61}$=3.010; P=0.0070; unpaired Welch's t test; n=13-14/group). Symbol: **P<0.01.

(E) Summary of currents evoked by baclofen, measured after quinpirole/sulpiride application (D), in VTA DA neurons from DATCre(+):Cas9GFP(+) mice treated with AAV8-U6- gGa_o -hSyn-NLSmCherry or AAV8-U6-gLacZ-hSyn-NLSmCherry control ($t_{20.22}$=6.845; P<0.0001; unpaired Welch's t test). Symbol: ***P<0.001.

Treatment	N/n	C_M (pF)	R_M (MΩ)	I_h (pA)	Frequency (Hz)	Rheobase (pA)
LacZ gRNA	7/14	62 ± 2	213 ± 25	316 ± 49	1.6 ± 0.2	-19 ± 4
Ga_o gRNA	7/13	70 ± 4	177 ± 13	382 ± 56	1.6 ± 0.3	-11 ± 4
		$t_{19.6}$=1.781	$t_{19.69}$=1.281	$t_{24.23}$=0.8928	$t_{18.21}$=0.0291	t_{25}=1.26
		P=0.0904	*P*=0.2150	*P*=0.3808	*P*=0.9771	*P*=0.2183
WT	12/24	72 ± 3	200 ± 19	413 ± 38	1.7 ± 0.2	-24 ± 3
$RGS6^{-/-}$	11/25	65 ± 3	216 ± 17	433 ± 52	1.9 ± 0.2	-22 ± 4
		t_{47}=1.850	$t_{45.93}$=0.6398	$t_{43.36}$=0.3178	$t_{45.2}$=0.666	$t_{46.69}$=0.372
		P=0.0707	*P*=0.5258	*P*=0.7522	*P*=0.5091	*P*=0.7115
LacZ gRNA	18/25	65 ± 3	185 ± 12	341 ± 31	1.3 ± 0.2	-12 ± 3
RGS6 gRNA	16/24	67 ± 2	189 ± 18	287 ± 27	1.5 ± 0.2	-18 ± 3
		$t_{46.4}$=0.3164	$t_{44.13}$=0.1817	$t_{46.36}$=1.318	$t_{44.83}$=0.522	$t_{46.98}$=1.50
		P=0.7531	*P*=0.8566	*P*=0.1939	*P*=0.6041	*P*=0.1412
GFP	6/12	63 ± 3	205 ± 23	301 ± 47	1.3 ± 0.2	-15 ± 4
RGS6(GFP)	9/14	61 ± 3	200 ± 15	292 ± 43	1.6 ± 0.2	-17 ± 5
		$t_{23.5}$=0.5474	$t_{19.48}$=0.1824	$t_{23.27}$=0.1300	$t_{23.91}$=1.21	$t_{21.39}$=0.313
		P=0.5893	*P*=0.8572	*P*=0.8977	*P*=0.2393	*P*=0.7573

Table 3.1. Electrophysiological properties of VTA DA neurons.

Data extracted from whole-cell recordings of VTA DA neurons from male and female DATCre(+):Cas9GFP(+) mice treated with intra-VTA control (LacZ), Ga_o, or RGS6 gRNA vectors; WT or constitutive RGS6–/– mice; or DATCre(+) mice treated with intra-VTA control (GFP) or RGS6(GFP) overexpression. Abbreviations: N/n - number of mice and individual experiments, C_M – apparent capacitance, R_M – input/membrane resistance, I_h – hyperpolarization-activated current.

3.4.3 VTA DA neuron D_2R- and $GABA_B$R-dependent signaling in RGS6$^{-/-}$ mice

We next examined the impact of RGS6 ablation on the kinetics and sensitivity of inhibitory G protein-dependent signaling mediated by D_2R and $GABA_B$R in VTA DA neurons, using slices from *RGS6*$^{-/-}$ and control mice. Baseline electrophysiological properties did not differ in VTA DA neurons from *RGS6*$^{-/-}$ and control mice, indicating that RGS6 does not regulate the baseline excitability of VTA DA neurons (**Table 3.1**). D_2R- and $GABA_B$R-dependent somatodendritic currents were measured (**Fig. 3.3B, E**). Consistent with previous studies (DeBaker et al., 2021; McCall et al., 2019), no sex differences were observed in baclofen-induced somatodendritic currents, so the data from male and female subjects were combined. No difference in maximal baclofen-induced current (**Fig. 3.3D**; unpaired Welch's t test; $t_{20.28}$=0.1525; P=0.8803; n=12/group) or sensitivity (**Fig. 3.3C**; unpaired Welch's t test; $t_{21.99}$=0.2519; P=0.8035) was observed in VTA DA neurons from *RGS6*$^{-/-}$ and WT mice. There was also no difference in sensitivity to quinpirole in VTA DA neurons from *RGS6*$^{-/-}$ and WT mice (**Fig. 3.3F**; unpaired Welch's t test; $t_{20.12}$=1.896, P=0.0724; n=11-13/group). Maximal quinpirole-induced currents, in contrast, were larger in VTA DA neurons from *RGS6*$^{-/-}$ mice (**Fig. 3.3G**; 2-way ANOVA; $F_{1,\ 21}$= 8.845, P=0.0072; n=6-7/group). In addition, VTA DA neurons from females exhibited larger maximal quinpirole-induced currents as compared to males of the same genotype ($F_{1,\ 21}$= 5.098, P=0.0347), consistent with previous reports (DeBaker et al., 2021). There was no interaction between sex and genotype ($F_{1,\ 21}$= 0.1029, P=0.7515). Thus, RGS6 regulates the amplitude of D_2R-dependent somatodendritic signaling in VTA DA neurons, but not $GABA_B$R.

As R7 RGS/Gβ5 complexes accelerate the kinetics of $GABA_B$R-dependent signaling in some neurons (Maity et al., 2012; Ostrovskaya et al., 2014), we used an

optogenetic approach to determine whether RGS6 ablation impacts the kinetics of synaptically evoked $GABA_BR$-dependent currents in VTA DA neurons. Synaptic $GABA_BR$-dependent responses were evoked by optogenetic stimulation of GABAergic release from NAc terminals in the VTA (Edwards et al., 2017)(**Fig. 3.3H,I**). While the activation rate of optically evoked $GABA_BR$-dependent responses in VTA DA neurons from *RGS6*$^{-/-}$ mice did not differ from the rate measured in WT controls (**Fig. 3.3J**; unpaired Welch's t test; $t_{22.18}$=1.355, P=0.1890; n=12-13/group), there was an interaction between sex and genotype for deactivation rate. Optically evoked $GABA_BR$-dependent responses were significantly prolonged in VTA DA neurons from *RGS6*$^{-/-}$ mice in slices from male (P=0.0419) and female (P<0.0001) mice (**Fig. 3.3K**). Thus, RGS6 negatively regulates discrete aspects of D_2R- and $GABA_BR$-dependent somatodendritic signaling dynamics in VTA DA neurons.

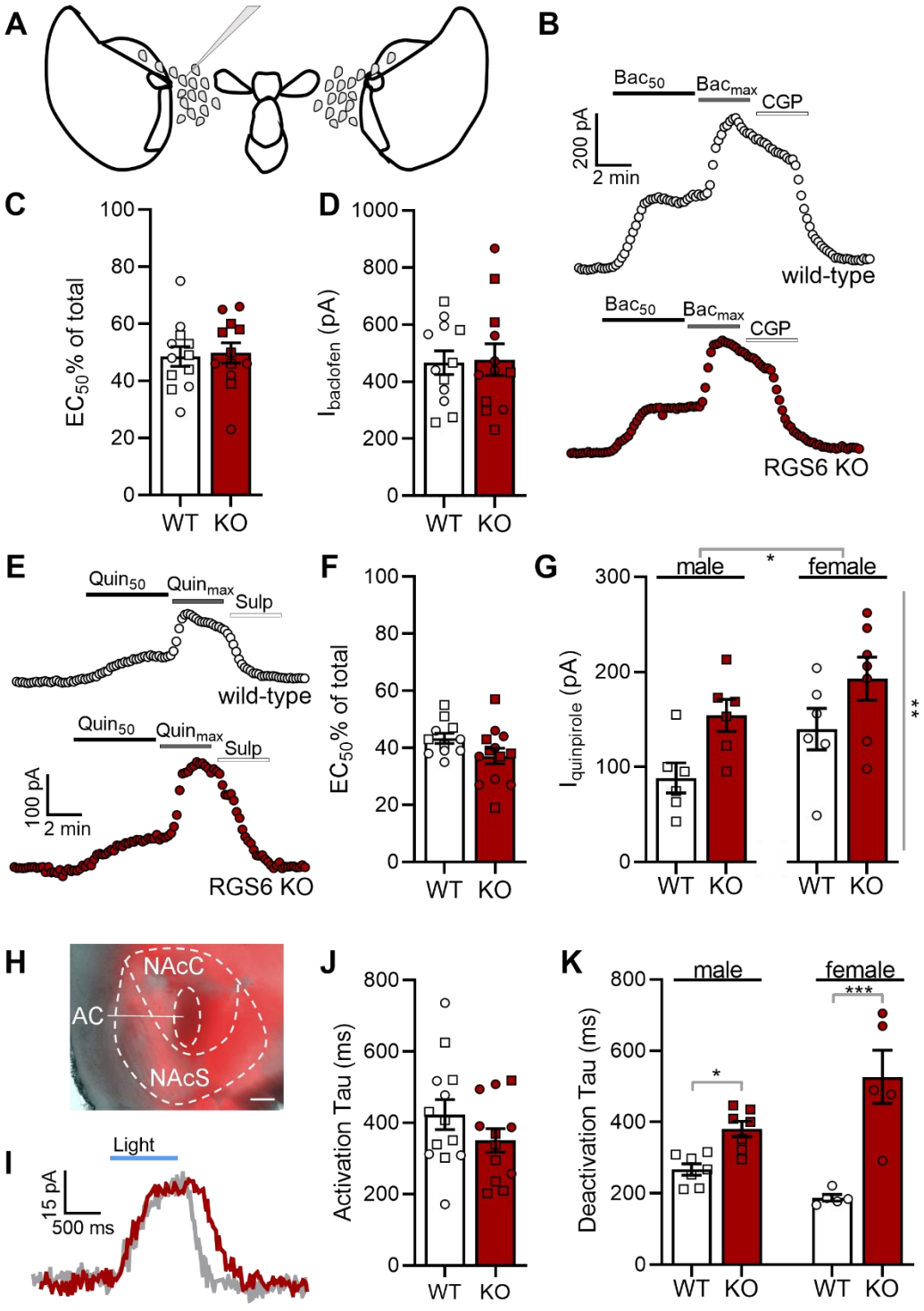

Figure 3.3. Electrophysiological analysis of somatodendritic $GABA_BR$- and D_2R-dependent signaling in VTA DA neurons of wild-type and RGS6–/– mice

(A) WT mice were processed for slice electrophysiology, targeting putative VTA DA neurons medial to the medial terminal nucleus of the accessory optic tract (MT).
(B) Somatodendritic inhibitory currents (V_{hold} =-60 mV) evoked by EC_{50} dose (Bac_{50}, 10 μM) followed by maximal dose (Bac_{max}, 200 μM) of baclofen recorded from putative DA neurons in VTA slices from WT and RGS6–/– mice. Currents were reversed by CGP54626 (CGP, 2 μM).
(C) Summary of sensitivity ratio of currents evoked by EC_{50} and maximal dose of baclofen in putative DA neurons in VTA slices from WT and RGS6–/– mice ($t_{21.99}$=0.2519, P=0.8035; unpaired Welch's t test; n=12/group).
(D) Summary of maximal currents evoked by baclofen in putative DA neurons in VTA slices from WT and RGS6–/– mice ($t_{20.28}$=0.1525; P=0.8803; unpaired Welch's t test; n=12/group).
(E) Somatodendritic inhibitory currents (V_{hold} =-60 mV) evoked by EC_{50} dose ($Quin_{50}$, 60 nM) followed by maximal dose ($Quin_{max}$, 20 μM) of quinpirole recorded from putative DA neurons in VTA slices from C57BL/6J (WT) and RGS6–/– mice. Currents were reversed by sulpiride (Sulp, 5 μM).
(F) Summary of sensitivity ratio of currents evoked by EC_{50} and maximal dose of quinpirole in putative DA neurons in VTA slices from WT and RGS6–/– mice ($t_{20.12}$=1.896, P=0.0724; unpaired Welch's t test; n=11-13/group).
(G) Summary of maximal currents evoked by quinpirole in putative DA neurons in VTA slices from WT and RGS6–/– mice. Main effect of genotype ($F_{1, 21}$= 8.845, P=0.0072; 2-way ANOVA; n=6-7/group) and sex ($F_{1, 21}$= 5.098, P=0.0347) but no interaction ($F_{1, 21}$= 0.1029, P=0.7515). Symbol: *P< 0.05; **P<0.01 (main effect).
(H) WT and RGS6–/– mice were treated with intra-NAc AAV8-CaMKIIa-hChR2(H134R)-mCherry. Example of viral targeting; mCherry fluorescence (red) highlights the anatomic scope of viral targeting. Abbreviations: NAcC – Nucleus Accumbens core, NAcS – Nucleus Accumbens shell, AC – anterior commisure. Scale bar: 250 μm.
(I) Somatodendritic inhibitory $GABA_BR$-dependent currents (V_{hold} =-60 mV) evoked by light stimulation of NAc terminals, recorded from putative DA neurons in VTA slices from WT and RGS6–/– mice.
(J) Summary of activation tau calculated from light-evoked $GABA_BR$-dependent currents in putative VTA DA neurons from WT and RGS6–/– mice ($t_{22.18}$=1.355, P=0.1890; unpaired Welch's t test; n=11-12/group).
(K) Summary of deactivation tau calculated from light-evoked $GABA_BR$-dependent currents in putative VTA DA neurons from WT and RGS6–/– mice. Main effect of genotype ($F_{1, 20}$= 41.42, P<0.0001; 2-way ANOVA; n=5-7/group), no main effect of sex ($F_{1, 20}$= 0.9083, P=0.3519) but a significant interaction ($F_{1, 20}$= 10.29, P=0.0044). Sidak's multiple comparisons test revealed differences between WT and RGS6–/– mice both for males (P=0.0419) and females (P<0.0001). Symbol: *P< 0.05; ***P<0.0001.

3.4.4 Selective manipulation of RGS6 expression in VTA DA neurons

As constitutive RGS6 ablation may provoke compensatory and/or developmental adaptations that could impact or obscure the role of RGS6 in VTA DA neurons, and because RGS6 is expressed in DAT-positive and DAT-negative neurons in the VTA, we used the VTA DA neuron-specific CRISPR/Cas9 approach to ablate RGS6 selectively in adult VTA DA neurons (**Fig. 3.4A**). Following infusion of vectors harboring either RGS6 or control gRNA into the VTA of adult DATCre(+):Cas9GFP(+) mice, we observed no impact of viral treatment on spontaneous activity, rheobase, or other parameters of VTA DA neurons (**Table 3.1**). Consistent with observations in VTA DA neurons from constitutive *RGS6*$^{-/-}$ mice, VTA DA neurons from mice treated with RGS6 gRNA exhibited larger maximal quinpirole-induced currents than LacZ control-treated subjects (**Fig. 3.4D**; unpaired Welch's t test; t_{47}=2.429; P=0.0192; n=24-25/group) with no effect on quinpirole sensitivity (**Fig. 3.4C**; unpaired Welch's t test; $t_{46.75}$=1.472; P=0.1478; n=24-25/group).

We also tested whether viral overexpression of RGS6 in VTA DA neurons exerted an opposite influence on D_2R-dependent somatodendritic signaling. Cre-dependent RGS6 overexpression or control AAV vector was infused into the VTA of adult male and female DATCre(+) mice (**Fig. 3.5A,B**). No differences in in VTA DA neuron parameters were observed across viral treatment groups (**Table 3.1**). Maximal somatodendritic currents evoked by bath application of quinpirole were smaller for mice treated with RGS6 overexpression compared to controls (**Fig. 3.5E**; 2-way ANOVA; $F_{1, 22}$=8.082, P=0.0095; n=6-7/group). We also saw a main effect of sex ($F_{1, 22}$=7.186, P=0.0137), consistent with constitutive *RGS6*$^{-/-}$, but no interaction ($F_{1, 22}$=0.6404, P=0.4321). Sensitivity was the same for mice treated with RGS6 overexpression or control (**Fig. 3.5D**; unpaired Welch's t test; $t_{21.46}$=0.8972, P=0.3796; n=12-14/group). Thus, RGS6 expression is negatively correlated with strength of D_2R-dependent somatodendritic signaling in VTA DA neurons.

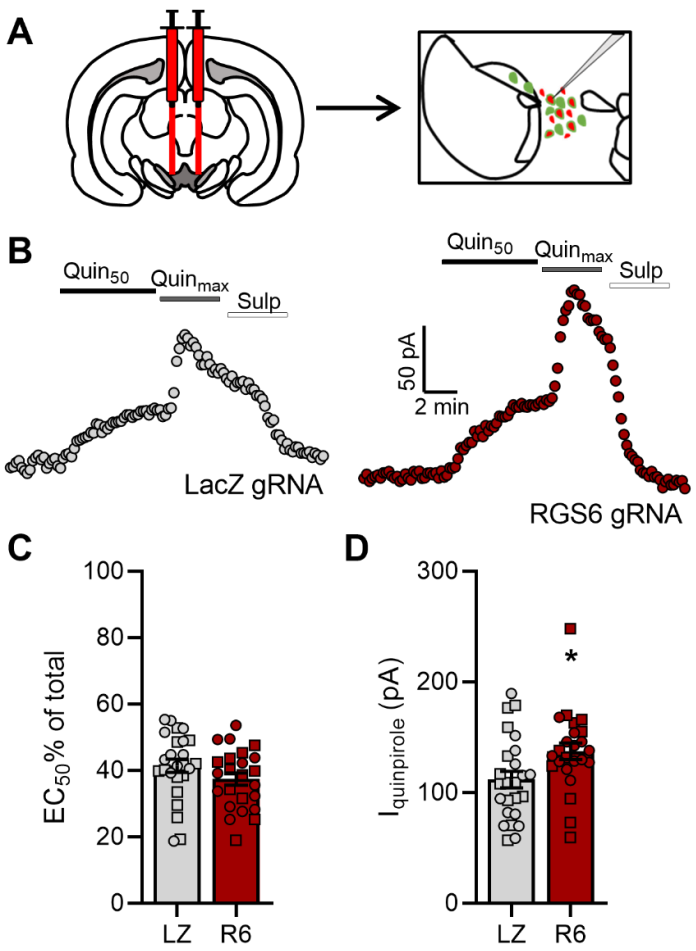

Figure 3.4. CRISPR/Cas9 ablation of RGS6 in VTA DA neurons

(A) DATCre(+):Cas9GFP(+) mice were treated with intra-VTA AAV8-U6-gRNA-hSyn-NLSmCherry. Following viral injection (5 w), mice were processed for slice electrophysiology.

(B) Somatodendritic inhibitory currents (V_{hold} =-60 mV) evoked by EC_{50} dose ($Quin_{50}$, 60 nM) followed by maximal dose ($Quin_{max}$, 20 μM) of quinpirole recorded in VTA DA neurons from DATCre(+):Cas9GFP(+) mice treated with AAV8-U6-gLacZ-hSyn-NLSmCherry control or AAV8-U6-gRGS6-hSyn-NLSmCherry. Currents were reversed by sulpiride (Sulp, 5 μM).

(C) Summary of sensitivity ratio of currents evoked by EC_{50} and maximal dose of quinpirole in VTA DA from DATCre(+):Cas9GFP(+) mice treated with AAV8-U6-gLacZ-hSyn-NLSmCherry control or AAV8-U6-gRGS6-hSyn-NLSmCherry ($t_{46.75}$=1.472; P=0.1478; unpaired Welch's t test; n=24-25/group).

(D) Summary of maximal currents evoked by quinpirole in VTA DA from DATCre(+):Cas9GFP(+) mice treated with AAV8-U6-gLacZ-hSyn-NLSmCherry control or AAV8-U6-gRGS6-hSyn-NLSmCherry (t_{47}=2.429; P=0.0192; unpaired Welch's t test; n=24-25/group). Symbol: *P<0.05.

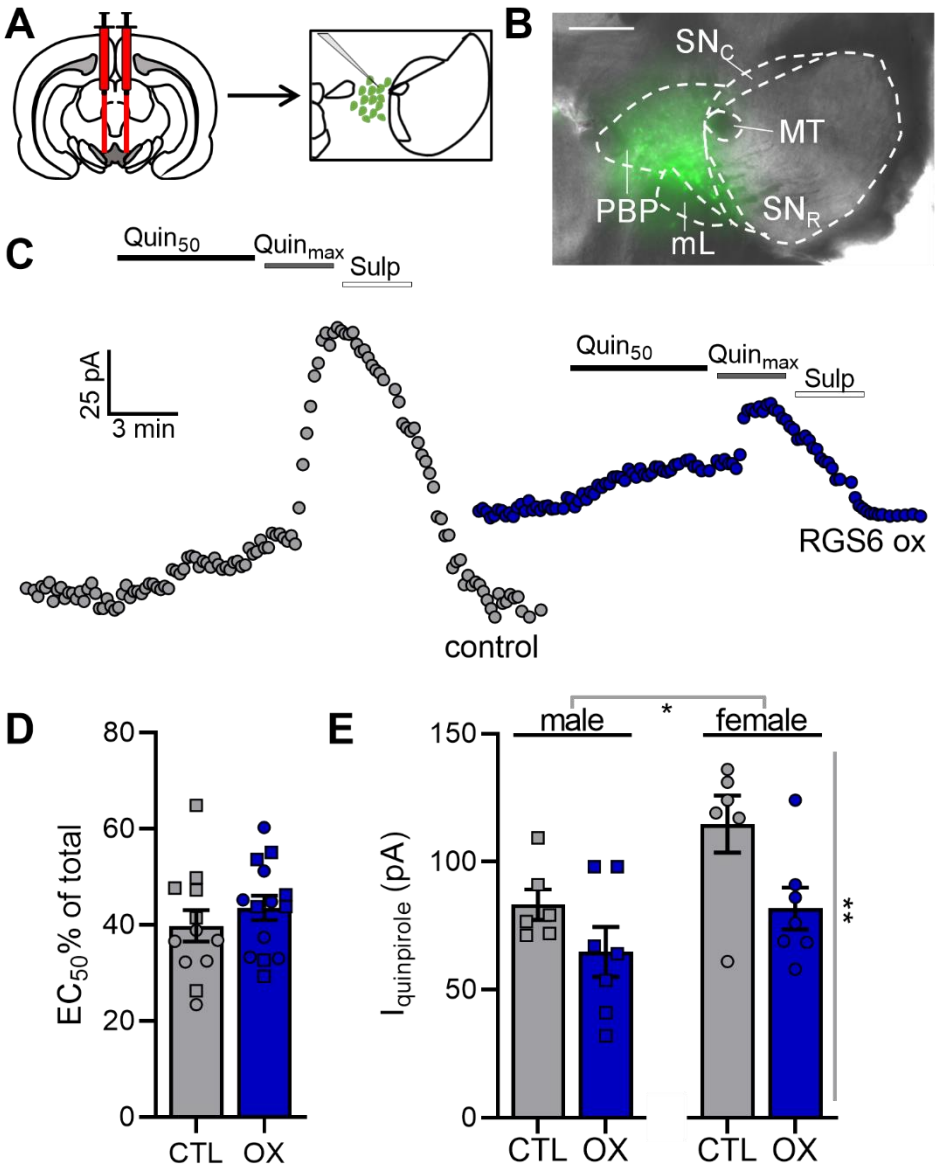

Figure 3.5. Overexpression of RGS6 in VTA DA neurons

(A) DATCre(+) mice were treated with intra-VTA AAV8-DIO-hSyn-RGS6-IRES-GFP or AAV8-DIO-hSyn-GFP control. Following viral injection (3 w), mice were processed for slice electrophysiology.

(B) Example of viral targeting; GFP fluorescence (green) denotes the Cre-dependent expression of viral targeting. Abbreviations: MT - medial terminal nucleus of the accessory optic tract, PBP - parabrachial pigmented nucleus of the VTA, SN_C - substantia nigra pars compacta, SN_R - substantia nigra pars reticulata, mL - medial lemniscus. Scale bar: 400 µm.

(C) Somatodendritic inhibitory currents (V_{hold} =-60 mV) evoked by EC_{50} dose ($Quin_{50}$, 60 nM) followed by maximal dose ($Quin_{max}$, 20 µM) of quinpirole recorded in VTA DA neurons from DATCre(+) mice treated with AAV8-DIO-hSyn-GFP control AAV8-DIO-hSyn-RGS6-IRES-GFP. Currents were reversed by sulpiride (Sulp, 5 µM).

(D) Summary of sensitivity ratio of currents evoked by EC_{50} and maximal dose of quinpirole in VTA DA neurons from DATCre(+) mice treated with AAV8-DIO-hSyn-GFP control AAV8-DIO-hSyn-RGS6-IRES-GFP ($t_{21.46}$=0.8972, P=0.3796; unpaired Welch's t test; n=12-14/group).

(E) Summary of maximal currents evoked by quinpirole in VTA DA neurons from DATCre(+) mice treated with AAV8-DIO-hSyn-GFP control AAV8-DIO-hSyn-RGS6-IRES-GFP. There was a main effect of genotype ($F_{1, 22}$=8.082, P=0.0095; 2-way ANOVA; n=6-7/group) and sex ($F_{1, 22}$=7.186, P=0.0137), but no interaction ($F_{1, 22}$=0.6404, P=0.4321). Symbol: *P< 0.05; **P<0.01 (main effect).

3.4.5 Impact of RGS6 ablation on binge alcohol consumption

RGS6$^{-/-}$ mice were reported to consume less alcohol in a 4 wk long, 24-h access alcohol consumption paradigm (Stewart et al., 2015). To assess if RGS6 ablation also impacts acute binge alcohol consumption, we utilized a well-established "drinking in the dark" (DID) model (Fritz & Boehm, 2016; Rhodes, Best, Belknap, Finn, & Crabbe, 2005; Thiele & Navarro, 2014). This model mimics human binge drinking, as mice can achieve blood alcohol concentrations of 0.08 g% or higher (Crabbe et al., 2017), a level considered to be intoxicating for humans (NIAAA, 2004). Briefly, alcohol consumption was measured during a limited timeframe over a total of 4 days, with day 4 considered as the "binge" day (**Fig. 3.6A**). During the day 4 binge session, *RGS6*$^{-/-}$ mice drank significantly less than WT counterparts (**Fig. 3.6B**; 2-way ANOVA; $F_{1, 43}$= 12.79, P=0.0009; n=11-12/group). While females drank significantly more than males during this session ($F_{1, 43}$= 5.841, P=0.0200), there was no interaction between sex and genotype ($F_{1, 43}$= 0.2097, P=0.6493). Male *RGS6*$^{-/-}$ mice also drank significantly less than WT counterparts on all 3 days leading up to the binge session (**Fig. 3.6C**; 2-way repeated measures ANOVA; $F_{1,21}$=4.530, P=0.0453; n=11-12/group) while females did not (**Fig. 3.6D**; 2-way repeated measures ANOVA; $F_{1,21}$=0.3356, P=0.5686).

We next examined the impact of VTA DA neuron-specific ablation of RGS6 on binge alcohol consumption in male and female DATCre(+):Cas9GFP(+) mice following intra-VTA infusion of RGS6 or LacZ control gRNA vectors. When comparing alcohol consumed during the day 4 binge session, mice that received RGS6 gRNA drank significantly less than LacZ gRNA controls (**Fig. 3.6F**; 2-way ANOVA; $F_{1,44}$=5.096, P=0.0290; n=11-13/group). Females again drank significantly more than males ($F_{1,44}$=38.52, P<0.0001), and an interaction between sex and viral treatment was observed ($F_{1,44}$=4.238, P=0.0455). Further analysis revealed a significant difference of viral

treatment in females only (P=0.0077). There was no main effect of virus on the 3 days leading up to the binge session for either males (**Fig. 3.6G**; 2-way repeated measures ANOVA; $F_{1, 22}$= 0.08891, P=0.7684; n=11-13/group) or females (**Fig. 3.6H**; 2-way repeated measures ANOVA; $F_{1, 22}$=0.3508, P=0.5597; n=11-13/group). Thus, while constitutive ablation of RGS6 affects alcohol consumption in both male and female mice, loss of RGS6 in VTA DA neurons affects alcohol consumption only in females.

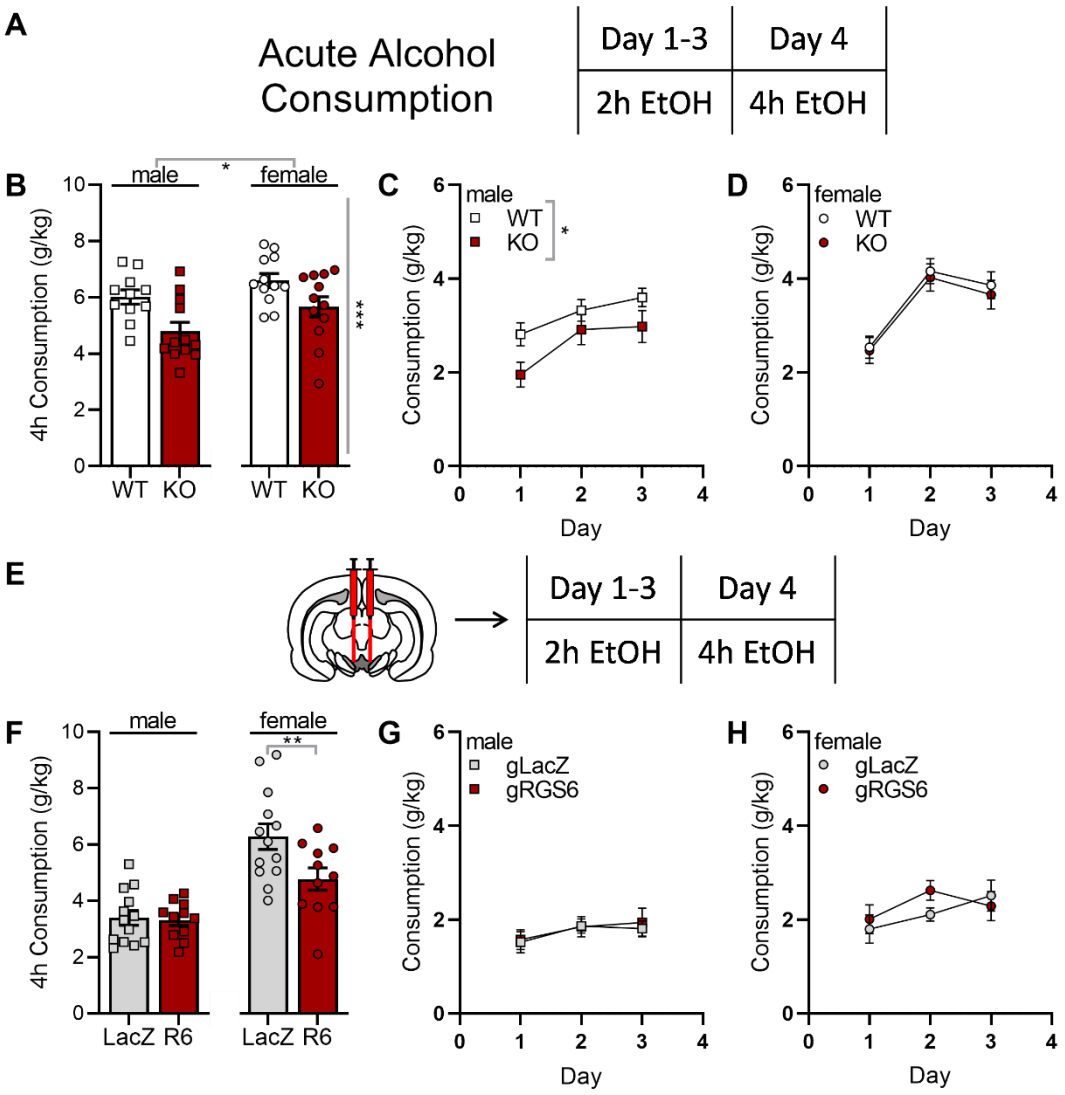

Figure 3.6. Behavioral analysis of mice lacking RGS6

(A) WT and *RGS6*$^{-/-}$ mice underwent an acute binge drinking paradigm that lasted 4 days. Mice received access to alcohol for 2 h on days 1-3 and 4 h on day 4.

(B) Summary of WT and *RGS6*$^{-/-}$ mouse alcohol consumption during the day 4, 4 h binge session. Main effect of genotype ($F_{1,\ 43}$= 12.79, P=0.0009; 2-way ANOVA; n=11-12/group) and sex ($F_{1,\ 43}$= 5.841, P=0.0200), with no interaction ($F_{1,\ 43}$= 0.2097, P=0.6493). Symbol: *P< 0.05; ***P<0.0001 (main effect).

(C) Alcohol consumption of male WT and *RGS6*$^{-/-}$ mice across the first 3 days of the procedure. There was a main effect based on procedure day ($F_{1.839,\ 38.63}$=9.658, P<0.001; 2-way repeated measures ANOVA; n=11-12/group) and a main effect of genotype ($F_{1,21}$=4.530, P=0.0453), but no interaction ($F_{2,42}$=0.5244, P=0.5957). Symbol: *P< 0.05 (main effect).

(D) Alcohol consumption of female WT and RGS6–/– mice across the first 3 days of the procedure. There was a main effect based on procedure day ($F_{1.969,41.34}$=18.32,

P<0.0001; 2-way repeated measures ANOVA; n=11-12/group), but no main effect of genotype ($F_{1,21}$=0.3356, P=0.5686) or interaction ($F_{2,42}$=0.02837, P=0.9721).

(E) DATCre(+):Cas9GFP(+) mice were treated with intra-VTA AAV8-U6-gRNA-hSyn-NLSmCherry. Following viral injection (5 w), mice underwent acute binge drinking.

(F) Summary of alcohol consumption of DATCre(+):Cas9GFP(+) mice treated with AAV8-U6-gLacZ-hSyn-NLSmCherry control or AAV8-U6-gRGS6-hSyn-NLSmCherry during the day 4, 4 h binge session. Main effect of genotype ($F_{1, 44}$=5.096, P=0.0290; 2-way ANOVA; n=11-13/group) and sex ($F_{1, 44}$=38.52, P<0.0001), in addition to a significant interaction ($F_{1, 44}$=4.238, P=0.0455). Sidak's multiple comparisons test revealed a significant difference between female LacZ gRNA and RGS6 gRNA mice (P=0.0077). Symbol: **P<0.01 (main effect).

(G) Alcohol consumption of male DATCre(+):Cas9GFP(+) mice treated with AAV8-U6-gLacZ-hSyn-NLSmCherry control or AAV8-U6-gRGS6-hSyn-NLSmCherry across first 3 days of the procedure. There was no main effect based on procedure day ($F_{1.872, 41.19}$=1.603, P=0.2145; 2-way repeated measures ANOVA; n=11-13/group), genotype ($F_{1, 22}$= 0.08891, P=0.7684), or interaction ($F_{2, 44}$=0.06039, P=0.9415).

(H) Alcohol consumption of female DATCre(+):Cas9GFP(+) mice treated with AAV8-U6-gLacZ-hSyn-NLSmCherry control or AAV8-U6-gRGS6-hSyn-NLSmCherry across first 3 days of the procedure. There was no main effect based on procedure day ($F_{1.962, 43.16}$=2.753, P=0.0759; 2-way repeated measures ANOVA; n=11-13/group), genotype ($F_{1, 22}$=0.3508, P=0.5597), or interaction ($F_{2,44}$=1.232, P=0.3017).

3.5 Discussion

Here, we examined the influence of RGS6 in the regulation of inhibitory G protein signaling in VTA DA neurons and on binge alcohol consumption. Relatively little is known about contribution of individual $G\alpha_{i/o}$ isoforms to inhibitory signaling in neurons. Previous reports have characterized GPCR-specific profiles of G protein engagement in cell lines (Masuho et al., 2020; Masuho, Martemyanov, & Lambert, 2015; Masuho, Ostrovskaya, et al., 2015). While $G\alpha$ signaling preferences for $GABA_BR$ have not been reported, D_2R can signal effectively through all $G\alpha_o$, $G\alpha_i$ and $G\alpha_z$ isoforms with the greatest response elicited through $G\alpha_o$ (Masuho, Ostrovskaya, et al., 2015). Our data suggest that $G\alpha_o$ contributes in part to the somatodendritic inhibitory effects evoked by $GABA_BR$ and D_2R activation in VTA DA neurons. Due to the reported preference of D_2R for $G\alpha_o$ (Masuho, Ostrovskaya, et al., 2015), the large residual current after loss of $G\alpha_o$ is somewhat surprising. Given the $G\alpha_o$ substrate preference of R7 RGS proteins (Hooks et al., 2003; Masuho et al., 2020), the relatively large residual current D_2R- and $GABA_BR$-dependent currents seen following $G\alpha_o$ ablation might suggest that a large proportion of inhibitory signaling mediated by these receptors is not subject to negative regulation by R7 RGS proteins. It is possible, however, that under normal conditions these receptors preferentially recruit $G\alpha_o$ but that under $G\alpha_o$ deficient conditions they are forced to compensate by recruiting other $G\alpha$ isoforms such as $G\alpha_i$ or $G\alpha_z$.

R7 RGS proteins are known to impact inhibitory G protein-dependent signaling in neurons. For example, RGS9 is important for accelerating the activation and deactivation kinetics of D_2R-dependent signaling in the striatum (Z. Rahman et al., 2003). RGS7, but not RGS6, has been implicated in the kinetics and sensitivity of $GABA_BR$-dependent signaling in hippocampal pyramidal neurons. For example, cultured hippocampal neurons

from *RGS7*$^{-/-}$ (and *Gb5*$^{-/-}$) mice display prolonged deactivation of baclofen-induced currents and increased sensitivity to baclofen (Ostrovskaya et al., 2014). Additionally, RGS6 regulates deactivation of $GABA_BR$-dependent signaling in cerebellar granule neurons (Maity et al., 2012), adenylyl cyclase activation by 5-hydroxytryptamine 1A receptor ($5HT_{1A}R$) in cortical and hippocampal pyramidal neurons (Stewart et al., 2014), and MOR-dependent signaling in multiple regions including the hypothalamus and cortex (Garzón et al., 2003). We show here that constitutive loss of RGS6 correlates with increased amplitude but not sensitivity of D_2R-dependent signaling, an effect recapitulated in a VTA DA neuron-specific RGS6 ablation model. While the amplitude of $GABA_BR$-dependent somatodendritic currents was not impacted by constitutive RGS6 ablation, the deactivation rate of evoked/synaptic $GABA_BR$-dependent currents was significantly prolonged in VTA DA neurons from *RGS6*$^{-/-}$ mice. These data suggest that RGS6 impacts discrete aspects of inhibitory G protein signaling dynamics in a receptor-dependent manner.

A GPCR-dependent influence of RGS6 on inhibitory G protein signaling was also reported in sinoatrial nodal cells (A. Anderson et al., 2020; Wydeven et al., 2014). The amplitude of A_1 adenosine receptor-mediated currents was higher in SAN cells from *RGS6*$^{-/-}$ mice, as compared to WT controls. In contrast, only the deactivation rate of M_2 muscarinic receptor-mediated signaling was impacted by RGS6 ablation (A. Anderson et al., 2020). Our observations in VTA DA neurons were similar; D_2R-dependent currents were larger in *RGS6*$^{-/-}$ mice, whereas loss of RGS6 only impacted $GABA_BR$-dependent signaling kinetics. All G protein-dependent signaling is limited by receptor, G protein, and/or effector availability. It is possible that $GABA_BR$-dependent signaling is limited by effector availability whereas D_2R-dependent signaling is limited by receptor or G protein availability. While the inhibitory effect of D_2R and $GABA_BR$ activation in VTA DA neurons

is mediated by multiple somatodendritic effectors, most (>80%) of the currents measured under the conditions used in this study reflect the activation of G protein-gated inwardly rectifying K^+ (GIRK/Kir3) channels(Arora et al., 2010; Bettler et al., 2004; Labouèbe et al., 2007; Steketee et al., 1992). The loss of RGS6 may lead to an increased pool of activated G proteins, allowing the opening of GIRK channels that are available but not typically utilized by D_2R activation, thereby yielding a larger current amplitude. $GABA_BR$-dependent signaling, on the other hand, normally produces a larger inhibitory current amplitude compared to D_2R-dependent signaling and may already be opening all available GIRK channels even with RGS6 intact. Consistent with this idea, overexpression of GIRK2, the subunit responsible for trafficking of functional GIRK channels, in VTA DA neurons did not significantly increase maximal amplitude of D_2R-dependent currents but it did increase maximal amplitude of $GABA_BR$-dependent currents (McCall et al., 2019). This suggests that availability of GIRK is the limiting agent of $GABA_BR$-dependent signaling but another factor, such as G protein or receptor availability, is limiting the activation of GIRK channels in D_2R-dependent signaling. Further, $GABA_BR$ in the brain often interact with KCTD proteins, which may facilitate the anchoring of proteins and effectors, such as GIRK channels, which may be responsible for allowing easier activation of GIRK channels by $GABA_BR$ (Rose & Wickman, 2022).

Several lines of evidence support the contention that modulation of inhibitory signaling within VTA DA neurons plays a role in response to drugs of abuse, including alcohol (Liu et al., 2020; Solecki et al., 2020; Valyear et al., 2020). Here, we report that mice constitutively lacking RGS6 displayed enhanced $GABA_BR$- and D_2R-mediated signaling in VTA DA neurons in addition to decreased binge alcohol consumption. This decreased binge consumption is recapitulated in female mice lacking RGS6 exclusively in VTA DA neurons. Further, VTA DA neuron-specific ablation and upregulation of RGS6

revealed a negative correlation between RGS6 and D_2R-dependent current amplitude, highlighting the role of RGS6 in negatively regulating VTA DA neuron inhibitory GPCR-dependent signaling. Previous studies have reported that intra-VTA infusions of the $GABA_B$R agonist baclofen decrease binge alcohol consumption in mice, but it is unclear whether this effect was mediated by DA neurons or other cells (Moore & Boehm, 2009). Additionally, systemic injections of the D_2R agonist quinpirole have been reported to decrease alcohol sensitivity, but this effect was not localized (Cohen, Perrault, & Sanger, 1997). Our results suggest that loss of RGS6, which enhances VTA DA neuron $GABA_B$R- and D_2R-dependent signaling, can reduce binge alcohol consumption. It is possible that RGS6 is upregulated as a form of plasticity after repeated drug administration to counteract activation of inhibitory GPCR-dependent signaling. Indeed, a previous study suggests that VTA RGS6 levels were increased after chronic alcohol consumption (Stewart et al., 2015).

We reported larger D_2R-dependent current amplitudes in females compared to males, as was reported previously (DeBaker et al., 2021), in our electrophysiological assessments of constitutive *RGS6*$^{-/-}$ and RGS6 overexpression. There was no sex difference in D_2R-dependent signaling amplitude in RGS6 gRNA studies. It is possible that this discrepancy is due to the high amount of variability in expression levels of D_2R across the heterogeneous population of VTA DA neurons (Morales & Margolis, 2017). We also report a sex difference in deactivation of $GABA_B$R-dependent signaling in RGS6-deficient VTA DA neurons, with female *RGS6*$^{-/-}$ having more prolonged deactivation than males.

Our behavioral assessments reveal novel insights about potential sex effects related to RGS6 loss on alcohol consumption, as male and female mice were combined in previous reports analyzing alcohol consumption in constitutive RGS6$^{-/-}$ mice (Stewart et al., 2015). Male and female constitutive *RGS6*$^{-/-}$ mice both showed decreased alcohol

consumption compared to WT during the binge session. There was also a main effect of sex, consistent with previous reports that female rodents tend to consume more alcohol than males (Cunningham & Shields, 2018; Li & Lumeng, 1984; Yoneyama et al., 2008).

We saw a sex-specific impact of VTA DA neuron-specific RGS6 ablation on alcohol consumption. Females had decreased alcohol consumption on day 4, similar to constitutive *RGS6*$^{-/-}$, while males did not decrease consumption compared to control on any day of the procedure. Our results suggest that VTA DA neuron specific manipulations of RGS6 exert a greater impact in female behaviors compared to males. This could be due in part to the higher proportion of VTA DA neurons that have been reported in female rodents compared to males (McArthur, McHale, & Gillies, 2007), resulting in a greater number of DA neurons being impacted in females relative to males. Females may also be more affected by loss of RGS6 in VTA DA neurons due to the larger amplitude of D_2R-dependent currents reported in females, together with the stronger effect of RGS6 on $GABA_B$R-dependent signaling kinetics in females compared to males. $GABA_B$R-dependent signaling may be more heavily moderated by RGS6 in females compared to males, therefore precluding effects of $GABA_B$R activation on drug-related behaviors in females with RGS6 intact. Loss of RGS6 could then permit the inhibitory effects of $GABA_B$R-dependent signaling to exert effects on behavior. Indeed, our previous work has shown that loss of VTA DA neuron D_2R-dependent signaling increases cocaine sensitivity in both males and females, but loss of $GABA_B$R-dependent signaling only affects cocaine sensitivity in males, suggesting a limited role of $GABA_B$R-dependent signaling in modulating drug-related behavior in females (DeBaker et al., 2021). Additionally, alcohol may be more reliant on $GABA_B$R-dependent signaling to exert reward-related behaviors compared to cocaine, as alcohol is known to play a role in modulating GABA transmission (Domi et al., 2021; Nora D. Volkow et al., 2011).

The female-specific reduction in alcohol consumption after intra-VTA RGS6 ablation may also be an artifact of the animals and timeframe employed in these experiments. It is important to note that VTA DA neuron-specific *RGS6*$^{-/-}$ mice were older than constitutive *RGS6*$^{-/-}$ mice at the time of behavioral assessment due to the viral injection and incubation period. It is possible that older male mice consume less alcohol relative to younger males whereas females do not differ based on age. It is not well understood whether age plays a large role in levels of alcohol consumption, or if this is a sex-dependent phenomenon, but studies suggest that older male rodents may be more sensitive to the negative effects of alcohol compared to younger males (Ott, Hunter, & Walker, 1985; Squeglia, Boissoneault, Van Skike, Nixon, & Matthews, 2014). Consistent with this premise, we saw that older male mice drank significantly less than younger males, but there was no age-related alcohol consumption difference for females (Supplementary **Fig. 3.7**). Thus, age may play a role in the lower alcohol consumption observed in the male VTA DA neuron-specific *RGS6*$^{-/-}$ mice, potentially limiting the ability to see any small decreases in consumption after loss of RGS6.

Taken together, our results show that loss of RGS6 in VTA DA neurons enhances inhibitory GPCR-dependent signaling, decreasing alcohol consumption in a sex-dependent manner. This work highlights novel insights about cellular and molecular mechanisms in the brain that regulate alcohol consumption and reward. The knowledge gained about RGS6 involvement in alcohol consumption may guide the identification of potential risk factors associated with AUD, as RGS6 levels were significantly associated with alcohol dependence symptom count, a quantitative measure of AUD, in a human Genome Wide Association Study (G. Chen et al., 2017). In addition, insights from these studies could inform investigations into new or improved therapeutic strategies for more targeted treatment of AUD.

Supplementary Figure:

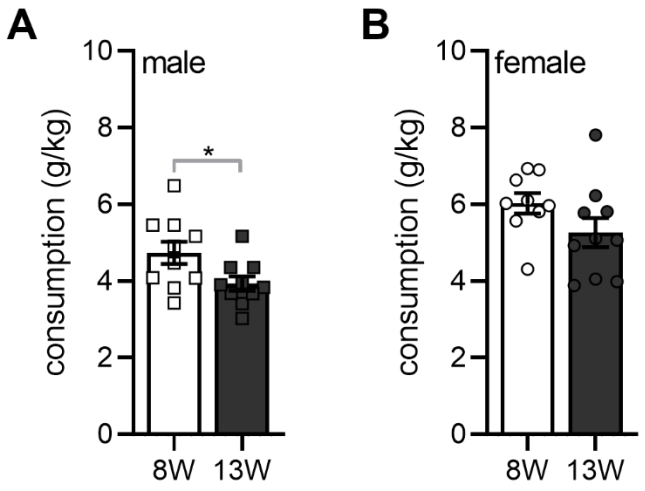

Figure 3.7. Comparison of age in alcohol consumption

(A) Summary of alcohol consumption of male 8 wk and 13 wk old WT mice during the 4 h binge session ($t_{15.19}$=2.306; P=0.0356; unpaired Welch's t test; n=10/group). Symbol: *P< 0.05.

(B) Summary of alcohol consumption of female 8 wk and 13 wk old WT mice during the 4 h binge session ($t_{15.75}$=1.634; P=0.1220; unpaired Welch's t test; n=9-10/group).

Chapter 4 : Unequal interactions between alcohol and nicotine co-consumption: Suppression and enhancement of concurrent drug intake

Chapter 4 contains work previously published in Psychopharmacology *2020, 237(4): 967-978. Published online 2019 Dec 20. "Unequal interactions between alcohol and nicotine co-consumption: suppression and enhancement of concurrent drug intake."* ***Margot C DeBaker****, Janna K Moen, Jenna M Robinson, Kevin Wickman and Anna M Lee.*

Reproduced with permission from Springer Nature.

Author Contributions: AML, MCD, JKM, and JMR designed the project. MCD planned, coordinated, and performed the majority of behavioral studies. JKM and JMR assisted with support of behavioral studies. KW provided co-mentorship support. MCD and AML wrote the manuscript, and all authors provided reviews.

4.1 Synopsis

Rationale Alcohol and nicotine addiction are prevalent conditions that co-occur. Despite the prevalence of co-use, factors that influence the suppression and enhancement of concurrent alcohol and nicotine intake are largely unknown.

Objectives Our goals were to assess how nicotine abstinence and availability influenced concurrent alcohol consumption, and to determine the impact of quinine adulteration of alcohol on aversion resistant alcohol consumption and concurrent nicotine consumption.

Methods Male and female C57BL/6J mice voluntarily consumed unsweetened alcohol, nicotine and water in a chronic 3-bottle choice procedure. In Experiment 1, nicotine access was removed for 1 week and re-introduced the following week, while the alcohol and water bottles remained available at all times. In Experiment 2, quinine (100-1000 μM) was added to the 20% alcohol bottle, while the nicotine and water bottles remained unaltered.

Results In Experiment 1, we found that alcohol consumption and preference were unaffected by the presence or absence of nicotine access in both male and female mice. In Experiment 2a, we found that quinine temporarily suppressed alcohol intake and enhanced concurrent nicotine, but not water, preference in both male and female mice. In Experiment 2b, chronic quinine suppression of alcohol intake increased nicotine consumption and preference in female mice without affecting water preference, whereas it increased water and nicotine preference in male mice.

Conclusions Quinine suppression of alcohol consumption enhanced the preference for concurrent nicotine preference in male and female mice, suggesting that mice compensate for the quinine adulteration of alcohol by increasing their nicotine preference.

4.2 Introduction

Alcohol and nicotine are the two most commonly abused addictive drugs and the majority of alcohol dependent individuals are also dependent on nicotine (Batel, Pessione, Maitre, & Rueff, 1995; Falk, Yi, & Hiller-Sturmhöfel, 2006; Miller & Gold, 1998). Persons co-dependent on alcohol and nicotine have more severe drug dependence symptoms such as greater craving and withdrawal signs, higher drug consumption, increased difficulty maintaining abstinence, and have higher mortality compared with persons dependent on alcohol or nicotine alone (Heffner, Mingione, Blom, & Anthenelli, 2011; Hurt, 1996; King, McNamara, Conrad, & Cao, 2009; Leeman et al., 2008; Marks, Hill, Pomerleau, Mudd, & Blow, 1997). Despite the high prevalence and increased health consequences of alcohol and nicotine co-dependence, there are currently no FDA-approved drugs for the treatment of alcohol and nicotine co-dependence. In human studies, it is difficult to dissect the effects of alcohol and nicotine from the genetic and environmental influences that also contribute to overall drug taking. Several reviews have highlighted key knowledge gaps that have limited the development of new drugs, such as the need to better understand the neurobiology of co-dependence and the need for identification of drug targets that mediate both alcohol and nicotine dependence (Tarren & Bartlett, 2017; Van Skike et al., 2016). To achieve this, the development of a greater variety of animal models that reflect alcohol and nicotine co-use is necessary, as this will enable the identification how alcohol and nicotine influence co-consumption while controlling for genetics and environment.

Many animal models of alcohol and nicotine co-dependence utilize investigator administered drugs (Blomqvist, Gelernter, & Kranzler, 2000; Hendrickson, Zhao-Shea, & Tapper, 2009; Lê et al., 2000; Lê, Wang, Harding, Juzytsch, & Shaham, 2003; Smith, Kelly, & Chen, 2002), and although these models allow for control of dose and timing, they

do not permit the animal to voluntarily consume both drugs. A limited number of studies in rats have examined voluntary alcohol and nicotine intake using several routes of administration, such as intravenous self-administration (IVSA) of nicotine with operant oral consumption of alcohol (Lê, Funk, Lo, & Coen, 2014; Lê et al., 2010), IVSA nicotine with oral alcohol consumption in a 2-bottle choice procedure (Maggio et al., 2018), operant intra-cranial self-administration of nicotine with operant alcohol consumption (Deehan et al., 2015), or operant intra-cranial self-administration of a mixture of alcohol and nicotine (Truitt et al., 2015). These studies provide valuable information, yet the procedures involve significant training as well as technical and surgical requirements. In contrast, 2-bottle choice studies are frequently used in rats and mice to assess alcohol or nicotine consumption (A. M. Lee & Messing, 2011; A. M. Lee et al., 2014; Locklear, McDonald, Smith, & Fryxell, 2012; Meliska, Bartke, McGlacken, & Jensen, 1995; Powers, Broderick, Drenan, & Chester, 2013; Simms et al., 2008). In these studies, the animals are individually housed with two fluid bottles, one containing drug and one water, and the animals are free to consume from both bottles. These bottle choice studies are less technically challenging and are more high-throughput compared with operant administration studies.

We have previously developed a novel 3-bottle choice co-consumption model where mice voluntarily consume unsweetened alcohol, unsweetened nicotine, and water from 3 separate drinking bottles (DeBaker, Robinson, Moen, Wickman, & Lee, 2020; O'Rourke, Touchette, Hartell, Bade, & Lee, 2016; Touchette, Maertens, Mason, O'Rourke, & Lee, 2018). Using this model, we investigated the effects of forced alcohol abstinence and intermittent drug access, and the impact of pre-clinical drug treatment on concurrent alcohol and nicotine consumption in male and female C57BL/6J mice (O'Rourke et al., 2016; Touchette et al., 2018). We reported that after 3 weeks of chronically co-consuming

alcohol and nicotine, forced alcohol abstinence resulted in an increase in concurrent nicotine consumption and preference in male and female C57BL/6J mice, suggesting that the mice compensated for the absence of alcohol by increasing their consumption of nicotine (O'Rourke et al., 2016). It is unclear if the reciprocal relationship between alcohol and nicotine is true, and in the current study one of our goals was to determine whether forced nicotine abstinence enhanced concurrent alcohol consumption in this model.

A prominent feature of alcohol use disorders (AUDs) in humans is consumption of alcohol despite adverse legal, health, economic, and societal consequences. The continued consumption of alcohol despite the addition of the bitter tastant quinine has been frequently used as a model of compulsive alcohol intake or aversion-resistant alcohol consumption in both rats and mice (F. Woodward Hopf & Lesscher, 2014; Frederic Woodward Hopf, Chang, Sparta, Bowers, & Bonci, 2010; Lei, Wegner, Yu, Simms, & Hopf, 2016; Sneddon, White, & Radke, 2018; Spanagel, Zieglgänsberger, & Hundt, 1996). Our second goal was to determine whether the alcohol-abstinence induced elevation of nicotine consumption that we previously reported in O'Rourke et al, 2016 could be produced by suppressing alcohol consumption instead of removing alcohol access. Moreover, quinine suppression of alcohol consumption has not yet been evaluated in a voluntary alcohol and nicotine co-consumption model.

Here, we report an unequal interaction between alcohol and nicotine, where alcohol consumption is unaffected by the presence or absence of nicotine access. In contrast, the addition of quinine temporarily suppressed alcohol preference and enhanced concurrent nicotine preference in both sexes. Chronic suppression of alcohol consumption with quinine produced a long-term enhancement of concurrent nicotine, but not water, preference in female mice, and enhanced both nicotine and water preference in male mice.

4.3 Materials and Methods

4.3.1 Animals and Reagents

12 male and 12 female C57BL/6J mice from The Jackson Laboratory (Sacramento, CA) acclimated to our facility for at least six days before beginning behavioral experiments at 55 days old. All mice underwent both experimental procedures. Mice were group housed in standard cages under a 12-h light/dark cycle until the start of behavioral experiments, after which they were individually housed. Food and water were freely available at all times. All animal procedures were in accordance with the Institutional Animal Care and Use Committee at the University of Minnesota, and conformed to NIH guidelines.

Alcohol (ethanol) (Decon Labs, King of Prussia, PA), and nicotine tartrate salt (Acros Organics, Thermo Fisher Scientific, Chicago, IL) were mixed with tap water to the concentrations reported for each experiment. The concentrations of nicotine are reported as free base, and nicotine solutions were not filtered or pH adjusted. The alcohol, nicotine and water bottles were unsweetened at all times. Quinine hydrochloride (Spectrum Chemical Manufacturing Corp, Gardena, CA) was added to the 20% alcohol bottle at concentrations of 100, 200, 500 and 1000 μM in Experiment 2.

4.3.2 Experiment 1: Effects of nicotine abstinence on concurrent alcohol consumption.

Mice were singly housed in custom cages that accommodated three drinking bottles (Ancare, Bellmore, NY) containing water, nicotine or alcohol at different concentrations. The concentrations for the first week consisted of 3% alcohol (v/v) in one bottle, 5 μg/mL nicotine in the second bottle and water in the third bottle. The concentrations for the second week were 10% alcohol and 15 μg/mL nicotine, and were 20% alcohol and 30 μg/mL nicotine for the third week. During the fourth week, the nicotine

bottle was removed and the 20% alcohol and water bottles remained available. During the fifth week, all three bottles were again presented at the 20% alcohol and 30 μg/mL nicotine concentrations. Food was freely available and the mice were not fluid restricted at any time. The bottles were weighed every other day and the solutions refreshed every 3-4 days. The positions of the bottles were alternated after each weighing to account for side preferences. Mice were weighed once a week. Fluid evaporation and potential dripping were accounted for by the presence of a set of alcohol, nicotine and water bottles on an empty control cage. The weight of fluid loss from these bottles was subtracted from all bottle weights throughout the study.

4.3.3 Experiment 2: The impact of quinine adulteration on concurrent alcohol and nicotine consumption.

Immediately after completion of Experiment 1, the mice proceeded to Experiment 2 without a break in alcohol or nicotine consumption. In Experiment 2a, quinine (100 μM) was added to the 20% alcohol bottle for 3 days (acute phase), while the water and 30 μg/mL nicotine bottles remained unaltered. In Experiment 2b, the quinine concentration in the 20% alcohol bottle was increased to 200, 500 and 1000 μM, with each concentration presented for 6 days (chronic phase). The 0 quinine concentrations reported were the average consumption and preference of 20% alcohol and 30 μg/mL nicotine during the prior week (Week 5 of Experiment 1). The bottles were weighed and rotated every day and the mice were weighed once a week. Fluid evaporation and bottle dripping were controlled for by the presence of a set of bottles on an empty control cage. The weight of fluid loss from these bottles was subtracted from all bottles throughout the study.

4.3.4 Statistical Analysis

The average daily alcohol (g/kg) and nicotine consumption (mg/kg) for each drug concentration was calculated based on the weight of the fluid consumed from the bottles,

the density of the solution (for alcohol only), and the weight of the individual mouse. The percent preference for alcohol, nicotine, and water bottles was calculated as the weight of the fluid consumed from the bottle of interest, divided by the summed weight of fluid consumed from all three bottles, multiplied by 100. All analyses were calculated using Prism 8.0 (GraphPad, La Jolla, CA). Data were tested for normality and variance.

For all experiments, data were analyzed by repeated measures (RM) 2-way ANOVA, followed by Sidak's multiple comparisons tests to examine the effect of sex and time. For all experiments, sex differences in the average consumption of alcohol (g/kg) and nicotine (mg/kg), and in the average preference for the alcohol, nicotine and water bottles are described first, followed by the time effects of forced nicotine abstinence (Experiment 1) or of quinine adulteration of alcohol (Experiment 2).

4.4 Results

4.4.1 Experiment 1: Effect of forced nicotine abstinence on concurrent alcohol consumption.

A schematic outline of our experiments is shown in **Figure 4.1**. In Experiment 1, we evaluated the effect of forced nicotine abstinence on concurrent alcohol consumption and preference. Male and female C57BL/6J mice had continuous access to alcohol (v/v), nicotine (μg/mL) and water for 3 weeks in a 3-bottle choice procedure, with drug concentrations of 3% alcohol and 5 μg/mL nicotine presented during Week 1, 10% alcohol and 15 μg/mL nicotine during Week 2 and 20% alcohol and 30 μg/mL nicotine presented during Week 3. During Week 4, the nicotine bottle was removed and mice had access to the 20% alcohol and water bottles. The nicotine bottle was re-introduced in Week 5. Drug consumption and preference data for the entire experiment (Weeks 1-5) was analyzed using RM 2-way ANOVA comparisons followed by Sidak's multiple comparisons tests.

We first examined the data for sex differences between male and female mice. For alcohol consumption, we found a significant sex by time interaction, a main effect of time and a main effect of sex ($F_{sexXtime}(4,88)=6.6061$, $P=0.0002$; $F_{sex}(1,22)=14.49$, $P=0.001$; $F_{time}(4,88)=26.39$, $P<0.0001$). Multiple comparisons tests showed that female mice consumed more average alcohol (g/kg/day) compared with male mice during Weeks 3-5 (**Figure 4.2A**). Female mice also consumed more nicotine (mg/kg/day) compared with male mice during Weeks 3 and 5 ($F_{sexXtime}(3,66)=3.070$, $P=0.03$; $F_{sex}(1,22)=8.776$, $P=0.007$; $F_{time}(3,66)=98.28$, $P<0.0001$, **Figure 4.2B**). For alcohol preference, we found a significant sex by time interaction, no main effect of sex and a main effect of time ($F_{sexXtime}(4,88)=2.928$, $P=0.03$; $F_{sex}(1,22)=0.4167$, $P=0.52$; $F_{time}(4,88)=19.84$, $P<0.0001$); however, multiple comparisons tests did not identify a difference between male and female alcohol preference at any week (**Figure 4.2C**). For nicotine preference, we found a main effect of time and no main effect of sex or a sex by time interaction ($F_{sexXtime}(3,66)=1.408$, $P=0.25$; $F_{sex}(1,22)=0.689$, $P=0.42$; $F_{time}(3,66)=7.631$, $P<0.001$, **Figure 4.2D**). Finally, for water preference we found main effects of sex and time without an interaction between sex and time ($F_{sexXtime}(4,88)=1.597$, $P=0.18$; $F_{sex}(1,22)=4.365$, $P=0.049$; $F_{time}(4,88)=78.26$, $P<0.0001$, **Figure 4.2E**).

We then examined the effect of forced nicotine abstinence during Week 4 on the consumption of 20% alcohol and 30 μg/mL nicotine, and the preference for each of the three bottles using Sidak's multiple comparisons tests, since we found main effects of time or interactions between sex and time. For alcohol consumption, we found that male mice had no significant differences in 20% alcohol consumption across Weeks 3-5, indicating that removal of the nicotine bottle had no effect on alcohol consumption (**Figure 4.3A**). Forced nicotine abstinence during Week 4 also did not affect 30 μg/mL nicotine consumption in male mice as the level of nicotine consumption for Weeks 3 and 5 were

not significantly different, indicating that no compensatory increase in nicotine consumption occurred after forced abstinence (**Figure 4.3A**). We found similar results in female mice, with no significant differences in 20% alcohol consumption across Weeks 3-5, and no significant differences in 30 μg/mL nicotine consumption across Weeks 3 and 5 (**Figure 4.3B**). For alcohol preference, we found no significant changes in alcohol preference across Weeks 3-5 in male mice (**Figure 4.3C**), or in female mice (**Figure 4.3D**). The preference for the 30 μg/mL nicotine bottle not significantly different across Weeks 3 and 5 for male (**Figure 4.3C**) or female mice (**Figure 4.3D**). Examining the water preference showed that the preference for the water bottle during Week 4 was significantly higher than during Weeks 3 or 5 in both males and females, suggesting that removal of the nicotine bottle elevated only water preference in both sexes (**Figure 4.3C-D**). Overall, Experiment 1 showed that female mice consumed more alcohol and nicotine than male mice, and forced nicotine abstinence during Week 4 had no effect on 20% alcohol or 30 μg/mL nicotine consumption or preference, but increased only the preference for the water bottle during Week 4 in both male and female mice.

	Expt 1					Expt 2			
Time	Week 1	Week 2	Week 3	Week 4	Week 5	3d	6d	6d	6d
A%:	3	10	20	20	20	20+100 Q	20+200 Q	20+500 Q	20+1000 Q
N μg/mL:	5	15	30		30	30	30	30	30
Water:	W	W	W	W	W	W	W	W	W

Figure 4.1. Schematic of experimental procedures.

Unsweetened alcohol % (A, v/v), nicotine (N, μg/mL) and water were presented in a 3-bottle choice consumption procedure. Quinine (Q, μM) was added to the 20% alcohol bottle in Experiment 2.

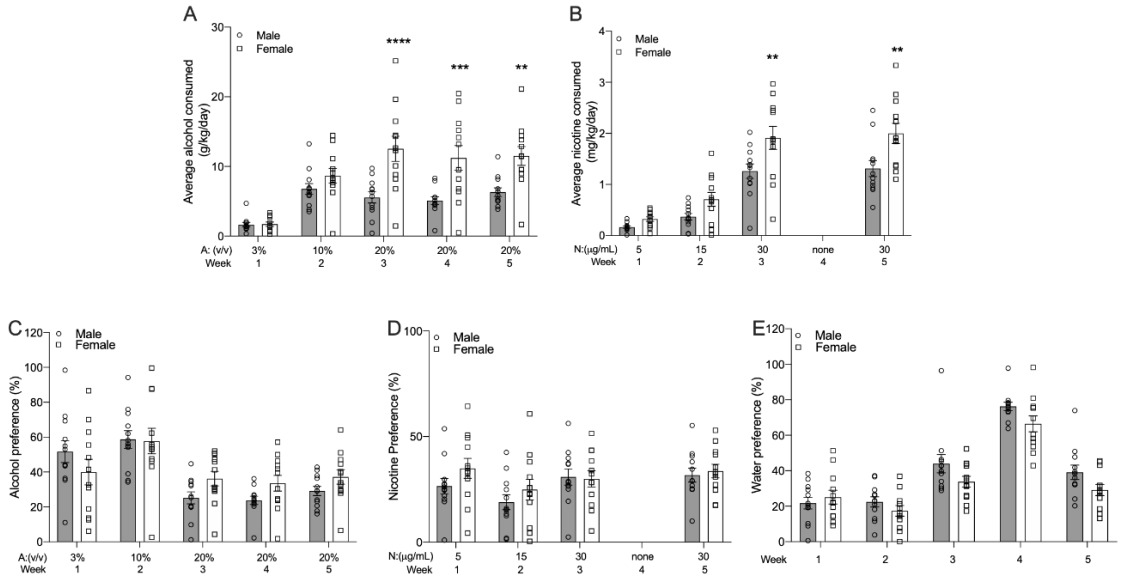

Figure 4.2. Female mice consume more alcohol and nicotine compared with male mice in Experiment 1 - effects of nicotine abstinence on concurrent alcohol consumption.

(A) Alcohol and **(B)** nicotine consumption by weight in male and female mice. **(C)** Alcohol, **(D)** nicotine and **(E)** water preference over time in male and female mice. Sidak's post-hoc test between male and female mice for the same week ***P*<0.01, ****P*<0.001, *****P*<0.0001. *n*=12 per sex, mean ± SEM.

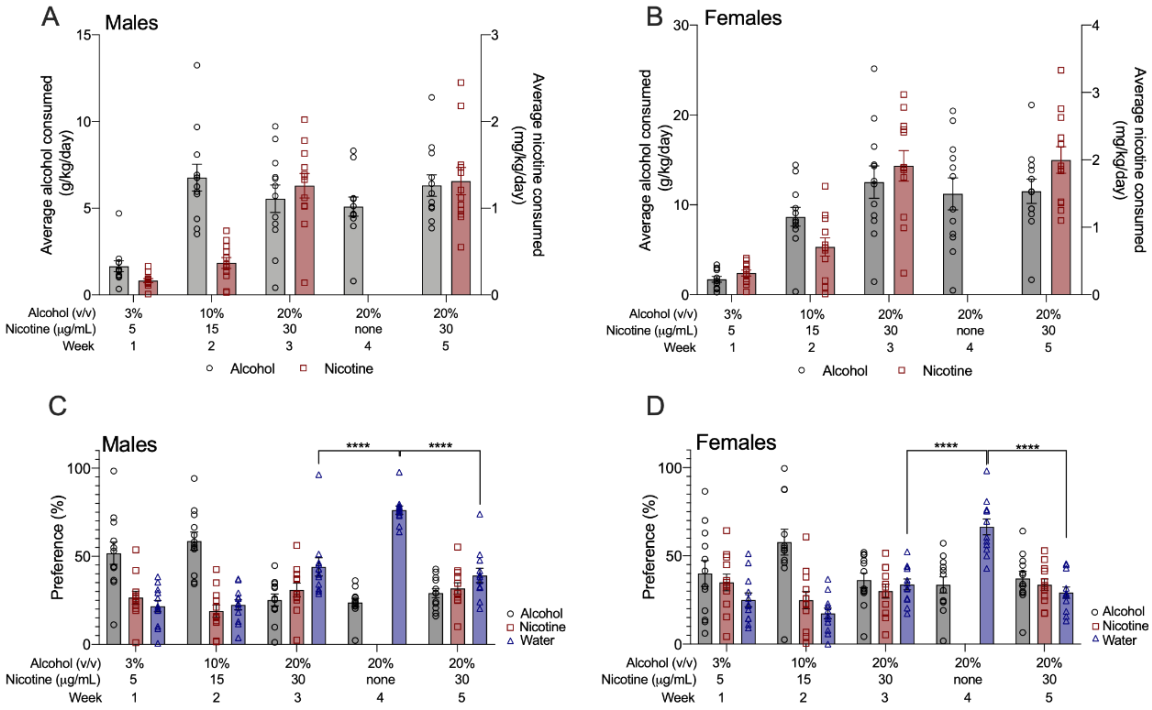

Figure 4.3. Nicotine forced abstinence increases concurrent water preference, and not alcohol preference, in male and female mice.

Average alcohol (g/kg) and nicotine (mg/kg) consumption in **(A)** male and **(B)** female mice. Preference for the alcohol, nicotine and water bottles for **(C)** male and **(D)** female mice. Removal of the nicotine bottle during Week 4 increased the preference for the water bottle but not the alcohol bottle in **(C)** male and **(D)** female mice. Sidak's post-hoc test ****P<0.0001 between Weeks 3 and 4, and between Weeks 4 and 5. n=12 per sex, mean ± SEM.

4.4.2 Experiment 2a: The impact of quinine adulteration on concurrent alcohol and nicotine consumption.

We tested the effect of quinine adulteration of 20% alcohol on concurrent alcohol and nicotine consumption in male and female C57BL/6J mice. Quinine (100 μM) was added to the 20% alcohol bottle for 3 days, and the average daily consumption of alcohol and nicotine during quinine adulteration was compared with the average daily consumption during the prior week when no quinine was present (Week 5 of Experiment 1). We first examined consumption and preference across sex as in Experiment 1. For alcohol consumption, we found a significant sex by time interaction, a main effect of sex and a main effect of time ($F_{sexXtime}(3,66)=4.142$, $P=0.009$; $F_{sex}(1,22)=9.280$, $P=0.006$; $F_{time}(3,66)=36.37$, $P<0.0001$). Multiple comparisons testing showed that female mice consumed more alcohol compared with male mice for all time points except for Day 1 (**Figure 4.4A**). For nicotine consumption, there were main effects of sex and time without a significant interaction, with females consuming more nicotine compared with males ($F_{sexXtime}(3,66)=0.2655$, $P=0.85$; $F_{time}(3,66)=3.367$, $P=0.02$; $F_{sex}(1,22)=8.908$, $P=0.007$, **Figure 4.4B**). For both alcohol and nicotine preference, there were main effects of time with no main effects of sex, or sex by time interactions (alcohol preference: $F_{sexXtime}(3,66)=2.415$, $P=0.07$; $F_{time}(3,66)=35.99$, $P<0.0001$; $F_{sex}(1,22)=0.87$, $P=0.36$; nicotine preference: $F_{sexXtime}(3,66)=0.088$, $P=0.97$; $F_{time}(3,66)=17.03$, $P<0.0001$; $F_{sex}(1,22)=0.2834$, $P=0.60$). For water preference, we found no main effect of sex or time, and no interaction between sex and time ($F_{sexXtime}(3,66)=1.450$, $P=0.24$; $F_{time}(3,66)=0.05$, $P=0.98$; $F_{sex}(1,22)=1.846$, $P=0.19$, preference data for all three bottles are shown separately by sex on **Figure 4.5C** and **4.5D**).

We then examined alcohol and nicotine consumption, and preference for each bottle over time, since we observed main effects of time or interactions between sex and

time. We found that 100 μM quinine temporarily suppressed alcohol consumption and alcohol preference in male mice (**Figure 4.5A** and **4.5C**) and in female mice (**Figure 4.5B** and **4.5D**) on Day 1. As female mice consumed more alcohol compared with male mice, we compared the magnitude of the quinine-adulterated alcohol suppression on Day 1 as a percent decrease from 0 levels, and found no significant difference between sexes (male: 74.5 ± 11.1% decrease; female: 76.7 ± 12.0% decrease, t=0.130, P=0.90). Quinine suppression of alcohol consumption and preference was temporary in both sexes, as both male and female mice overcame the 100 μM quinine suppression on Day 2. For concurrent nicotine preference, we found that the addition of 100 μM quinine to the 20% alcohol bottle produced a temporary increase in nicotine preference on Day 1 in male and female mice (**Figure 4.5C** and **4.5D**). There was no significant increase in nicotine consumption on Day 1 in either sex. As there were no main effects of sex or time on water preference, as described above, the overall effect of 100 μM quinine adulteration of 20% alcohol was to reduce alcohol consumption and preference, and increase nicotine but not water preference in male and female mice.

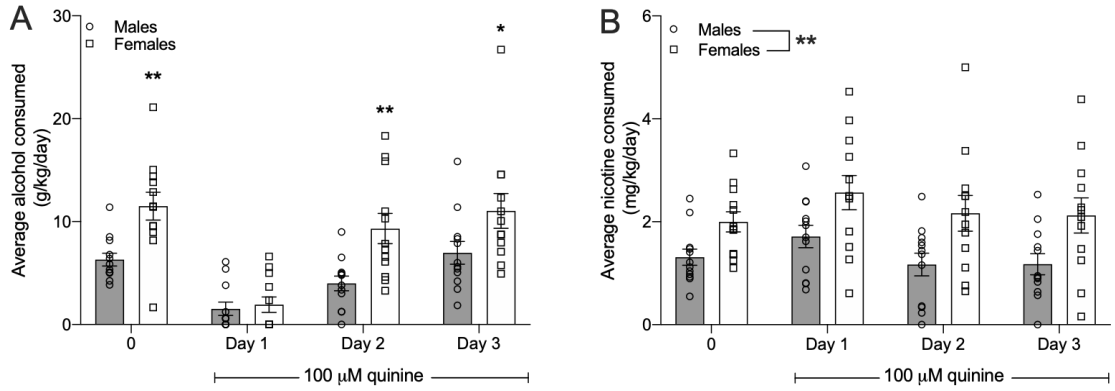

Figure 4.4. Female mice consume more alcohol and nicotine compared with male mice in Experiment 2a – effects of acute quinine adulteration of alcohol.

(A) Alcohol consumption by weight in male and female mice. Sidak's post-hoc test between male and female mice for the same time point *P<0.05, **P<0.01.

(B) Nicotine consumption by weight in male and female mice. There was a main effect of sex on nicotine consumption. n=12 per sex, mean ± SEM

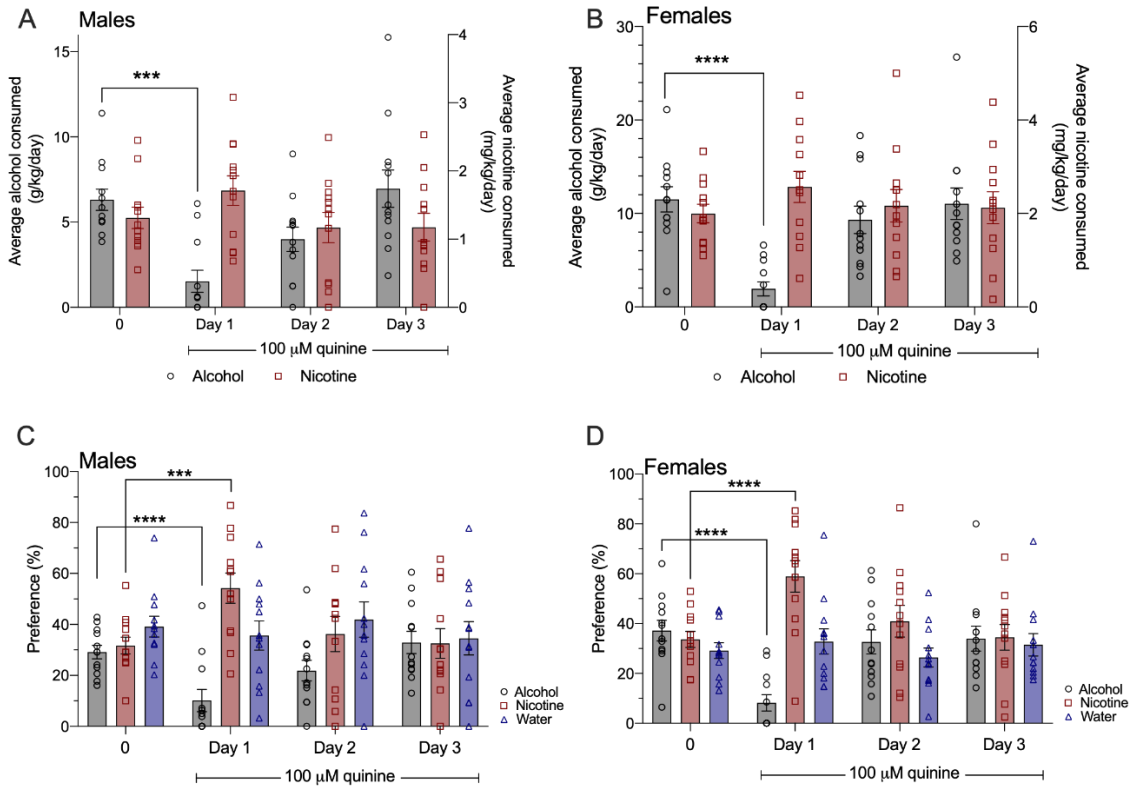

Figure 4.5. Temporary quinine-induced suppression of alcohol intake produces an increase in concurrent nicotine preference.

Addition of 100 μM quinine to the 20% alcohol bottle occurred on Days 1-3. Quinine suppressed alcohol consumption on Day 1 in **(A)** male mice and **(B)** female mice compared to the average alcohol consumption at the 0 quinine concentration. Sidak's multiple comparisons test ***P<0.0001, ****P<0.0001 for Day 1 compared with 0. Quinine suppressed alcohol preference and increased nicotine preference on Day 1 in **(C)** male mice and **(D)** female mice. Sidak's multiple comparisons test ***P<0.0001, ****P<0.0001 for Day 1 compared with the 0 quinine concentration for alcohol and nicotine preference. n=12 per sex, mean ± SEM

4.4.3 Experiment 2b: The impact of chronic quinine adulteration on concurrent alcohol and nicotine consumption.

To determine the effect of chronic quinine adulteration of alcohol consumption on concurrent alcohol and nicotine intake, the quinine concentration in the 20% alcohol bottle was increased to 200, 500 and 1000 μM, with each concentration presented for 6 days. We first examined average daily drug consumption and preference across sex as in Experiment 1. For alcohol consumption, we found a significant interaction between sex and concentration, a main effect of sex and a main effect of concentration ($F_{sexXconcentration}(4,88)=3.602$, $P=0.009$; $F_{sex}(1,22)=14.01$, $P=0.001$; $F_{concentration}(4,88)=47.13$, $P<0.0001$). Multiple comparisons tests showed that female mice consumed more alcohol compared with male mice at the 0, 100 and 200 μM quinine concentrations (**Figure 4.6A**). For 30 μg/mL nicotine consumption, we found a significant interaction between sex and concentration, a main effect of sex and a main effect of concentration ($F_{sexXconcentration}(4,88)=5.156$, $P=0.0009$; $F_{sex}(1,22)=14.37$, $P=0.001$; $F_{concentration}(4,88)=8.044$, $P<0.0001$). Multiple comparisons tests showed that female mice consumed more nicotine compared with male mice at the 200, 500 and 1000 μM quinine concentrations (**Figure 4.6B**). For alcohol preference, we found a main effect of concentration with no main effect of sex, or a sex by concentration interaction ($F_{sexXconcentration}(4,88)=0.958$, $P=0.43$; $F_{concentration}(4,88)=52.54$, $P<0.0001$; $F_{sex}(1,22)=1.318$, $P=0.26$, alcohol preference for each sex is shown separately in **Figure 4.6F** and **4.6G**). For nicotine preference, we found a significant interaction between sex and concentration, a main effect of concentration and no main effect of sex ($F_{sexXconcentration}(4,88)=2.835$, $P=0.03$; $F_{sex}(1,22)=1.704$, $P=0.21$; $F_{concentration}(4,88)=13.76$, $P<0.0001$); however, multiple comparisons tests did not reveal a significant difference in nicotine preference between sex at any concentration (**Figure 4.6F** and **4.6G**). We also found main effects of sex and

concentration with no interaction between sex and concentration for water preference, with male mice having an overall greater preference for water compared with female mice ($F_{sexXconcentration}(4,88)=0.893$, $P=0.47$; $F_{concentration}(4,88)=8.695$, $P<0.0001$; $F_{sex}(1,22)=5.033$, $P=0.04$; **Figure 4.6F** and **4.6G**).

We then examined alcohol and nicotine consumption, and preference for each bottle over the increasing quinine concentrations, since we observed main effects of quinine concentration or interactions between sex and quinine concentration. We found that the average daily consumption and preference of 20% alcohol was significantly suppressed at all quinine concentrations in both male (**Figure 4.6D** and **4.6F**) and female mice (**Figure 4.6E** and **4.6G**). As female mice consumed more alcohol compared with male mice, we calculated the quinine-induced alcohol suppression as a percent of baseline alcohol consumption at the 0 quinine level. We found no significant difference in the magnitude of quinine-induced suppression between sexes over the increasing quinine concentrations, suggesting that quinine suppressed alcohol consumption to the same proportion in males and females, even though female mice consume more g/kg alcohol ($F_{sexXconcentration}(3,66)=0.05$, $P=0.99$; $F_{sex}(1,22)=0.397$, $P=0.53$, $F_{time}(3,66)=31.99$, $P<0.0001$, **Figure 4.6C**).

Chronic quinine adulteration of alcohol did not alter nicotine consumption at any time point in male mice (**Figure 4.6D**), whereas female mice increased their nicotine consumption at the 200, 500 and 1000 μM quinine concentrations compared with the 0 quinine concentration (**Figure 4.6E**). In male mice, we found that nicotine preference significantly increased when 100 and 1000 μM quinine was added to the 20% alcohol bottle, and water preference was significantly increased when 500 and 1000 μM quinine was added to the 20% alcohol bottle (**Figure 4.6F**). In female mice, the preference for the nicotine bottle was increased at all quinine concentrations, whereas water preference was

not significantly changed at any quinine concentration (**Figure 4.6G**). Overall, these data showed that quinine suppressed alcohol consumption and preference equally in male and female mice, but female mice responded to chronic quinine adulteration of alcohol by increasing the consumption and preference of nicotine without changing water preference, whereas male mice increased both nicotine and water preference.

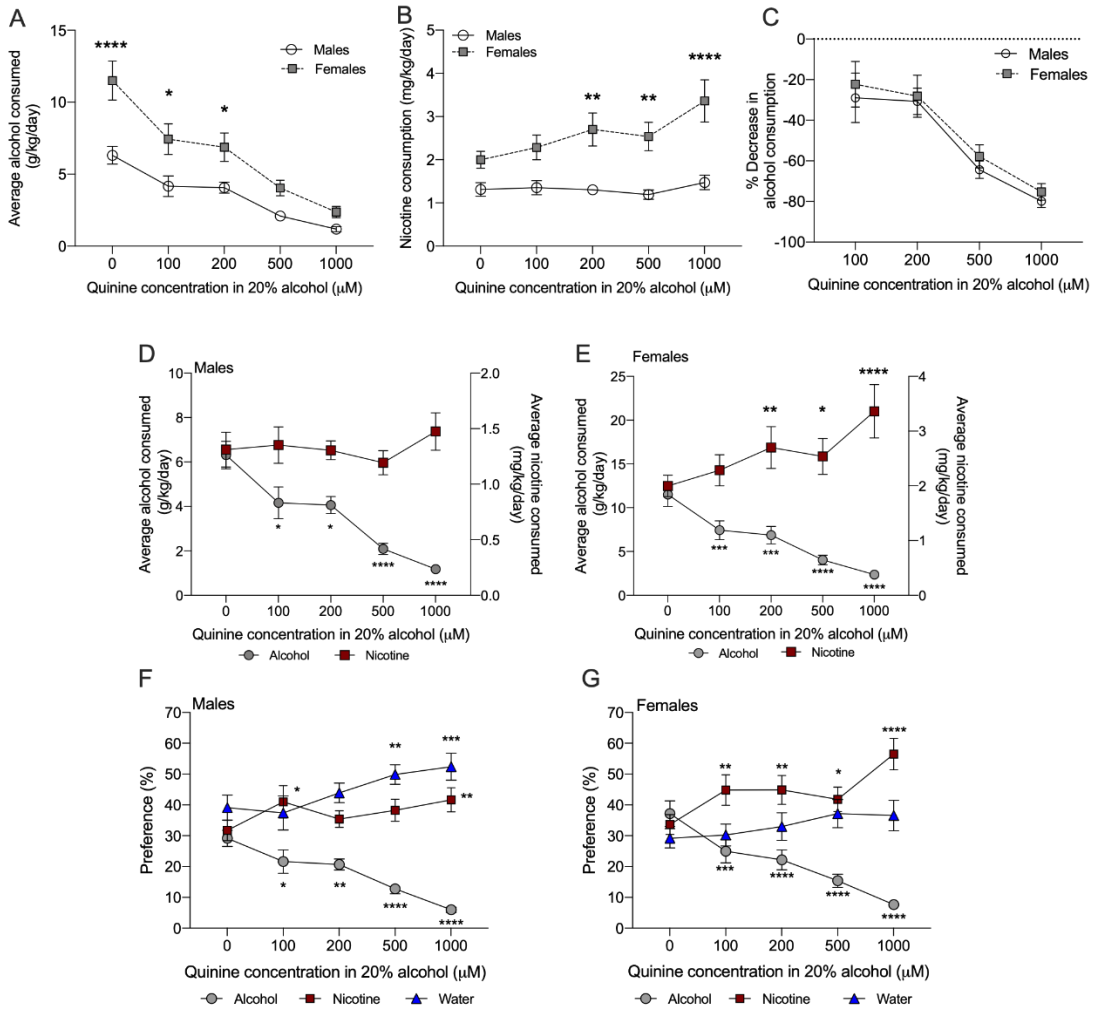

Figure 4.6. Chronic suppression of alcohol intake by quinine increases nicotine consumption and preference.

(A) Female mice consume more alcohol and **(B)** more nicotine compared with male mice. Sidak's post-hoc test between male and female mice at the same concentration **P*<0.05, ***P*<0.01, *****P*<0.0001. **(C)** Male and female mice have the same percent decrease in alcohol consumption over increasing quinine concentrations. **(D)** In male mice, increasing concentrations of quinine suppressed alcohol consumption without increasing nicotine consumption, whereas **(E)** in female mice, increasing concentrations of quinine suppressed alcohol consumption and increased concurrent nicotine consumption. Sidak's multiple comparisons tests ***P*<0.01, ****P*<0.001, *****P*<0.0001 compared with the 0 quinine level within drug. **(F)** In male mice, increasing concentrations of quinine reduced alcohol preference, and increased nicotine and water preference, whereas **(G)** in female mice, increasing concentrations of quinine reduced alcohol preference and increased nicotine, but not water, preference. Sidak's post-hoc test **P*<0.05, ***P*<0.01, ****P*<0.001, *****P*<0.0001 compared with the 0 quinine level within each bottle. *n*=12 per sex, mean ± SEM.

4.5 Discussion

In this study, we used a 3-bottle choice procedure that allows for voluntary, chronic co-consumption of alcohol and nicotine to investigate the suppression and enhancement of concurrent drug intake in male and female C57BL/6J mice. We and others have published data showing that female mice consume significantly more drug compared with male mice (Hwa et al., 2011; Kamens, Andersen, & Picciotto, 2010; Kamens, Hoft, Cox, Miyamoto, & Ehringer, 2012; O'Rourke et al., 2016; Touchette et al., 2018), and here we also report significant sex differences in alcohol and nicotine consumption in all our experiments. When we examined the impact of forced nicotine abstinence in Experiment 1, we found that alcohol consumption and preference is unaffected by forced nicotine abstinence or the re-introduction of nicotine access in both male and female C57BL/6J mice. In Experiment 2a, we found that addition of 100 μM quinine to the 20% alcohol bottle temporarily suppressed alcohol consumption and preference, while increasing concurrent nicotine preference in both male and female mice. In Experiment 2b, we found that chronic suppression of alcohol consumption with increasing concentrations of quinine increased both nicotine and water preference in male mice, and increased nicotine preference without affecting water preference in female mice. Our previous study showed that forced alcohol abstinence produced an enhancement in concurrent nicotine consumption and preference in male and female C57BL/6J mice (O'Rourke et al., 2016). Together with this study, our work showed that alcohol intake is unresponsive to the presence or absence of the nicotine bottle, but nicotine intake is influenced by the absence of alcohol consumption or by the adulteration of the alcohol bottle with quinine. In both studies, we used a 1-week forced abstinence period and it is possible that changes in concurrent alcohol consumption may require a longer abstinence duration.

One characteristic of AUD is the continued consumption of alcohol despite adverse consequences. Quinine adulteration of alcohol consumption in rodents has been frequently used to model aversion-resistant alcohol intake using quinine concentrations ranging from 25-500 μM (F. Woodward Hopf & Lesscher, 2014; Frederic Woodward Hopf et al., 2010; Lei et al., 2016; Lesscher, Van Kerkhof, & Vanderschuren, 2010; Sneddon et al., 2018; Spanagel et al., 1996). Quinine adulteration of alcohol consumption had not been previously examined in conjunction with concurrent nicotine consumption. In this study, we found that addition of 100 μM quinine to the alcohol bottle temporarily suppressed alcohol consumption and preference in both male and female mice. Interestingly, the suppression of alcohol intake was associated with increased preference for the nicotine bottle and not the water bottle. These data suggest that the mice compensate for the reduction in quinine-adulterated alcohol intake by selectively increasing preference for the unsweetened nicotine bottle, even though the water bottle is readily available. These results support our previous findings that nicotine consumption and preference is enhanced during forced alcohol abstinence (O'Rourke et al., 2016), and show that suppression of alcohol consumption, either by removing access to the alcohol bottle or reducing the palatability of alcohol, produces an enhancement of concurrent nicotine consumption.

The suppression of alcohol intake with 100 μM quinine was transient, as male and female mice overcame the aversion within one day. Our mice had been co-consuming alcohol and nicotine for 5 weeks prior to the introduction of quinine. A prior study in male C57BL/6J mice required 8 weeks of intermittent access consumption of 15% alcohol before resistance to 100 and 250 μM quinine develops (Lesscher et al., 2010). In addition, prior studies in rats have required a minimum of 3 months of intermittent alcohol consumption before the development of aversion resistant alcohol consumption to 0.1 g/L

quinine (277 μM) in 5-20% alcohol concentrations (Frederic Woodward Hopf et al., 2010; Spanagel et al., 1996). However, a recent study by Lei and colleagues (2016) shows that a single session of unadulterated alcohol consumption is sufficient to produce aversion-resistant alcohol consumption to 100 μM quinine in 15% alcohol in male C57BL/6J mice (Lei et al., 2016), suggesting the duration of alcohol consumption required to achieve quinine resistance may be days, rather than weeks.

We increased the concentration of quinine in the alcohol bottle to determine the effect of long-term suppression of alcohol consumption on concurrent nicotine intake. We found that alcohol consumption was suppressed in a concentration-dependent manner in both male and female mice. Male mice showed increased preference for the nicotine and water bottles as the quinine concentration increased, suggesting that male mice compensated for the long-term suppression of alcohol intake by increasing their nicotine and water preference. In contrast, female mice showed increased nicotine consumption and preference as the quinine concentration increased, and did not show any increase in water preference. Thus, our data suggest that female mice compensated for the long-term suppression of alcohol intake by increasing their nicotine intake. These data illustrate an important sex difference in compensatory drug consumption and highlight the need to continue investigating both sexes to identify important differences that can influence addiction-related behaviors and potential treatment strategies. Nearly all of the prior research on aversion-resistant drinking has focused on male animals. One recent study by Sneddon and colleagues (2019) shows no sex difference in the proportion of 100 or 250 μM quinine-suppression of alcohol drinking in male and female C57BL/6J mice, even though female mice consume more 15% alcohol than males (Sneddon et al., 2018). Our data supports this finding, as male and female mice showed similar percent suppression of alcohol consumption as a result of increasing concentrations of quinine.

One limitation of our study is the lack of blood alcohol and nicotine levels. Since the mice are receiving access to the alcohol and nicotine bottles 24 hours a day, the consumption of alcohol and nicotine is spread out over time. Measuring blood alcohol and nicotine concentrations at an arbitrary time point is difficult due to the unsynchronized drug consumption and the fast metabolism of alcohol and nicotine in mice.

Alcohol and nicotine addiction are heritable disorders that share common genetic factors (Swan, Carmelli, & Cardon, 1996, 1997; True et al., 1999). The majority of tobacco smokers also use alcohol, yet smoking cessation trials frequently incorporate alcohol-related exclusion criteria and do not track co-use of alcohol in their subjects (Leeman, Huffman, & O'Malley, 2007), thus data on the treatment of co-users are lacking. Nearly one quarter of smokers report hazardous alcohol consumption patterns as defined by the NIAAA (Toll et al., 2012). These individuals have lower smoking cessation rates compared with moderate alcohol drinkers, highlighting that some co-users are less likely to successfully quit alcohol and nicotine use compared with other co-users (Toll et al., 2012). Varenicline (an $\alpha 4\beta 2$ nicotinic acetylcholine receptor (nAChR) partial agonist) is approved for smoking cessation (Rollema et al., 2010), and naltrexone (an opioid receptor antagonist) and acamprosate (an NMDA receptor antagonist) are approved for alcohol use disorder in the United States (Franck & Jayaram-Lindström, 2013). Studies in alcohol-preferring female rats shows that varenicline reduces nicotine self-administration but has no effect on concurrent alcohol intake, and naltrexone reduces alcohol intake but has no effect on concurrent nicotine self-administration (Maggio et al., 2018; Waeiss et al., 2019), suggesting that monotherapy may be ineffective for combination alcohol and nicotine use disorder. Indeed, varenicline has shown mixed results in reducing alcohol consumption in human studies (de Bejczy et al., 2015; Litten et al., 2013; Mitchell, Teague, Kayser, Bartlett, & Fields, 2012; O'Malley et al., 2018; Plebani et al., 2013), and naltrexone and

acamprosate fail to reduce cigarette smoking (Fucito et al., 2012; Kahler et al., 2017). Dual pharmacological treatment, such as combining naltrexone with nicotine replacement therapy, has been incorporated in trials to enhance the likelihood of successful alcohol and smoking abstinence (Kahler et al., 2017; Toll et al., 2010).

Pre-clinical research on combination alcohol and nicotine consumption will be necessary to understand the complex relationship between alcohol and nicotine co-use to help identify novel drug targets and strategies that may be more helpful in treating human co-use. Our mouse model can assist in the investigation of alcohol and nicotine interactions and optimization of treatment strategies, as it enables us identify how alcohol and nicotine influence co-consumption while controlling for environment, experience and genetics. Our previous work using this 3-bottle choice model showed that forced alcohol abstinence increased nicotine consumption, and resumption of alcohol access produced a compensatory increase in alcohol consumption (O'Rourke et al., 2016). In this study, we find that forced nicotine abstinence does not affect alcohol consumption, and there is no compensatory increase in nicotine consumption after nicotine access has resumed. Together, our work demonstrates that in mice, alcohol intake is unresponsive to the presence or absence of the nicotine bottle, but nicotine intake is influenced by the absence of alcohol consumption or by the adulteration of the alcohol bottle with quinine. Our data suggest that if alcohol and nicotine cessation cannot occur simultaneously, then nicotine cessation, rather than alcohol cessation, should occur first so that the increased nicotine consumption due to alcohol unavailability can be avoided. In summary, our data highlight a complex interaction between alcohol and nicotine co-consumption. Further behavioral and molecular dissection of these interactions will provide a better understanding of the neurobiology underlying alcohol and nicotine co-use.

4.6 Funding and Disclosures

This work was supported by the National Institute of Health grants T32DA007234 (MCD, JKM), F31AA026782 (JKM), R01DA034696 (KW) and R01AA026598 (AML). The authors have no conflicts of interest.

Chapter 5 : Discussion

5.1 General Summary

Substance Use disorder accounts for a substantial proportion of healthcare costs, negative health outcomes and deaths in America each year. Effective treatments for SUD are currently lacking, highlighting the need to gain a greater understanding of brain mechanisms underlying SUD and resulting drug use patterns in order to better inform targets for medications and other treatment strategies. Although mechanisms underlying SUD are not well understood, DA neurons in the VTA have been implicated in numerous drug-related behaviors, and therefore serve as a promising node to be assessed.

This dissertation contains information discussing how drugs of abuse are known to increase DA levels in the VTA and downstream regions in order to exert their effects. **Chapters 2** and **3** have a particular focus on regulation of VTA DA neurons, and how disruptions in this regulatory system can lead to adverse outcomes. In addition to discussing how changes in regulation of neural circuits can affect drug-related behaviors, this dissertation work also discusses how consumption of one drug of abuse can affect the consumption of another drug of abuse in **Chapter 4**. The conclusions from this work provide insights that are beneficial to inform further research into pharmacotherapies and other treatment strategies for patients with SUD.

5.1.1 VTA DA neurons affect sensitivity to and consumption of drugs

Drugs of abuse are typically studied in isolation, as it gives a clearer picture of how the drug is acting in the brain and how changes in brain circuitry can affect this action. As such, **Chapters 2** and **3** discuss how manipulations of VTA DA neuron inhibitory signaling affect the sensitivity to and consumption of 3 different drugs of abuse administered independently. Previous work from our lab and others has shown that VTA DA $G_{i/o}$ coupled

GPCR-dependent signaling plays a critical role in dug sensitivity, but the relative influence of individual GPCRs was not assessed (Kotecki et al., 2015; McCall et al., 2019). Work in **Chapter 2** addresses this question, as it describes how loss of either $GABA_BR$ or D_2R in VTA DA neurons affects cocaine and morphine sensitivity (**Fig. 2.3, 2.4, 2.5**). Results show that individual GPCR ablation leads to increased cocaine sensitivity but has no effect on morphine sensitivity (**Fig. 2.3, 2.5**). This is in line with previous studies that showed the importance of D_2R- and $GABA_BR$-dependent signaling in cocaine sensitivity, but that $GABA_BR$-dependent signaling didn't seem to play a role in morphine sensitivity (De Jong et al., 2015; Edwards et al., 2017). Our manipulations provide the added benefit of producing a complete ablation of GPCR-dependent currents, as the previous studies mentioned only reported partial GPCR knock-down. In addition, our approach allows direct comparison between $GABA_BR$ or D_2R manipulations, as the same mice and behavior are used for all conditions.

Further, our results show that there is a sex difference in the relative influence of D_2R- and $GABA_BR$-dependent signaling on VTA DA neuron inhibition and cocaine sensitivity. D_2R-dependent somatodendritic currents in VTA DA neurons were significantly larger in drug-naive females compared to males (**Fig. 2.2**), suggesting a greater influence of D_2R-dependent signaling in the somatodendritic compartment of VTA DA neurons in females. Female control animals also displayed a different cocaine-induced activity pattern compared to males; females had a rapid increase in activity followed by a fairly rapid decrease after the peak, whereas males had a slower increase followed by a plateau and a gradual decrease (**Fig. 2.4**). Additionally, loss of D_2R-dependent inhibitory signaling significantly increased cocaine sensitivity in both males and females, but loss of $GABA_BR$-dependent inhibitory signaling only significantly increased cocaine sensitivity in males (**Fig. 2.3**). Together these data suggest that D_2R- but not $GABA_BR$-dependent inhibition

of VTA DA neurons plays an important role in modulating response to cocaine in females, whereas both D_2R- and $GABA_B$R-dependent inhibition of VTA DA neurons modulates response to cocaine in males. It is possible that the D_2R plays a more important role in the somatodendritic region in females and the terminal region in males, therefore mediating larger amplitude of somatodendritic D_2R-dependent currents in females compared to males, and locomotor activity pattern differences in male and female control mice. In further support of this, loss of VTA DA neuron D_2R normalized the sex difference in males and females, suggesting that this receptor plays an important role in mediating sex-dependent differences in drug response. These results highlight sex differences in the underlying inhibitory architecture moderating VTA DA neurons, which plays an important role in drug-related behaviors.

Work in **Chapter 3** expands upon the idea that GPCR-dependent inhibition of VTA DA neurons is critical to modulate drug-related behaviors. We utilized an RGS protein, which is a regulator of GPCR-dependent signaling, to enhance and diminish VTA DA neuron GPCR-dependent signaling. The R7 family of RGS proteins plays a critical role in promoting the deactivation of $G_{i/o}$ coupled GPCRs, therefore loss of R7 RGS proteins results in the enhancement of GPCR dependent inhibition. The effects of R7 RGS proteins on GPCR-dependent currents have been reported in various cell populations, but data in VTA DA neurons had not previously been explored. Experiments in **Chapter 3** address how loss of the R7 RGS protein RGS6 affects VTA DA neuron D_2R- and $GABA_B$R-dependent signaling and alcohol consumption. Results indicate that loss of RGS6 produces enhanced amplitude of D_2R-dependent signaling and prolonged deactivation of $GABA_B$R-dependent signaling (**Fig. 3.3, 3.4**). Additionally, manipulations overexpressing RGS6 in VTA DA neurons produced diminished amplitude of D_2R-dependent currents, suggesting a negative regulatory role for RGS6 in D_2R-dependent inhibition (**Fig. 3.5**).

These changes in current dynamics are consistent with previous reports assessing R7 RGS proteins in other cell types, as RGS proteins have been reported to modulate both signaling amplitude and kinetics in a cell type- and GPCR-specific manner (A. Anderson et al., 2020; Maity et al., 2012; Ostrovskaya et al., 2014; Z. Rahman et al., 2003).

We also tested how loss of RGS6 in VTA DA neurons affects binge alcohol consumption. We first tested constitutive *RGS6*$^{-/-}$ mice and saw that both male and female *RGS6*$^{-/-}$ mice consumed less alcohol compared to WT, mirroring previous studies assessing constitutive *RGS6*$^{-/-}$ in a continuous-access alcohol consumption paradigm (Stewart et al., 2015). Similar to constitutive *RGS6*$^{-/-}$, female mice lacking RGS6 specifically in VTA DA neurons consumed less alcohol compared to controls (**Fig. 3.6**). Male mice lacking RGS6 specifically in VTA DA neurons, on the other hand, consumed the same amount of alcohol compared to controls (**Fig. 3.6**). These data suggest that RGS6 is important for modulating alcohol consumption in both male and female mice, as constitutive *RGS6*$^{-/-}$ mice of both sexes consume less alcohol, but this effect may only be mediated by VTA DA neurons in females. This is not completely surprising, as numerous sexually dimorphic brain circuits have been reported, resulting in distinct behavioral patterns between males and females (Anker & Carroll, 2011; Becker & Koob, 2016; Fattore et al., 2008). The sex effect reported here may also be due to confounding variables, such as age or weight of the mice, resulting in very low levels of alcohol consumption in males resulting in a possible floor effect (**Fig. 3.6, 3.7**). Together, work in **Chapter 3** characterizes RGS6 as an important modulator of GPCR-dependent inhibition of VTA DA neurons and alcohol consumption.

As a whole, work in **Chapter 2 and 3** expand the understanding of how different aspects of GPCR-dependent inhibition play similar yet distinct roles in modulating VTA DA neuron signaling and drug-related behavior. This enhanced understanding of

mesocorticolimbic communication may provide insights into potential drug targets to exploit for pharmacotherapies to treat SUD. Drug treatments that enhance inhibitory signaling in the mesocorticolimbic system have been an enticing avenue of research, but many of these substances come with mixed efficacy for various SUDs and are accompanied by many negative side effects such as sedation and anhedonia (Chan et al., 2019; Kampman, 2019; K Witkiewitz et al., 2019). One such drug, the $GABA_BR$ agonist baclofen, has been approved for treatment for AUD in Europe. Baclofen has shown some promise in reducing harmful alcohol consumption, withdrawal symptoms, and relapse, but only in certain patient populations (De Beaurepaire, Sinclair, et al., 2019). The dosing for baclofen is especially difficult, as there are many $GABA_BRs$ expressed throughout the brain being affected by this drug therapy and therefore many negative off-target effects. Finding a way to target specific elements of GPCR-dependent signaling within VTA DA neurons may be one way to take advantage of the positive outcomes from baclofen treatment while reducing the unwanted side effects. A greater understanding of the GPCR-dependent signaling architecture within VTA DA neurons would provide a critical steppingstone in this endeavor.

5.1.2 Patterns of concurrent drug consumption

As humans tend to have multiple co-occurring substance use and/or mental health disorders, assessing drugs administered together as well as individually could provide insights into potential synergies that affect behavioral or neural processes differently than when used in isolation. Although studying concurrent use of drugs could make it difficult to understand mechanistic insights, it is important to assess the effects drugs might have on one another in order to adequately address the human condition. In this vein, work in **Chapter 4** delves into behavioral differences when drugs are consumed both alone and together. Previously our lab developed a 3-bottle choice oral consumption paradigm where

mice had concurrent access to alcohol, nicotine and water (O'Rourke et al., 2016). After 3 weeks of continuous access to 3 separate solutions of alcohol, nicotine and water, the alcohol bottle was removed for one week to assess nicotine consumption during forced alcohol abstinence. Mice increased the amount of nicotine that they consumed during alcohol abstinence, suggesting that mice compensated for the lack of alcohol with excess nicotine consumption. The work in **Chapter 4** addresses the reciprocal question; after 3 weeks of access to 3 separate solutions of alcohol, nicotine and water, the nicotine bottle was removed for one week to assess alcohol consumption during forced nicotine abstinence. Interestingly, during the period of nicotine abstinence the mice did not change the level of alcohol consumed to compensate for the absence of nicotine (**Fig. 4.3**). This discrepancy points out a key difference in consumption patterns of alcohol and nicotine and provides interesting insights about how abstaining from one substance may affect seeking/taking of another.

Chapter 4 also assesses outcomes of a more "voluntary" decrease in alcohol consumption on concurrent nicotine consumption. The same 3-bottle choice paradigm was used but rather than forcing abstinence by removing the alcohol bottle, increasing concentrations of quinine, a bitter tastant, were added to the alcohol bottle. Quinine adds an aversive taste, resulting in mice choosing to drink less of the alcohol solution. Drug dependent rodents have been shown to continue seeking and taking drug despite negative consequences such as the addition of quinine or administration of a foot-shock (Domi et al., 2021; F. Woodward Hopf & Lesscher, 2014; Frederic Woodward Hopf et al., 2010; Lei et al., 2016; Lesscher et al., 2010; Sneddon et al., 2018; Spanagel et al., 1996). The addition of quinine to the alcohol solution allowed the assessment of whether mice continue to drink alcohol despite the aversive taste, or if they decrease alcohol consumption and compensate with nicotine as seen with forced alcohol abstinence in

O'Rourke et al. 2016. We saw that similar to the previous study, mice initially decrease their alcohol consumption and compensate with increased nicotine consumption (**Fig. 4.5**). After chronically increasing the amount of quinine in the alcohol solution, we observed a sex difference in levels of compensatory nicotine consumption; females tended to escalate their nicotine intake and males tended to escalate their water intake to a greater degree than nicotine (**Fig. 4.6**). This sex difference further emphasizes the necessity to gain a greater understanding of the underlying circuitry driving alcohol and nicotine co-consumption in order to develop more personalized treatment strategies.

Although mice are different from humans in many ways, this model of alcohol vs. nicotine compensation can provide insights into potential patterns and interactions of drug consumption, as attempting to discontinue drug use is frequently a chosen behavior rather than forced. Human clinical data is still inconclusive as there is a lot of heterogeneity in patient populations, but many people with alcohol and nicotine dependence who choose to abstain from alcohol report smoking to cope with urges to drink alcohol (O'Malley et al., 2018). Conversely, studies report that there is not a significant increase in binge alcohol consumption during smoking cessation treatment (Hammett et al., 2019; Verplaetse & McKee, 2017). Our results along with these human reports suggest that quitting nicotine use before quitting alcohol use may provide better patient outcomes for certain populations, as it could result in less drug compensation.

5.2 Future Directions

The work presented in this dissertation provides novel insights into how elements of the natural reward circuitry play a role in drug-related behaviors, and how patterns of behavior vary based on sex and drug(s) of abuse available. These insights provide the

groundwork for future studies to build a more complete framework of understanding around the biological substrates underlying SUD.

5.2.1 Specific Neuron Populations

The VTA consists of a wide variety of neurons, with the largest proportion being DA neurons. VTA DA neurons, once considered to be a homogeneous population of neurons, are actually diverse in electrical properties, expression profiles, morphology, location, inputs, and outputs (De Jong et al., 2022). Classically, DA neurons have been defined as neurons that express TH, DAT, VMAT2, and D_2R, in addition to having specific electrical properties such as slow pacemaker activity and presence of an I_h (Lammel et al., 2014; Morales & Margolis, 2017). The electrophysiological experiments discussed in this dissertation used DAT as a fluorescent dopamine marker when possible, and/or classical electrical properties in order to identify lateral VTA DA neurons. As other researchers have found that DA neurons in the lateral portion of the VTA that display these classical characteristics tend to project mainly to the NAc lateral shell, electrophysiological measurements reported here are likely suggestive of this neuronal projection. Viral infusions for behavioral studies reported here, on the other hand, cover most of the VTA and rely on DAT-driven viral infection. DAT-expressing neurons are enriched in the lateral VTA, but they also exist in more medial regions, suggesting that the neurons targeted for electrophysiology are likely within the group of neurons targeted for behavior but do not make up the entire population of VTA DA neurons (Morales & Margolis, 2017).

Using a viral manipulation that could more specifically target the sub-population of VTA DA neurons that project to the NAc lateral shell would allow a more homogeneous assessment of neuron functional relevance in electrophysiological recordings and behavior. Other labs have performed experiments utilizing dual-virus approaches or neuronal tracers that target specific sub-populations within VTA DA neurons based on

both projection inputs and projection outputs (Beier et al., 2019; Lammel et al., 2012). Future studies could use a dual-virus approach to alter GPCR function as outlined in **Chapters 2** and **3** exclusively in a specific VTA DA neuron sub-population based on output target. This assessment would greatly enhance the understanding of how projection-specific cellular communication in the mesocorticolimbic system affects drug-related behaviors.

Another important factor to consider when assessing DA neuron output is that DA levels released in target regions may be controlled independently from DA neuron cell body firing (Collins & Saunders, 2020; De Jong et al., 2022; Mohebi et al., 2019). That means that an increase or decrease in GPCR-dependent inhibition, as reported in **Chapter 2** and **3**, may change somatodendritic DA neuron activity but may not lead to an accompanying change of DA release in the terminal. One way to address whether DA release is actually altered in these manipulations would be to use fiber photometry to measure DA levels in projection targets. Since electrophysiological manipulations discussed in these projects were likely enriched with DA neurons projecting to the NAc lateral shell, measuring DA levels in this area during drug administration would provide further insights about VTA DA neuron to NAc communication. It would be expected that loss of inhibitory GPCRs in VTA DA neurons would augment DA release in the NAc, and enhanced GPCR-dependent signaling due to loss of RGS6 would diminish DA release in the NAc.

5.2.2 Further Behavioral Assessments

Animal behavioral models are a great way to translate what is happening on the cellular and molecular level in the brain into a concrete output. While no single animal model can truly embody the human condition, different behavioral models are useful for evaluating specific aspects of the process leading from drug use to SUD. Each animal

model can be used only to address very specific questions, and therefore testing a multitude of animal behaviors can be beneficial to parse out nuances in behavioral attributes related to drugs of abuse. In **Chapter 2**, our behavioral model assesses drug sensitivity whereas in **Chapters 3** and **4** our behavioral models address voluntary drug consumption.

The model used to assess drug sensitivity in **Chapter 2** utilized a passive injection of cocaine or morphine followed by measurement of drug-induced locomotor stimulation. It has been shown that locomotor stimulation is a relatively simple way to measure behavior resulting from increased VTA DA output (Di Chiara & Imperato, 1988). While this model provides important insights about the way brain circuitry is affected by drugs of abuse, it does not provide us with answers about the voluntary components of drug use. One way to expand on this data would be to evaluate how viral ablation of D_2R- or $GABA_BR$-dependent signaling affects self-administration of cocaine and morphine. It is possible that the enhanced locomotor stimulating effects of cocaine due to loss of GPCR-dependent signaling do not lead to enhanced drug consumption, but rather mice with heightened sensitivity to cocaine may actually need to consume less drug to receive the same amount of reward reinforcement. It is also possible that although loss of GPCR-dependent signaling has no effect on morphine-induced locomotor stimulation at the particular dose tested, it still enhances sensitivity to morphine and could alter morphine self-administration. Indeed, low doses of morphine have been shown to produce locomotor stimulation, while higher doses of morphine produce an initial decreases in locomotor stimulation followed by an increase (Vezina, Kalivas, & Stewart, 1987). Increased sensitivity to morphine, therefore, could mimic effects of a higher dose of morphine and actually result in no overall difference in measured locomotor stimulation.

Another model of behavior that would provide valuable insights about how brain circuits affect drug reward is the conditioned place preference assay. This assay repeatedly pairs one context with a drug of abuse and another context with a neutral stimulus, and then tests which context is preferred by the animal. Animals typically display greater approach behavior to the drug-paired context because it is associated with positive reward reinforcement. Future studies could use this assay to provide insights into whether or not the loss of VTA DA neuron GPCR-dependent inhibition in **Chapter 2** that increased cocaine locomotor stimulation (**Fig. 2.3**) also increases cocaine reward. Additionally, CPP could provide insights into whether the decreased alcohol consumption (**Fig. 3.6**) reported in females after loss of VTA DA neuron RGS6 in **Chapter 3** is due to an increase or decrease in the reward reinforcing aspect of alcohol. It is expected that VTA DA neuron specific loss of RGS6 decreases alcohol reward resulting in decreased consumption, as previous studies using constitutive *RGS6*$^{-/-}$ mice reported decreased time spent in the alcohol-paired context during a CPP assay (Stewart et al., 2015). It is possible, however, that the decrease in alcohol reward reported in Stewart et al., 2015 is mediated by a different brain region, and that loss of RGS6 in VTA DA neurons actually produces an increase in reward which results in less alcohol consumption necessary to achieve the same reward reinforcement. Testing alcohol reward may also provide further insights into the sex difference reported in RGS6 gRNA treated mice (**Fig. 3.6**). It is possible that the age and weight of mice obscures differences in alcohol consumption between male RGS6 gRNA and LacZ control treated mice, but that differences would be revealed when testing alcohol reward.

Manipulations in **Chapters 2** and **3** assess different aspects of VTA DA neuron inhibitory signaling, and they both support the idea that this signaling is critical for drug-related behaviors. Decreased GPCR-dependent inhibitory signaling in **Chapter 2** results

in increased cocaine sensitivity (**Fig. 2.3**) and enhanced GPCR-dependent inhibitory signaling in **Chapter 3** results in decreased alcohol consumption (**Fig. 3.6**). Future work could expand on these insights by assessing whether manipulations in **Chapter 2** affect alcohol consumption and whether manipulations in **Chapter 3** affect cocaine sensitivity, in addition to testing whether and how each of these manipulations modulate the co-consumption patterns of alcohol and nicotine discussed in **Chapter 4.** These experiments would provide a greater understanding about how VTA DA neurons modulate behaviors in a drug-specific manner.

5.2.3 Other R7 RGS proteins in VTA DA neurons

The work in **Chapter 3** addresses the role of RGS6 in negatively regulating GPCR-dependent signaling in VTA DA neurons. RGS6 is a member of the R7 family of RGS proteins, which also contains RGS7, RGS9, and RGS11. RGS9 and RGS11 have been most strongly associated with activity in the visual system, and RGS9 in the brain is thought to be highly localized to the striatum (G. R. Anderson et al., 2009; Z. Rahman et al., 2003). RGS7, on the other hand, has been implicated in GPCR-dependent signaling in multiple brain regions. Deactivation of $GABA_BR$-mediated currents in hippocampal neurons from *RGS7*$^{-/-}$ or *G*β*5*$^{-/-}$ mice is prolonged relative to wild-type controls (Ostrovskaya et al., 2014; Xie et al., 2010). Additionally, RGS7 knockdown in the striatum leads to enhanced cocaine-induced locomotor stimulation and stress induced reinstatement of cocaine seeking (G. R. Anderson et al., 2010; Sutton, Khalatyan, Savas, & Martemyanov, 2021). Therefore, it would be advantageous to assess if RGS7 also plays a role in regulating GPCR-dependent signaling in VTA DA neurons, and if this regulation in turn modulates drug-related behaviors.

Studies from our lab have already begun to assess the role of RGS7 in VTA DA neurons, as *in situ* hybridization studies in WT mice have revealed RGS7 mRNA co-

localization with DAT expressing neurons (**Fig. 5.1A, B**). In mice constitutively lacking RGS7, amplitude of D_2R-dependent signaling was increased while amplitude of $GABA_B$R-dependent signaling was unaffected (**Fig. 5.1C, D**). Further, deactivation tau of $GABA_B$R-dependent signaling was enhanced (**Fig. 5.1E**). Together these data suggest that GPCR-dependent currents in VTA DA neurons are enhanced in the absence of RGS7, mimicking the GPCR-dependent effects reported in **Chapter 3** from mice constitutively lacking RGS6 (**Fig. 3.3**). It is interesting that RGS6 and RGS7 seem to be playing a similar role in regulating D_2R- and $GABA_B$R-dependent signaling, but this is not the first instance where multiple R7 RGS family members play a regulatory role in the same cell and receptor populations (Masuho et al., 2013; Wydeven et al., 2014). It is possible that RGS6 and RGS7 have more nuanced differences that are missed by our electrophysiological measurements, or that are muddled due to the lack of differentiation between VTA DA neuron sub-populations. Indeed, a large proportion of VTA DA neurons express both RGS6 and RGS7, but there is also a population that only expresses one of these proteins (**Fig. 5.1A, B**). Projection specific assessments of R7 RGS expression patterns and inhibitory current modulation in VTA DA neurons could provide additional insights about differences in RGS6 and RGS7 regulation. It is also important to note that these recordings are from mice constitutively lacking RGS7, which could result in confounding variables such as compensation of other regulatory elements and effects in other brain regions or cell types. Future studies measuring effects of VTA DA neuron specific RGS7 loss using our CRISPR/Cas9 ablation technique described in **Chapters 2** and **3** would allow a more refined assessment of the effects of RGS7 on inhibitory GPCR-dependent signaling exclusively in VTA DA neurons. Furthermore, assessing whether drug-related behaviors differ between VTA DA neuron specific *RGS6*$^{-/-}$ and *RGS7*$^{-/-}$ mice will further enlighten our understanding of how modulation by these proteins may be redundant or disparate.

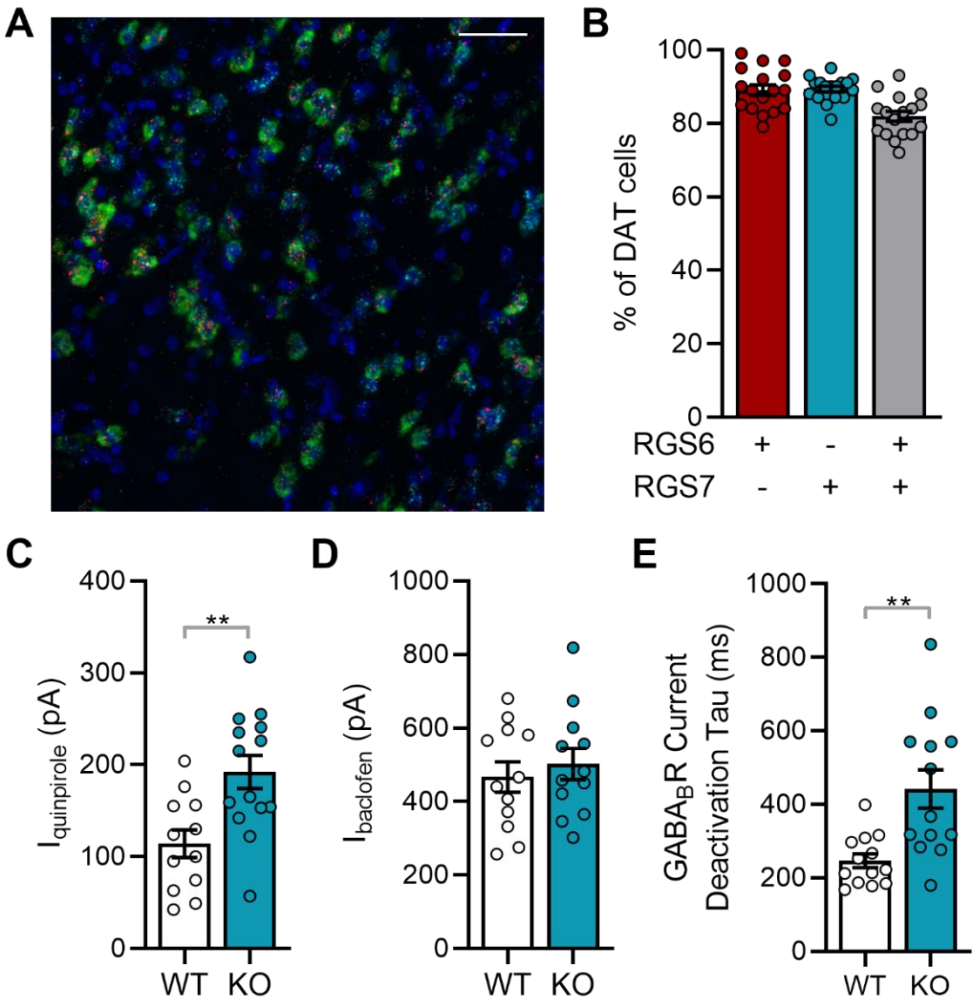

Figure 5.1. RGS7$^{-/-}$ and GPCR-dependent current modulation in VTA DA neurons

(A) Example image of fluorescent in situ hybridization used to detect RGS6 (red) and RGS7 (cyan) transcript in cells of the VTA that express the dopamine transporter (DAT, green) in WT mice; 20x magnification, scale bar: 50 µm.

(B) Summary of coded analysis of images indicating that 89% of DAT expressing cells also expressed RGS6, 89% express RGS7, and 82% express both RGS6 and RGS7.

(C) Summary of maximal currents evoked by quinpirole baclofen in putative DA neurons in VTA slices from WT and *RGS7*$^{-/-}$ mice ($t_{23.77}$=3.324; P=0.0029; unpaired Welch's t test; n=12-14/group). Symbol: **P<0.01.

(D) Summary of maximal currents evoked by baclofen in putative DA neurons in VTA slices from WT and *RGS7*$^{-/-}$ mice ($t_{21.97}$=0.5992; P=0.5552; unpaired Welch's t test; n=12/group).

(E) Summary of deactivation tau calculated from light-evoked $GABA_BR$-dependent currents in putative VTA DA neurons from WT and *RGS7*$^{-/-}$ mice ($t_{15.15}$=3.522; P=0.0030; unpaired Welch's t test; n=13/group). Symbol: **P<0.01.

5.3 Conclusion

In conclusion, the work discussed here provides insights into numerous ways that sensitivity to and consumption of drugs of abuse can be altered. Decreased inhibitory GPCR-dependent signaling in VTA DA neurons increases the sensitivity to cocaine in a receptor and sex-dependent manner (**Chapter 2**) but does not increase the sensitivity to morphine. Increased inhibitory GPCR-dependent signaling in VTA DA neurons via loss of RGS6 regulation decreases alcohol consumption in females but not males (**Chapter 3**). In addition, the method of RGS6 modulation of GPCR-dependent signaling differs for D_2R- and $GABA_B$R-dependent currents; RGS6 modulates amplitude of D_2R-dependent currents and deactivation kinetics of $GABA_B$R-dependent currents. Co-consumption of alcohol and nicotine also tempers drug consumption in a drug dependent manner; both forced and aversion-induced abstinence from alcohol increases nicotine consumption, whereas abstinence from nicotine has no effect on alcohol consumption (**Chapter 4**). Together, these studies provide insights into the complex circuits and behavior underlying substance use and abuse and inform further studies to identify potential drug targets and treatment strategies for people with SUD.

Bibliography

Ackerman, J. M., Johansen, P. A., Clark, D., & White, F. J. (1993). Electrophysiological effects of putative autoreceptor-selective dopamine agonists on A10 dopamine neurons. *Journal of Pharmacology and Experimental Therapeutics*, *265*(2), 963–970.

Ackerman, J. M., & White, F. J. (1990). A10 somatodendritic dopamine autoreceptor sensitivity following withdrawal from repeated cocaine treatment. *Neuroscience Letters*, *117*(1–2), 181–187. https://doi.org/10.1016/0304-3940(90)90141-U

Adell, A., & Artigas, F. (2004). The somatodendritic release of dopamine in the ventral tegmental area and its regulation by afferent transmitter systems. *Neuroscience and Biobehavioral Reviews*, *28*(4), 415–431. https://doi.org/10.1016/j.neubiorev.2004.05.001

Adrover, M. F., Shin, J. H., & Alvarez, V. A. (2014). Glutamate and dopamine transmission from midbrain dopamine neurons share similar release properties but are differentially affected by cocaine. *Journal of Neuroscience*, *34*(9), 3183–3192. https://doi.org/10.1523/JNEUROSCI.4958-13.2014

Agabio, R., & Colombo, G. (2014). GABAB receptor ligands for the treatment of alcohol use disorder: Preclinical and clinical evidence. *Frontiers in Neuroscience*. Frontiers Media SA. https://doi.org/10.3389/fnins.2014.00140

Amano, T., Matsubayashi, H., Seki, T., Sasa, M., & Sakai, N. (2003). Repeated administration of methamphetamine causes hypersensitivity of D2 receptor in rat ventral tegmental area. *Neuroscience Letters*, *347*(2), 89–92. https://doi.org/10.1016/S0304-3940(03)00673-6

Anderson, A., Masuho, I., De Velasco, E. M. F., Nakano, A., Birnbaumer, L., Birnbaumer, L., … Wickman, K. (2020). GPCR-dependent biasing of GIRK channel signaling dynamics by RGS6 in mouse sinoatrial nodal cells. *Proceedings of the National Academy of Sciences of the United States of America*, *117*(25), 14522–14531. https://doi.org/10.1073/pnas.2001270117

Anderson, G. R., Cao, Y., Davidson, S., Truong, H. V, Pravetoni, M., Thomas, M. J., … Martemyanov, K. A. (2010). R7BP Complexes With RGS9-2 and RGS7 in the Striatum Differentially Control Motor Learning and Locomotor Responses to Cocaine. *Neuropsychopharmacology*, *35*(4), 1040–1050. https://doi.org/10.1038/npp.2009.212

Anderson, G. R., Posokhova, E., & Martemyanov, K. A. (2009). The R7 RGS protein family: Multi-subunit regulators of neuronal G protein signaling. *Cell Biochemistry and Biophysics*. NIH Public Access. https://doi.org/10.1007/s12013-009-9052-9

Anker, J. J., & Carroll, M. E. (2011). Females are more vulnerable to drug abuse than males: Evidence from preclinical studies and the role of ovarian hormones. *Current Topics in Behavioral Neurosciences*, *8*, 73–96. https://doi.org/10.1007/7854_2010_93

Aragona, B. J., Cleaveland, N. A., Stuber, G. D., Day, J. J., Carelli, R. M., & Wightman, R. M. (2008). Preferential enhancement of dopamine transmission within the nucleus accumbens shell by cocaine is attributable to a direct increase in phasic dopamine release events. *Journal of Neuroscience*, *28*(35), 8821–8831. https://doi.org/10.1523/JNEUROSCI.2225-08.2008

Aragona, Brandon J, Day, J. J., Roitman, M. F., Cleaveland, N. A., Mark Wightman, R., & Carelli, R. M. (2009). Regional specificity in the real-time development of phasic dopamine transmission patterns during acquisition of a cue-cocaine association in

rats. *European Journal of Neuroscience*, *30*(10), 1889–1899. https://doi.org/10.1111/j.1460-9568.2009.07027.x

Arora, D., Haluk, D. M., Kourrich, S., Pravetoni, M., Fernández-Alacid, L., Nicolau, J. C., … Wickman, K. (2010). Altered neurotransmission in the mesolimbic reward system of Girk-/-mice. *Journal of Neurochemistry*, *114*(5), 1487–1497. https://doi.org/10.1111/j.1471-4159.2010.06864.x

Arora, D., Hearing, M., Haluk, D. M., Mirkovic, K., Fajardo-Serrano, A., Wessendorf, M. W., … Wickman, K. (2011). Acute cocaine exposure weakens GABAB receptor-dependent G-protein-gated inwardly rectifying K+ signaling in dopamine neurons of the ventral tegmental area. *Journal of Neuroscience*, *31*(34), 12251–12257. https://doi.org/10.1523/JNEUROSCI.0494-11.2011

Backes, E. N., & Hemby, S. E. (2008). Contribution of ventral tegmental GABA receptors to cocaine self-administration in rats. *Neurochemical Research*, *33*(3), 459–467. https://doi.org/10.1007/s11064-007-9454-2

Bäckman, C. M., Malik, N., Zhang, Y., Shan, L., Grinberg, A., Hoffer, B. J., … Tomac, A. C. (2006). Characterization of a mouse strain expressing Cre recombinase from the 3′ untranslated region of the dopamine transporter locus. *Genesis*, *44*(8), 383–390. https://doi.org/10.1002/dvg.20228

Batel, P., Pessione, F., Maitre, C., & Rueff, B. (1995). Relationship between alcohol and tobacco dependencies among alcoholics who smoke. *Addiction*, *90*(7), 977–980. https://doi.org/10.1046/j.1360-0443.1995.90797711.x

Beart, P. M., McDonald, D., & Gundlach, A. L. (1979). Mesolimbic dopaminergic neurones and somatodendritic mechanisms. *Neuroscience Letters*, *15*(2–3), 165–170.

Bechtholt, A. J., & Cunningham, C. L. (2005). Ethanol-induced conditioned place preference is expressed through a ventral tegmental area dependent mechanism. *Behavioral Neuroscience*, *119*(1), 213–223. https://doi.org/10.1037/0735-7044.119.1.213

Becker, J. B., & Koob, G. F. (2016). Sex differences in animal models: Focus on addiction. *Pharmacological Reviews*. https://doi.org/10.1124/pr.115.011163

Beckstead, M. J., Grandy, D. K., Wickman, K., & Williams, J. T. (2004). Vesicular dopamine release elicits an inhibitory postsynaptic current in midbrain dopamine neurons. *Neuron*, *42*(6), 939–946. https://doi.org/10.1016/j.neuron.2004.05.019

Beier, K. T., Gao, X. J., Xie, S., DeLoach, K. E., Malenka, R. C., & Luo, L. (2019). Topological Organization of Ventral Tegmental Area Connectivity Revealed by Viral-Genetic Dissection of Input-Output Relations. *Cell Reports*, *26*(1), 159-167.e6. https://doi.org/10.1016/j.celrep.2018.12.040

Bell, J., & Strang, J. (2020). Medication Treatment of Opioid Use Disorder. *Biological Psychiatry*, *87*(1), 82–88. https://doi.org/10.1016/j.biopsych.2019.06.020

Bello, E. P., Mateo, Y., Gelman, D. M., Noaín, D., Shin, J. H., Low, M. J., … Rubinstein, M. (2011). Cocaine supersensitivity and enhanced motivation for reward in mice lacking dopamine D2 autoreceptors. *Nature Neuroscience*, *14*(8), 1033–1038. https://doi.org/10.1038/nn.2862

Berke, J. D., & Hyman, S. E. (2000, March 1). Addiction, dopamine, and the molecular mechanisms of memory. *Neuron*. Elsevier. https://doi.org/10.1016/S0896-6273(00)81056-9

Bernosky-Smith, K. A., Qiu, Y. Y., Feja, M., Lee, Y. B., Loughlin, B., Li, J. X., & Bass, C. E. (2018). Ventral tegmental area D2 receptor knockdown enhances choice impulsivity in a delay-discounting task in rats. *Behavioural Brain Research*, *341*, 129–134. https://doi.org/10.1016/j.bbr.2017.12.029

Bettler, B., Kaupmann, K., Mosbacher, J., & Gassmann, M. (2004). Molecular Structure and Physiological Functions of GABA B Receptors. *Physiological Reviews*, *84*(3), 835–867. https://doi.org/10.1152/physrev.00036.2003

Bifsha, P., Yang, J., Fisher, R. A., & Drouin, J. (2014). Rgs6 is Required for Adult Maintenance of Dopaminergic Neurons in the Ventral Substantia Nigra. *PLoS Genetics*, *10*(12), 1004863. https://doi.org/10.1371/journal.pgen.1004863

Blomqvist, O., Gelernter, J., & Kranzler, H. R. (2000). Family-based study of DRD2 alleles in alcohol and drug dependence. *American Journal of Medical Genetics - Neuropsychiatric Genetics*, *96*(5), 659–664. https://doi.org/10.1002/1096-8628(20001009)96:5<659::AID-AJMG12>3.0.CO;2-G

Bocarsly, M. E., da Silva e Silva, D., Kolb, V., Luderman, K. D., Shashikiran, S., Rubinstein, M., … Alvarez, V. A. (2019). A Mechanism Linking Two Known Vulnerability Factors for Alcohol Abuse: Heightened Alcohol Stimulation and Low Striatal Dopamine D2 Receptors. *Cell Reports*, *29*(5), 1147-1163.e5. https://doi.org/10.1016/j.celrep.2019.09.059

Boender, A. J., De Jong, J. W., Boekhoudt, L., Luijendijk, M. C. M., Van Der Plasse, G., & Adan, R. A. H. (2014). Combined use of the canine adenovirus-2 and DREADDtechnology to activate specific neural pathways in vivo. *PLoS ONE*, *9*(4). https://doi.org/10.1371/journal.pone.0095392

Bowery, B., Rothwell, L. A., & Seabrook, G. R. (1994). Comparison between the pharmacology of dopamine receptors mediating the inhibition of cell firing in rat brain slices through the substantia nigra pars compacta and ventral tegmental area. *British Journal of Pharmacology*, *112*(3), 873–880. https://doi.org/10.1111/j.1476-5381.1994.tb13161.x

Bradberry, C. W., & Roth, R. H. (1989). Cocaine increases extracellular dopamine in rat nucleus accumbens and ventral tegmental area as shown by in vivo microdialysis. *Neuroscience Letters*, *103*(1), 97–102. https://doi.org/10.1016/0304-3940(89)90492-8

Brady, K. T., & Randall, C. L. (1999). Gender differences in substance use disorders. *Psychiatric Clinics of North America*, *22*(2), 241–252. https://doi.org/10.1016/S0193-953X(05)70074-5

Brebner, K., Phelan, R., & Roberts, D. C. S. (2000). Intra-VTA baclofen attenuates cocaine self-administration on a progressive ratio schedule of reinforcement. *Pharmacology Biochemistry and Behavior*, *66*(4), 857–862. https://doi.org/10.1016/S0091-3057(00)00286-0

Brodie, M. S. (2002). Increased ethanol excitation of dopaminergic neurons of the ventral tegmental area after chronic ethanol treatment. *Alcoholism: Clinical and Experimental Research*, *26*(7), 1024–1030. https://doi.org/10.1111/j.1530-0277.2002.tb02637.x

Brodie, M. S., & Dunwiddie, T. V. (1990). Cocaine effects in the ventral tegmental area: Evidence for an indirect dopaminergic mechanism of action. *Naunyn-Schmiedeberg's Archives of Pharmacology*, *342*(6), 660–665. https://doi.org/10.1007/BF00175709

Bunney, E. B., Appel, S. B., & Brodie, M. S. (2001). Electrophysiological effects of cocaethylene, cocaine, and ethanol on dopaminergic neurons of the ventral tegmental area. *Journal of Pharmacology and Experimental Therapeutics*, *297*(2), 696–703. Retrieved from http://jpet.aspetjournals.org

Bunney, W. C., Massari, V. J., & Pert, A. (1984). Chronic morphine-induced hyperactivity in rats is altered by nucleus accumbens and ventral tegmental lesions. *Psychopharmacology*, *82*(4), 318–321. https://doi.org/10.1007/BF00427677

Caine, S. B., Thomsen, M., Gabriel, K. I., Berkowitz, J. S., Gold, L. H., Koob, G. F., … Xu, M. (2007). Lack of self-administration of cocaine in dopamine D1 receptor knock-out mice. *Journal of Neuroscience*, *27*(48), 13140–13150. https://doi.org/10.1523/JNEUROSCI.2284-07.2007

Calipari, E. S., Sun, H., Eldeeb, K., Luessen, D. J., Feng, X., Howlett, A. C., … Chen, R. (2014). Amphetamine self-administration attenuates dopamine D2 autoreceptor function. *Neuropsychopharmacology*, *39*(8), 1833–1842. https://doi.org/10.1038/npp.2014.30

Carlezon, W. A., & Thomas, M. J. (2009). Biological substrates of reward and aversion: A nucleus accumbens activity hypothesis. *Neuropharmacology*. NIH Public Access. https://doi.org/10.1016/j.neuropharm.2008.06.075

Carpenter, A. E., Jones, T. R., Lamprecht, M. R., Clarke, C., Kang, I. H., Friman, O., … Sabatini, D. M. (2006). CellProfiler: image analysis software for identifying and quantifying cell phenotypes. *Genome Biology*, *7*(10), R100. https://doi.org/10.1186/GB-2006-7-10-R100

Chan, B., Kondo, K., Freeman, M., Ayers, C., Montgomery, J., & Kansagara, D. (2019, December 1). Pharmacotherapy for Cocaine Use Disorder—a Systematic Review and Meta-analysis. *Journal of General Internal Medicine*. Springer New York LLC. https://doi.org/10.1007/s11606-019-05074-8

Chefer, V I, Denoroy, L., Zapata, A., & Shippenberg, T. S. (2009). Mu opioid receptor modulation of somatodendritic dopamine overflow: GABAergic and glutamatergic mechanisms. *European Journal of Neuroscience*, *30*(2), 272–278. https://doi.org/10.1111/j.1460-9568.2009.06827.x

Chefer, Vladimir I., Kieffer, B. L., & Shippenberg, T. S. (2003). Basal and morphine-evoked dopaminergic neurotransmission in the nucleus accumbens of MOR- and DOR-knockout mice. *European Journal of Neuroscience*, *18*(7), 1915–1922. https://doi.org/10.1046/j.1460-9568.2003.02912.x

Chen, C. K., Eversole-Cire, P., Zhang, H., Mancino, V., Chen, Y. J., He, W., … Simon, M. I. (2003). Instability of GGL domain-containing RGS proteins in mice lacking the G protein β-subunit Gβ5. *Proceedings of the National Academy of Sciences of the United States of America*, *100*(11), 6604–6609. https://doi.org/10.1073/pnas.0631825100

Chen, G., Zhang, F., Xue, W., Wu, R., Xu, H., Wang, K., & Zhu, J. (2017). An association study revealed substantial effects of dominance, epistasis and substance dependence co-morbidity on alcohol dependence symptom count. *Addiction Biology*, *22*(6), 1475–1485. https://doi.org/10.1111/adb.12402

Chen, N. H., & Reith, M. E. A. (1994). Autoregulation and monoamine interactions in the ventral tegmental area in the absence and presence of cocaine: A microdialysis study in freely moving rats. *Journal of Pharmacology and Experimental Therapeutics*, *271*(3), 1597–1610.

Chen, N. N. H., & Pan, W. H. T. (2000). Regulatory effects of D2 receptors in the ventral tegmental area on the mesocorticolimbic dopaminergic pathway. *Journal of Neurochemistry*, *74*(6), 2576–2582. https://doi.org/10.1046/j.1471-4159.2000.0742576.x

Chen, R., McIntosh, S., Hemby, S. E., Sun, H., Sexton, T., Martin, T. J., & Childers, S. R. (2018). High and low doses of cocaine intake are differentially regulated by dopamine D2 receptors in the ventral tegmental area and the nucleus accumbens. *Neuroscience Letters*, *671*, 133–139. https://doi.org/10.1016/j.neulet.2018.02.026

Chen, S. H., Haam, J., Walker, M., Scappini, E., Naughton, J., & Martin, N. P. (2019). Production of Viral Constructs for Neuroanatomy, Calcium Imaging, and

Optogenetics. *Current Protocols in Neuroscience*, *87*(1), 66. https://doi.org/10.1002/cpns.66
Chen, S. Y., Burger, R. L., & Reith, M. E. A. (1996). Extracellular dopamine in the rat ventral tegmental area and nucleus accumbens following ventral tegmental infusion of cocaine. *Brain Research*, *729*(2), 294–296. https://doi.org/10.1016/0006-8993(96)00671-3
Cheng, Y., Huang, C. C. Y., Ma, T., Wei, X., Wang, X., Lu, J., & Wang, J. (2017). Distinct Synaptic Strengthening of the Striatal Direct and Indirect Pathways Drives Alcohol Consumption. *Biological Psychiatry*, *81*(11), 918–929. https://doi.org/10.1016/j.biopsych.2016.05.016
Cohen, C., Perrault, G., & Sanger, D. J. (1997). Evidence for the involvement of dopamine receptors in ethanol-induced hyperactivity in mice. *Neuropharmacology*, *36*(8), 1099–1108. https://doi.org/10.1016/S0028-3908(97)00100-7
Collins, A. L., & Saunders, B. T. (2020, June 1). Heterogeneity in striatal dopamine circuits: Form and function in dynamic reward seeking. *Journal of Neuroscience Research*. John Wiley & Sons, Ltd. https://doi.org/10.1002/jnr.24587
Costall, B., Fortune, D. H., & Naylor, R. J. (1978). The induction of catalepsy and hyperactivity by morphine administered directly into the nucleus accumbens of rats. *European Journal of Pharmacology*, *49*(1), 49–64. https://doi.org/10.1016/0014-2999(78)90221-2
Crabbe, J. C., Ozburn, A. R., Metten, P., Barkley-Levenson, A., Schlumbohm, J. P., Spence, S. E., … Huang, L. C. (2017). High Drinking in the Dark (HDID) mice are sensitive to the effects of some clinically relevant drugs to reduce binge-like drinking. *Pharmacology Biochemistry and Behavior*, *160*, 55–62. https://doi.org/10.1016/j.pbb.2017.08.002
Cruz, H. G., Ivanova, T., Lunn, M. L., Stoffel, M., Slesinger, P. A., & Lüscher, C. (2004). Bi-directional effects of GABAB receptor agonists on the mesolimbic dopamine system. *Nature Neuroscience*, *7*(2), 153–159. https://doi.org/10.1038/nn1181
Cunningham, C. L., & Shields, C. N. (2018). Effects of sex on ethanol conditioned place preference, activity and variability in C57BL/6J and DBA/2J mice. *Pharmacology Biochemistry and Behavior*, *173*(July), 84–89. https://doi.org/10.1016/j.pbb.2018.07.008
De Beaurepaire, R., Heydtmann, M., & Agabio, R. (2019). Editorial: Baclofen in the treatment of alcohol use disorder. *Frontiers in Psychiatry*. Frontiers Media SA. https://doi.org/10.3389/fpsyt.2019.00338
De Beaurepaire, R., Sinclair, J. M. A., Heydtmann, M., Addolorato, G., Aubin, H. J., Beraha, E. M., … Agabio, R. (2019). The use of baclofen as a treatment for alcohol use disorder: A clinical practice perspective. *Frontiers in Psychiatry*. Frontiers Media SA. https://doi.org/10.3389/fpsyt.2018.00708
de Bejczy, A., Löf, E., Walther, L., Guterstam, J., Hammarberg, A., Asanovska, G., … Söderpalm, B. (2015). Varenicline for Treatment of Alcohol Dependence: A Randomized, Placebo-Controlled Trial. *Alcoholism: Clinical and Experimental Research*, *39*(11), 2189–2199. https://doi.org/10.1111/acer.12854
De Jong, J. W., Fraser, K. M., & Lammel, S. (2022). Mesoaccumbal Dopamine Heterogeneity: What Do Dopamine Firing and Release Have to Do with It? *Annual Review of Neuroscience*, *45*, 109–129. https://doi.org/10.1146/annurev-neuro-110920
De Jong, J. W., Roelofs, T. J. M., Mol, F. M. U., Hillen, A. E. J., Meijboom, K. E., Luijendijk, M. C. M., … Adan, R. A. H. (2015). Reducing Ventral Tegmental Dopamine D2 Receptor Expression Selectively Boosts Incentive Motivation.

Neuropsychopharmacology, *40*(9), 2085–2095. https://doi.org/10.1038/npp.2015.60
DeBaker, M. C., Marron Fernandez de Velasco, E., McCall, N. M., Lee, A. M., & Wickman, K. (2021). Differential Impact of Inhibitory G-Protein Signaling Pathways in Ventral Tegmental Area Dopamine Neurons on Behavioral Sensitivity to Cocaine and Morphine. *ENeuro*, *8*(2), ENEURO.0081-21.2021. https://doi.org/10.1523/ENEURO.0081-21.2021
DeBaker, M. C., Robinson, J. M., Moen, J. K., Wickman, K., & Lee, A. M. (2020). Differential patterns of alcohol and nicotine intake: Combined alcohol and nicotine binge consumption behaviors in mice. *Alcohol*, *85*(2020), 57–64. https://doi.org/10.1016/j.alcohol.2019.09.006
Deehan, G. A., Hauser, S. R., Waeiss, R. A., Knight, C. P., Toalston, J. E., Truitt, W. A., … Rodd, Z. A. (2015). Co-administration of ethanol and nicotine: The enduring alterations in the rewarding properties of nicotine and glutamate activity within the mesocorticolimbic system of female alcohol-preferring (P) rats. *Psychopharmacology*, *232*(23), 4293–4302. https://doi.org/10.1007/s00213-015-4056-1
Delfs, J. M., Schreiber, L., & Kelley, A. E. (1990). Microinjection of cocaine into the nucleus accumbens elicits locomotor activation in the rat. *Journal of Neuroscience*, *10*(1), 303–310. https://doi.org/10.1523/jneurosci.10-01-00303.1990
Delgado, M. R. (2007). Reward-related responses in the human striatum. In *Annals of the New York Academy of Sciences* (Vol. 1104, pp. 70–88). John Wiley & Sons, Ltd. https://doi.org/10.1196/annals.1390.002
Di Chiara, G., & Imperato, A. (1988). Drugs abused by humans preferentially increase synaptic dopamine concentrations in the mesolimbic system of freely moving rats. *Proceedings of the National Academy of Sciences of the United States of America*, *85*(14), 5274–5278. https://doi.org/10.1073/pnas.85.14.5274
Ding, Z. M., Ingraham, C. M., Rodd, Z. A., & McBride, W. J. (2015). The reinforcing effects of ethanol within the posterior ventral tegmental area depend on dopamine neurotransmission to forebrain cortico-limbic systems. *Addiction Biology*, *20*(3), 458–468. https://doi.org/10.1111/adb.12138
Domi, E., Domi, A., Adermark, L., Heilig, M., & Augier, E. (2021, June 1). Neurobiology of alcohol seeking behavior. *Journal of Neurochemistry*. John Wiley and Sons Inc. https://doi.org/10.1111/jnc.15343
Durieux, P. F., Bearzatto, B., Guiducci, S., Buch, T., Waisman, A., Zoli, M., … De Kerchove D'Exaerde, A. (2009). D2R striatopallidal neurons inhibit both locomotor and drug reward processes. *Nature Neuroscience 2009 12:4*, *12*(4), 393–395. https://doi.org/10.1038/NN.2286
Edwards, N. J., Tejeda, H. A., Pignatelli, M., Zhang, S., McDevitt, R. A., Wu, J., … Bonci, A. (2017). Circuit specificity in the inhibitory architecture of the VTA regulates cocaine-induced behavior. *Nature Neuroscience*, *20*(3), 438–448. https://doi.org/10.1038/nn.4482
Einhorn, L. C., Johansen, P. A., & White, F. J. (1988). Electrophysiological effects of cocaine in the mesoaccumbens dopamine system: Studies in the Ventral Tegmental Area. *Journal of Pharmacology and Experimental Therapeutics*, *8*(1), 100–112.
Erhardt, S., Mathé, J. M., Chergui, K., Engberg, G., & Svensson, T. H. (2002). GABAB receptor-mediated modulation of the firing pattern of ventral tegmental area dopamine neurons in vivo. *Naunyn-Schmiedeberg's Archives of Pharmacology*, *365*(3), 173–180. https://doi.org/10.1007/s00210-001-0519-5
Falk, D. E., Yi, H. Y., & Hiller-Sturmhöfel, S. (2006). An epidemiologic analysis of co-

occurring alcohol and tobacco use and disorders: Findings from the National Epidemiologic Survey on Alcohol and Related Conditions. *Alcohol Research and Health*, *29*(3), 162–171.
Fattore, L., Altea, S., & Fratta, W. (2008). Sex differences in drug addiction: A review of animal and human studies. *Women's Health*. https://doi.org/10.2217/17455057.4.1.51
Filip, M., Frankowska, M., Sadakierska-Chudy, A., Suder, A., Szumiec, Ł., Mierzejewski, P., … Cryan, J. F. (2015). GABAB receptors as a therapeutic strategy in substance use disorders: Focus on positive allosteric modulators. *Neuropharmacology*, *88*, 36–47. https://doi.org/10.1016/j.neuropharm.2014.06.016
Ford, C. P., Mark, G. P., & Williams, J. T. (2006). Properties and opioid inhibition of mesolimbic dopamine neurons vary according to target location. *Journal of Neuroscience*, *26*(10), 2788–2797. https://doi.org/10.1523/JNEUROSCI.4331-05.2006
Ford, Christopher P. (2014). The role of D2-autoreceptors in regulating dopamine neuron activity and transmission. *Neuroscience*. https://doi.org/10.1016/j.neuroscience.2014.01.025
Francis, T. C., Gantz, S. C., Moussawi, K., & Bonci, A. (2019). Synaptic and intrinsic plasticity in the ventral tegmental area after chronic cocaine. *Current Opinion in Neurobiology*. https://doi.org/10.1016/j.conb.2018.08.013
Franck, J., & Jayaram-Lindström, N. (2013). Pharmacotherapy for alcohol dependence: Status of current treatments. *Current Opinion in Neurobiology*. https://doi.org/10.1016/j.conb.2013.05.005
Fritz, B. M., & Boehm, S. L. (2016). Rodent models and mechanisms of voluntary binge-like ethanol consumption: Examples, opportunities, and strategies for preclinical research. *Progress in Neuro-Psychopharmacology and Biological Psychiatry*, *65*, 297–308. https://doi.org/10.1016/j.pnpbp.2015.05.012
Fucito, L. M., Park, A., Gulliver, S. B., Mattson, M. E., Gueorguieva, R. V, & O'Malley, S. S. (2012). Cigarette smoking predicts differential benefit from naltrexone for alcohol dependence. *Biological Psychiatry*, *72*(10), 832–838. https://doi.org/10.1016/j.biopsych.2012.03.023
Garzón, J., López-Fando, A., & Sánchez-Blázquez, P. (2003). The R7 Subfamily of RGS Proteins Assists Tachyphylaxis and Acute Tolerance at μ-Opioid Receptors. *Neuropsychopharmacology*, *28*(11), 1983–1990. https://doi.org/10.1038/sj.npp.1300263
Gold, S. J., Ni, Y. G., Dohlman, H. G., & Nestler, E. J. (1997). Regulators of G-protein signaling (RGS) proteins: Region-specific expression of nine subtypes in rat brain. *Journal of Neuroscience*, *17*(20), 8024–8037. https://doi.org/10.1523/JNEUROSCI.17-20-08024.1997
Groves, P. M., Wilson, C. J., Young, S. J., & Rebec, G. V. (1975). Self-inhibition by dopaminergic neurons. *Science (New York, N.Y.)*, *190*(4214), 522–528.
Grucza, R. A., & Bierut, L. J. (2006). Co-occurring risk factors for alcohol dependence and habitual smoking: Update on findings from the Collaborative Study on the Genetics of Alcoholism. *Alcohol Research and Health*. National Institute on Alcohol Abuse and Alcoholism. Retrieved from /pmc/articles/PMC6527048/
Guo, S., Chen, S., Zhang, Q., Wang, Y., Xu, K., & Zheng, X. (2014). Optogenetic activation of the excitatory neurons expressing CaMKII α in the ventral tegmental area upregulates the locomotor activity of free behaving rats. *BioMed Research International*, *2014*. https://doi.org/10.1155/2014/687469
Hammett, P. J., Lando, H. A., Taylor, B. C., Widome, R., Erickson, D. J., Joseph, A. M.,

… Fu, S. S. (2019). The relationship between smoking cessation and binge drinking, depression, and anxiety symptoms among smokers with serious mental illness. *Drug and Alcohol Dependence*, *194*, 128–135. https://doi.org/10.1016/j.drugalcdep.2018.08.043

Hearing, M. C., Zink, A. N., & Wickman, K. (2012). Cocaine-induced adaptations in metabotropic inhibitory signaling in the mesocorticolimbic system. *Reviews in the Neurosciences*. NIH Public Access. https://doi.org/10.1515/revneuro-2012-0045

Heffner, J. L., Mingione, C., Blom, T. J., & Anthenelli, R. M. (2011). Smoking history, nicotine dependence, and changes in craving and mood during short-term smoking abstinence in alcohol dependent vs. control smokers. *Addictive Behaviors*, *36*(3), 244–247. https://doi.org/10.1016/j.addbeh.2010.10.008

Hendrickson, L. M., Zhao-Shea, R., & Tapper, A. R. (2009). Modulation of ethanol drinking-in-the-dark by mecamylamine and nicotinic acetylcholine receptor agonists in C57BL/6J mice. *Psychopharmacology*, *204*(4), 563–572. https://doi.org/10.1007/s00213-009-1488-5

Henry, D. J., Greene, M. A., & White, F. J. (1989). Electrophysiological effects of cocaine in the mesoaccumbens dopamine system: Repeated administration. *Journal of Pharmacology and Experimental Therapeutics*, *251*(3), 833–839.

Henry, D. J., Hu, X. T., & White, F. J. (1998). Adaptations in the mesoaccumbens dopamine system resulting from repeated administration of dopamine D1 and D2 receptor-selective agonists: Relevance to cocaine sensitization. *Psychopharmacology*, *140*(2), 233–242. https://doi.org/10.1007/s002130050762

Hikosaka, O., Bromberg-Martin, E., Hong, S., & Matsumoto, M. (2008). New insights on the subcortical representation of reward. *Current Opinion in Neurobiology*. https://doi.org/10.1016/j.conb.2008.07.002

Holroyd, K. B., Adrover, M. F., Fuino, R. L., Bock, R., Kaplan, A. R., Gremel, C. M., … Alvarez, V. A. (2015). Loss of Feedback Inhibition via D2 Autoreceptors Enhances Acquisition of Cocaine Taking and Reactivity to Drug-Paired Cues. *Neuropsychopharmacology*, *40*(6), 1495–1509. https://doi.org/10.1038/npp.2014.336

Hooks, S. B., Waldo, G. L., Corbitt, J., Bodor, E. T., Krumins, A. M., & Harden, T. K. (2003). RGS6, RGS7, RGS9, and RGS11 stimulate GTPase activity of Gi family G-proteins with differential selectivity and maximal activity. *Journal of Biological Chemistry*, *278*(12), 10087–10093. https://doi.org/10.1074/jbc.M211382200

Hopf, F. Woodward, & Lesscher, H. M. (2014). Rodent models for compulsive alcohol intake. *Alcohol*. Tiffany & Conklin. https://doi.org/10.1016/j.alcohol.2014.03.001

Hopf, Frederic Woodward, Chang, S.-J., Sparta, D. R., Bowers, M. S., & Bonci, A. (2010). Motivation for Alcohol Becomes Resistant to Quinine Adulteration After 3 to 4 Months of Intermittent Alcohol Self-Administration. *Alcoholism: Clinical and Experimental Research*, *34*(9), 1565–1573. https://doi.org/10.1111/j.1530-0277.2010.01241.x

Hurt, R. D. (1996). Mortality Following Inpatient Addictions Treatment. *JAMA*, *275*(14), 1097. https://doi.org/10.1001/jama.1996.03530380039029

Hwa, L. S., Chu, A., Levinson, S. A., Kayyali, T. M., DeBold, J. F., & Miczek, K. A. (2011). Persistent escalation of alcohol drinking in C57BL/6J mice with intermittent access to 20% ethanol. *Alcoholism, Clinical and Experimental Research*, *35*(11), 1938–1947. https://doi.org/10.1111/j.1530-0277.2011.01545.x

Hyman, S. E., Malenka, R. C., & Nestler, E. J. (2006). Neural Mechanisms of Addiction: The Role of Reward-Related Learning and Memory. https://doi.org/10.1146/annurev.neuro.29.051605.113009

Iravani, M. M., Muscat, R., & Kruk, Z. L. (1996). Comparison of somatodendritic and axon terminal dopamine release in the ventral tegmental area and the nucleus accumbens. *Neuroscience*, *70*(4), 1025–1037. https://doi.org/10.1016/0306-4522(95)00396-7

Jalabert, M., Bourdy, R., Courtin, J., Veinante, P., Manzoni, O. J., Barrot, M., & Georges, F. (2011). Neuronal circuits underlying acute morphine action on dopamine neurons. *Proceedings of the National Academy of Sciences of the United States of America*, *108*(39), 16446–16450. https://doi.org/10.1073/pnas.1105418108

Jhou, T. C., Fields, H. L., Baxter, M. G., Saper, C. B., & Holland, P. C. (2009). The rostromedial tegmental nucleus (RMTg), a GABAergic afferent to midbrain opamine neurons, encodes aversive stimuli and inhibits motor responses. *Neuron*, *61*(5), 786–800. https://doi.org/10.1016/j.neuron.2009.02.001

Johnson, S. W., & North, R. A. (1992). Opioids excite dopamine neurons by hyperpolarization of local interneurons. *Journal of Neuroscience*, *12*(2), 483–488. https://doi.org/10.1523/jneurosci.12-02-00483.1992

Jordan, C. J., & Xi, Z.-X. (2022). Identification of the Risk Genes Associated With Vulnerability to Addiction: Major Findings From Transgenic Animals. *Frontiers in Neuroscience*, *15*. https://doi.org/10.3389/fnins.2021.811192

Joseph, M. H., & Hodges, H. (1990). Lever pressing for food reward and changes in dopamine turnover and uric acid in rat caudate and nucleus accumbens studied chronically by in vivo voltammetry. *Journal of Neuroscience Methods*, *34*(1–3), 143–149. https://doi.org/10.1016/0165-0270(90)90052-H

Joyce, E. M., & Iversen, S. D. (1979). The effect of morphine applied locally to mesencephalic dopamine cell bodies on spontaneous motor activity in the rat. *Neuroscience Letters*, *14*(2–3), 207–212. https://doi.org/10.1016/0304-3940(79)96149-4

Juarez, B., & Han, M.-H. (2016). Diversity of dopaminergic neural circuits in response to drug exposure. *Neuropsychopharmacology*, *41*(10), 2424–2446. https://doi.org/10.1038/npp.2016.32

Kahler, C. W., Cioe, P. A., Tzilos, G. K., Spillane, N. S., Leggio, L., Ramsey, S. E., … O'Malley, S. S. (2017). A Double-Blind Randomized Placebo-Controlled Trial of Oral Naltrexone for Heavy-Drinking Smokers Seeking Smoking Cessation Treatment. *Alcoholism: Clinical and Experimental Research*, *41*(6), 1201–1211. https://doi.org/10.1111/acer.13396

Kalivas, P. W., & Duffy, P. (1993). Time course of extracellular dopamine and behavioral sensitization to cocaine. II. Dopamine perikarya. *Journal of Neuroscience*, *13*(1), 276–284. https://doi.org/10.1523/jneurosci.13-01-00276.1993

Kalivas, P. W., Duffy, P., & Eberhardt, H. (1990). Modulation of A10 dopamine neurons by γ-aminobutyric acid agonists. *Journal of Pharmacology and Experimental Therapeutics*, *253*(2), 858–866.

Kalivas, P. W., & O'Brien, C. (2008, September 5). Drug addiction as a pathology of staged neuroplasticity. *Neuropsychopharmacology*. Nature Publishing Group. https://doi.org/10.1038/sj.npp.1301564

Kalivas, P. W., Taylor, S., & Miller, J. S. (1985). Sensitization to repeated enkephalin administration into the ventral tegmental area of the rat. I. Behavioral characterization. *Journal of Pharmacology and Experimental Therapeutics*, *235*(2), 537–543.

Kalivas, P. W., & Volkow, N. D. (2005). The neural basis of addiction: a pathology of motivation and choice. *The American Journal of Psychiatry*, *162*(8), 1403–1413. https://doi.org/10.1176/appi.ajp.162.8.1403

Kamens, H. M., Andersen, J., & Picciotto, M. R. (2010). Modulation of ethanol consumption by genetic and pharmacological manipulation of nicotinic acetylcholine receptors in mice. *Psychopharmacology*, *208*(4), 613–626. https://doi.org/10.1007/s00213-009-1759-1

Kamens, H. M., Hoft, N. R., Cox, R. J., Miyamoto, J. H., & Ehringer, M. A. (2012). The α6 nicotinic acetylcholine receptor subunit influences ethanol-induced sedation. *Alcohol*, *46*(5), 463–471. https://doi.org/10.1016/j.alcohol.2012.03.001

Kamentsky, L., Jones, T. R., Fraser, A., Bray, M. A., Logan, D. J., Madden, K. L., … Carpenter, A. E. (2011). Improved structure, function and compatibility for CellProfiler: modular high-throughput image analysis software. *Bioinformatics*, *27*(8), 1179. https://doi.org/10.1093/BIOINFORMATICS/BTR095

Kampman, K. M. (2019). The treatment of cocaine use disorder. *Science Advances*, *5*(10), 1532–1548. https://doi.org/10.1126/sciadv.aax1532

Karami, M., & Zarrindast, M. R. (2008). Morphine sex-dependently induced place conditioning in adult Wistar rats. *European Journal of Pharmacology*, *582*(1–3), 78–87. https://doi.org/10.1016/j.ejphar.2007.12.010

Kelley, A. E. (2004). Ventral striatal control of appetitive motivation: Role in ingestive behavior and reward-related learning. In *Neuroscience and Biobehavioral Reviews* (Vol. 27, pp. 765–776). https://doi.org/10.1016/j.neubiorev.2003.11.015

Kelly, P. H., Seviour, P. W., & Iversen, S. D. (1975). Amphetamine and apomorphine responses in the rat following 6-OHDA lesions of the nucleus accumbens septi and corpus striatum. *Brain Research*, *94*(3), 507–522. https://doi.org/10.1016/0006-8993(75)90233-4

Keyes, K. M., Grant, B. F., & Hasin, D. S. (2008). Evidence for a closing gender gap in alcohol use, abuse, and dependence in the United States population. *Drug and Alcohol Dependence*, *93*(1–2), 21–29. https://doi.org/10.1016/j.drugalcdep.2007.08.017

Kim, K. M., Baratta, M. V, Yang, A., Lee, D., Boyden, E. S., & Fiorillo, C. D. (2012). Optogenetic mimicry of the transient activation of dopamine neurons by natural reward is sufficient for operant reinforcement. *PLoS ONE*, *7*(4), 33612. https://doi.org/10.1371/journal.pone.0033612

King, A., McNamara, P., Conrad, M., & Cao, D. (2009). Alcohol-induced increases in smoking behavior for nicotinized and denicotinized cigarettes in men and women. *Psychopharmacology*, *207*(1), 107–117. https://doi.org/10.1007/s00213-009-1638-9

Kita, J. M., Kile, B. M., Parker, L. E., & Wightman, R. M. (2009). In vivo measurement of somatodendritic release of dopamine in the ventral tegmental area. *Synapse*, *63*(11), 951–960. https://doi.org/10.1002/syn.20676

Knutson, B., & Cooper, J. C. (2005). Functional magnetic resonance imaging of reward prediction. *Current Opinion in Neurology*, *18*(4), 411–417. https://doi.org/10.1097/01.wco.0000173463.24758.f6

Koob, G. F. (2013). Negative reinforcement in drug addiction: The darkness within. *Current Opinion in Neurobiology*. https://doi.org/10.1016/j.conb.2013.03.011

Koob, G. F. (2020). Neurobiology of Opioid Addiction: Opponent Process, Hyperkatifeia, and Negative Reinforcement. *Biological Psychiatry*. https://doi.org/10.1016/j.biopsych.2019.05.023

Koob, G. F., & Le Moal, M. (1997). Drug abuse: Hedonic homeostatic dysregulation. *Science*, *278*(5335), 52–58. https://doi.org/10.1126/science.278.5335.52

Koob, G. F., & Nestler, E. J. (1997, April 1). The neurobiology of drug addiction. *Journal of Neuropsychiatry and Clinical Neurosciences*. American Psychiatric Publishing. https://doi.org/10.1176/jnp.9.3.482

Koob, G. F., & Volkow, N. D. (2016, August 1). Neurobiology of addiction: a neurocircuitry analysis. *The Lancet Psychiatry*. NIH Public Access. https://doi.org/10.1016/S2215-0366(16)00104-8

Kosten, T. A., Gawin, F. H., Kosten, T. R., & Rounsaville, B. J. (1993). Gender differences in cocaine use and treatment response. *Journal of Substance Abuse Treatment*, *10*(1), 63–66. https://doi.org/10.1016/0740-5472(93)90100-G

Kotecki, L., Hearing, M., McCall, N. M., de Velasco, E. M. F., Pravetoni, M., Arora, D., … Wickman, K. (2015). GIRK channels modulate opioid-induced motor activity in a cell type- and subunit-dependent manner. *Journal of Neuroscience*, *35*(18), 7131–7142. https://doi.org/10.1523/JNEUROSCI.5051-14.2015

Koulchitsky, S., Delairesse, C., Beeken, T., Monteforte, A., Dethier, J., Quertemont, E., … Seutin, V. (2016). Activation of D2 autoreceptors alters cocaine-induced locomotion and slows down local field oscillations in the rat ventral tegmental area. *Neuropharmacology*, *108*, 120–127. https://doi.org/10.1016/j.neuropharm.2016.04.034

Koyrakh, L., Luján, R., Colón, J., Karschin, C., Kurachi, Y., Karschin, A., & Wickman, K. (2005). Molecular and cellular diversity of neuronal G-protein-gated potassium channels. *Journal of Neuroscience*, *25*(49), 11468–11478. https://doi.org/10.1523/JNEUROSCI.3484-05.2005

Kushner, S. A., & Unterwald, E. M. (2001). Chronic cocaine administration decreases the functional coupling of GABA B receptors in the rat ventral tegmental area as measured by baclofen-stimulated 35S-GTPγS binding. *Life Sciences*, *69*(9), 1093–1102. https://doi.org/10.1016/S0024-3205(01)01203-6

Labouèbe, G., Lomazzi, M., Cruz, H. G., Creton, C., Luján, R., Li, M., … Lüscher, C. (2007). RGS2 modulates coupling between GABAB receptors and GIRK channels in dopamine neurons of the ventral tegmental area. *Nature Neuroscience*, *10*(12), 1559–1568. https://doi.org/10.1038/nn2006

Lammel, S., Hetzel, A., Häckel, O., Jones, I., Liss, B., & Roeper, J. (2008). Unique Properties of Mesoprefrontal Neurons within a Dual Mesocorticolimbic Dopamine System. *Neuron*, *57*(5), 760–773. https://doi.org/10.1016/j.neuron.2008.01.022

Lammel, S., Lim, B. K., & Malenka, R. C. (2014). Reward and aversion in a heterogeneous midbrain dopamine system. *Neuropharmacology*. NIH Public Access. https://doi.org/10.1016/j.neuropharm.2013.03.019

Lammel, S., Lim, B. K., Ran, C., Huang, K. W., Betley, M. J., Tye, K. M., … Malenka, R. C. (2012). Input-specific control of reward and aversion in the ventral tegmental area. *Nature*, *491*(7423), 212–217. https://doi.org/10.1038/nature11527

Layer, R. T., Uretsky, N. J., & Wallace, L. J. (1991). Effects of morphine in the nucleus accumbens on stimulant-induced locomotion. *Pharmacology, Biochemistry and Behavior*, *40*(1), 21–26. https://doi.org/10.1016/0091-3057(91)90315-S

Lê, A. D., Corrigall, W. A., Watchus, J., Harding, S., Juzytsch, W., & Li, T. K. (2000). Involvement of nicotinic receptors in alcohol self-administration. *Alcoholism: Clinical and Experimental Research*, *24*(2), 155–163. https://doi.org/10.1111/j.1530-0277.2000.tb04585.x

Lê, A. D., Funk, D., Lo, S., & Coen, K. (2014). Operant self-administration of alcohol and nicotine in a preclinical model of co-abuse. *Psychopharmacology*, *231*(20), 4019–4029. https://doi.org/10.1007/s00213-014-3541-2

Lê, A. D., Lo, S., Harding, S., Juzytsch, W., Marinelli, P. W., & Funk, D. (2010). Coadministration of intravenous nicotine and oral alcohol in rats. *Psychopharmacology*, *208*(3), 475–486. https://doi.org/10.1007/s00213-009-1746-6

Lê, A. D., Wang, A., Harding, S., Juzytsch, W., & Shaham, Y. (2003). Nicotine increases

alcohol self-administration and reinstates alcohol seeking in rats. *Psychopharmacology*, *168*(1–2), 216–221. https://doi.org/10.1007/s00213-002-1330-9

Lee, A. M., & Messing, R. O. (2011). Protein kinase C epsilon modulates nicotine consumption and dopamine reward signals in the nucleus accumbens. *Proceedings of the National Academy of Sciences of the United States of America*, *108*(38), 16080–16085. https://doi.org/10.1073/pnas.1106277108

Lee, A. M., Zou, M. E., Lim, J. P., Stecher, J., Mcmahon, T., & Messing, R. O. (2014). Deletion of Prkcz Increases Intermittent Ethanol Consumption in Mice. *Alcoholism: Clinical and Experimental Research*, *38*(1), 170–178. https://doi.org/10.1111/acer.12211

Lee, C. W. S., & Ho, I. K. (2013). Sex differences in opioid analgesia and addiction: Interactions among opioid receptors and estrogen receptors. *Molecular Pain*. https://doi.org/10.1186/1744-8069-9-45

Lee, Y. K., Gold, M. S., & Fuehrlein, B. S. (2022). Looking beyond the opioid receptor: A desperate need for new treatments for opioid use disorder. *Journal of the Neurological Sciences*, *432*, 120094. https://doi.org/10.1016/j.jns.2021.120094

Leeman, R. F., Huffman, C. J., & O'Malley, S. S. (2007). Alcohol history and smoking cessation in nicotine replacement therapy, bupropion sustained release and varenicline trials: A review. *Alcohol and Alcoholism*. https://doi.org/10.1093/alcalc/agm022

Leeman, R. F., McKee, S. A., Toll, B. A., Krishnan-Sarin, S., Cooney, J. L., Makuch, R. W., & O'Malley, S. S. (2008). Risk factors for treatment failure in smokers: Relationship to alcohol use and to lifetime history of an alcohol use disorder. *Nicotine and Tobacco Research*, *10*(12), 1793–1809. https://doi.org/10.1080/14622200802443742

Lei, K., Wegner, S. A., Yu, J. H., Simms, J. A., & Hopf, F. W. (2016). A single alcohol drinking session is sufficient to enable subsequent aversion-resistant consumption in mice. *Alcohol*, *55*, 9–16. https://doi.org/10.1016/j.alcohol.2016.07.008

Leite-Morris, K. A., Fukudome, E. Y., & Kaplan, G. B. (2002). Opiate-induced motor stimulation is regulated by γ-aminobutyric acid type B receptors found in the ventral tegmental area in mice. *Neuroscience Letters*, *317*(3), 119–122. https://doi.org/10.1016/S0304-3940(01)02457-0

Leite-Morris, K. A., Fukudome, E. Y., Shoeb, M. H., & Kaplan, G. B. (2004). GABAB Receptor Activation in the Ventral Tegmental Area Inhibits the Acquisition and Expression of Opiate-Induced Motor Sensitization. *Journal of Pharmacology and Experimental Therapeutics*, *308*(2), 667–678. https://doi.org/10.1124/jpet.103.058412

Lesscher, H. M. B., Van Kerkhof, L. W. M., & Vanderschuren, L. J. M. J. (2010). Inflexible and indifferent alcohol drinking in male mice. *Alcoholism: Clinical and Experimental Research*, *34*(7), 1219–1225. https://doi.org/10.1111/j.1530-0277.2010.01199.x

Li, T.-K., & Lumeng, L. (1984). Alcohol Preference and Voluntary Alcohol Intakes of Inbred Rat Strains and the National Institutes of Health Heterogeneous Stock of Rats. *Alcoholism, Clinical and Experimental Research*, *8*(5), 485–486.

Litten, R. Z., Ryan, M. L., Fertig, J. B., Falk, D. E., Johnson, B., Dunn, K. E., … Stout, R. (2013). A double-blind, placebo-controlled trial assessing the efficacy of varenicline tartrate for alcohol dependence. *Journal of Addiction Medicine*, *7*(4), 277–286. https://doi.org/10.1097/ADM.0b013e31829623f4

Liu, Y., Jean-Richard-dit-Bressel, P., Yau, J. O.-Y., Willing, A., Prasad, A. A., Power, J.

M., … McNally, G. P. (2020). The Mesolimbic Dopamine Activity Signatures of Relapse to Alcohol-Seeking. *The Journal of Neuroscience*, *40*(33), 6409–6427. https://doi.org/10.1523/jneurosci.0724-20.2020

Locklear, L. L., McDonald, C. G., Smith, R. F., & Fryxell, K. J. (2012). Adult mice voluntarily progress to nicotine dependence in an oral self-selection assay. *Neuropharmacology*, *63*(4), 582–592. https://doi.org/10.1016/j.neuropharm.2012.04.037

Lomazzi, M., Slesinger, P. A., & Lüscher, C. (2008). Addictive drugs modulate GIRK-channel signaling by regulating RGS proteins. *Trends in Pharmacological Sciences*, *29*(11), 544–549. https://doi.org/10.1016/j.tips.2008.07.011

Longabaugh, R., & Magill, M. (2011). Recent advances in behavioral addiction treatments: Focusing on mechanisms of change. *Current Psychiatry Reports*, *13*(5), 382–389. https://doi.org/10.1007/s11920-011-0220-4

Lorrai, I., Maccioni, P., Gessa, G. L., & Colombo, G. (2016). R(+)-baclofen, but not S(-)-baclofen, alters alcohol self-administration in alcohol-preferring rats. *Frontiers in Psychiatry*, *7*(APR), 68. https://doi.org/10.3389/fpsyt.2016.00068

Lüscher, C. (2016). The Emergence of a Circuit Model for Addiction. *Annual Review of Neuroscience*, *39*, 257–276. https://doi.org/10.1146/annurev-neuro-070815-013920

Lüscher, C., & Ungless, M. A. (2006). The mechanistic classification of addictive drugs. *PLoS Medicine*, *3*(11), 2005–2010. https://doi.org/10.1371/journal.pmed.0030437

Maccioni, P., Lorrai, I., Contini, A., Leite-Morris, K., & Colombo, G. (2018). Microinjection of baclofen and CGP7930 into the ventral tegmental area suppresses alcohol self-administration in alcohol-preferring rats. *Neuropharmacology*, *136*(Pt A), 146–158. https://doi.org/10.1016/j.neuropharm.2017.10.012

Maggio, S. E., Saunders, M. A., Nixon, K., Prendergast, M. A., Zheng, G., Crooks, P. A., … Bardo, M. T. (2018). An improved model of ethanol and nicotine co-use in female P rats: Effects of naltrexone, varenicline, and the selective nicotinic α6β2* antagonist r-bPiDI. *Drug and Alcohol Dependence*, *193*, 154–161. https://doi.org/10.1016/j.drugalcdep.2018.09.008

Maity, B., Stewart, A., Yang, J., Loo, L., Sheff, D., Shepherd, A. J., … Fisher, R. A. (2012). Regulator of G protein signaling 6 (RGS6) protein ensures coordination of motor movement by modulating GABA B receptor signaling. *Journal of Biological Chemistry*, *287*(7), 4972–4981. https://doi.org/10.1074/jbc.M111.297218

Maldonado, R., Saiardi, A., Valverde, O., Samad, T. A., Roques, B. P., & Borrelli, E. (1997). Absence of opiate, rewarding effects in mice lacking dopamine D2 receptors. *Nature*, *388*(6642), 586–589. https://doi.org/10.1038/41567

Margolis, E. B., Mitchell, J. M., Ishikawa, J., Hjelmstad, G. O., & Fields, H. L. (2008). Midbrain dopamine neurons: Projection target determines action potential duration and dopamine D2 receptor inhibition. *Journal of Neuroscience*, *28*(36), 8908–8913. https://doi.org/10.1523/JNEUROSCI.1526-08.2008

Marinelli, M., Cooper, D. C., Baker, L. K., & White, F. J. (2003). Impulse activity of midbrain dopamine neurons modulates drug-seeking behavior. *Psychopharmacology*, *168*(1–2), 84–98. https://doi.org/10.1007/s00213-003-1491-1

Marks, J. L., Hill, E. M., Pomerleau, C. S., Mudd, S. A., & Blow, F. C. (1997). Nicotine dependence and withdrawal in alcoholic and nonalcoholic ever- smokers. *Journal of Substance Abuse Treatment*, *14*(6), 521–527. https://doi.org/10.1016/S0740-5472(97)00049-4

Marron Fernandez de Velasco, E., McCall, N., & Wickman, K. (2015). GIRK channel plasticity and implications for drug addiction. In *International review of neurobiology* (Vol. 123, pp. 201–238). https://doi.org/10.1016/bs.irn.2015.05.011

Martin, T. A., Smith, H. R., Luessen, D. J., Chen, R., & Porrino, L. J. (2020). Functional brain activity is globally elevated by dopamine D2 receptor knockdown in the ventral tegmental area. *Brain Research*, *1727*, 146552. https://doi.org/10.1016/j.brainres.2019.146552

Masuho, I., Balaji, S., Muntean, B. S., Skamangas, N. K., Chavali, S., Tesmer, J. J. G., … Martemyanov, K. A. (2020). A Global Map of G Protein Signaling Regulation by RGS Proteins. *Cell*, *183*(2), 503-521.e19. https://doi.org/10.1016/j.cell.2020.08.052

Masuho, I., Martemyanov, K. A., & Lambert, N. A. (2015). Monitoring G protein activation in cells with BRET. *Methods in Molecular Biology*, *1335*, 107–113. https://doi.org/10.1007/978-1-4939-2914-6_8

Masuho, I., Ostrovskaya, O., Kramer, G. M., Jones, C. D., Xie, K., & Martemyanov, K. A. (2015). Distinct profiles of functional discrimination among G proteins determine the actions of G protein-coupled receptors. *Science Signaling*, *8*(405), ra123–ra123. https://doi.org/10.1126/scisignal.aab4068

Masuho, I., Xie, K., & Martemyanov, K. A. (2013). Macromolecular composition dictates receptor and G protein selectivity of regulator of G protein signaling (RGS) 7 and 9-2 protein complexes in living cells. *Journal of Biological Chemistry*, *288*(35), 25129–25142. https://doi.org/10.1074/jbc.M113.462283

McArthur, S., McHale, E., & Gillies, G. E. (2007). The size and distribution of midbrain dopaminergic populations are permanently altered by perinatal glucocorticoid exposure in a sex- region- and time-specific manner. *Neuropsychopharmacology*, *32*(7), 1462–1476. https://doi.org/10.1038/sj.npp.1301277

McCall, N. M., Kotecki, L., Dominguez-Lopez, S., Marron Fernandez De Velasco, E., Carlblom, N., Sharpe, A. L., … Wickman, K. (2017). Selective Ablation of GIRK Channels in Dopamine Neurons Alters Behavioral Effects of Cocaine in Mice. *Neuropsychopharmacology*, *42*(3), 707–715. https://doi.org/10.1038/npp.2016.138

McCall, N. M., Marron Fernandez De Velasco, E., & Wickman, K. (2019). GIRK channel activity in dopamine neurons of the ventral tegmental area bidirectionally regulates behavioral sensitivity to cocaine. *Journal of Neuroscience*, *39*(19), 3600–3610. https://doi.org/10.1523/JNEUROSCI.3101-18.2019

McClure, S. M., York, M. K., & Montague, P. R. (2004, June 29). The neural substrates of reward processing in humans: The modern role of fMRI. *Neuroscientist*. Sage PublicationsSage CA: Thousand Oaks, CA. https://doi.org/10.1177/1073858404263526

McLellan, A. T. (2017). Substance Misuse and Substance use Disorders: Why do they Matter in Healthcare? *Transactions of the American Clinical and Climatological Association*, *128*, 112–130.

McQuin, C., Goodman, A., Chernyshev, V., Kamentsky, L., Cimini, B. A., Karhohs, K. W., … Carpenter, A. E. (2018). CellProfiler 3.0: Next-generation image processing for biology. *PLoS Biology*, *16*(7). https://doi.org/10.1371/JOURNAL.PBIO.2005970

Meliska, C. J., Bartke, A., McGlacken, G., & Jensen, R. A. (1995). Ethanol, nicotine, amphetamine, and aspartame consumption and preferences in C57BL/6 and DBA/2 mice. *Pharmacology, Biochemistry and Behavior*, *50*(4), 619–626. https://doi.org/10.1016/0091-3057(94)00354-8

Menegas, W., Bergan, J. F., Ogawa, S. K., Isogai, Y., Venkataraju, K. U., Osten, P., … Watabe-Uchida, M. (2015). Dopamine neurons projecting to the posterior striatum form an anatomically distinct subclass. *ELife*, *4*(AUGUST2015). https://doi.org/10.7554/eLife.10032

Mercuri, N. B., Saiardi, A., Bonci, A., Picetti, R., Calabresi, P., Bernardi, G., & Borrelli, E. (1997). Loss of autoreceptor function in dopaminergic neurons from dopamine D2

receptor deficient mice. *Neuroscience*, *79*(2), 323–327. https://doi.org/10.1016/S0306-4522(97)00135-8
Mickley, G. A., Mulvihill, M. A., & Postler, M. A. (1990). *Brain p and 6 opioid receptors mediate different locomotor hyperactivity responses of the C57BL]6J mouse*. *Psychopharmacology* (Vol. 101).
Miller, N. S., & Gold, M. S. (1998). Comorbid cigarette and alcohol addiction: Epidemiology and treatment. *Journal of Addictive Diseases*, *17*(1), 55–66. https://doi.org/10.1300/J069v17n01_06
Mitchell, J. M., Teague, C. H., Kayser, A. S., Bartlett, S. E., & Fields, H. L. (2012). Varenicline decreases alcohol consumption in heavy-drinking smokers. *Psychopharmacology*, *223*(3), 299–306. https://doi.org/10.1007/s00213-012-2717-x
Mohebi, A., Pettibone, J. R., Hamid, A. A., Wong, J. M. T., Vinson, L. T., Patriarchi, T., … Berke, J. D. (2019). Dissociable dopamine dynamics for learning and motivation. *Nature*, *570*(7759), 65–70. https://doi.org/10.1038/s41586-019-1235-y
Moore, E. M., & Boehm, S. L. (2009). Site-Specific Microinjection of Baclofen Into the Anterior Ventral Tegmental Area Reduces Binge-Like Ethanol Intake in Male C57BL/6J Mice. *Behavioral Neuroscience*, *123*(3), 555–563. https://doi.org/10.1037/a0015345
Morales, M., & Margolis, E. B. (2017, February 5). Ventral tegmental area: Cellular heterogeneity, connectivity and behaviour. *Nature Reviews Neuroscience*. Nature Publishing Group. https://doi.org/10.1038/nrn.2016.165
Munoz, M. B., Padgett, C. L., Rifkin, R., Terunuma, M., Wickman, K., Contet, C., … Slesinger, P. A. (2016). A Role for the GIRK3 Subunit in Methamphetamine-Induced Attenuation of GABAB Receptor-Activated GIRK Currents in VTA Dopamine Neurons. *Journal of Neuroscience*, *36*(11), 3106–3114. https://doi.org/10.1523/JNEUROSCI.1327-15.2016
Narayanan, S., Wallace, L., & Uretsky, N. (1996). Spontaneous and drug-stimulated locomotor activity after the administration of pertussis toxin into the ventral tegmental area. *Journal of Psychiatry and Neuroscience*, *21*(3), 172–180.
National Institute of Mental Health. (2021). Substance Use and Co-Occurring Mental Disorders. Retrieved February 24, 2022, from https://www.nimh.nih.gov/health/topics/substance-use-and-mental-health
Nelson, J., Bundoc-Baronia, R., Comiskey, G., & McGovern, T. F. (2017). Facing Addiction in America: The Surgeon General's Report on Alcohol, Drugs, and Health: A Commentary. *Alcoholism Treatment Quarterly*, *35*(4), 445–454. https://doi.org/10.1080/07347324.2017.1361763
NIAAA. (2004). *NIAAA Council Approves Definition of Binge Drinking*. Retrieved from www.psych.org/
O'Doherty, J. P. (2004). Reward representations and reward-related learning in the human brain: Insights from neuroimaging. *Current Opinion in Neurobiology*. https://doi.org/10.1016/j.conb.2004.10.016
O'Malley, S. S., Zweben, A., Fucito, L. M., Wu, R., Piepmeier, M. E., Ockert, D. M., … Gueorguieva, R. (2018). Effect of varenicline combined with medical management on alcohol use disorder with comorbid cigarette smoking: A randomized clinical trial. *JAMA Psychiatry*, *75*(2), 129–138. https://doi.org/10.1001/jamapsychiatry.2017.3544
O'Rourke, K. Y., Touchette, J. C., Hartell, E. C., Bade, E. J., & Lee, A. M. (2016). Voluntary co-consumption of alcohol and nicotine: Effects of abstinence, intermittency, and withdrawal in mice. *Neuropharmacology*, *109*, 236–246. https://doi.org/10.1016/j.neuropharm.2016.06.023

Ostrovskaya, O., Xie, K., Masuho, I., Fajardo-Serrano, A., Lujan, R., Wickman, K., & Martemyanov, K. A. (2014). RGS7/Gβ5/R7BP complex regulates synaptic plasticity and memory by modulating hippocampal GABABR-GIRK signaling. *ELife*, *3*, e02053. https://doi.org/10.7554/eLife.02053

Ott, J. F., Hunter, B. E., & Walker, D. W. (1985). The Effect of Age on Ethanol Metabolism and on the Hypothermic and Hypnotic Responses to Ethanol in the Fischer 344 Rat. *Alcoholism: Clinical and Experimental Research*, *9*(1), 59–65. https://doi.org/10.1111/j.1530-0277.1985.tb05051.x

Pfaus, J. G., Damsma, G., Nomikos, G. G., Wenkstern, D. G., Blaha, C. D., Phillips, A. G., & Fibiger, H. C. (1990). Sexual behavior enhances central dopamine transmission in the male rat. *Brain Research*, *530*(2), 345–348. https://doi.org/10.1016/0006-8993(90)91309-5

Philippart, F., & Khaliq, Z. M. (2018). Gi/o protein-coupled receptors in dopamine neurons inhibit the sodium leak channel NALCN. *ELife*, *7*. https://doi.org/10.7554/eLife.40984

Phillips, A. G., & LePiane, F. G. (1980). Reinforcing effects of morphine microinjection into the ventral tegmental area. *Pharmacology, Biochemistry and Behavior*, *12*(6), 965–968. https://doi.org/10.1016/0091-3057(80)90460-8

Pignatelli, M., & Bonci, A. (2018, January 17). Spiraling Connectivity of NAc-VTA Circuitry. *Neuron*. Elsevier. https://doi.org/10.1016/j.neuron.2017.12.046

Pijnenburg, A. J. J., & van Rossum, J. M. (1973). Stimulation of locomotor activity following injection of dopamine into the nucleus accumbens. *Journal of Pharmacy and Pharmacology*, *25*(12), 1003–1005.

Pinard, A., Seddik, R., & Bettler, B. (2010). GABA B receptors. Physiological functions and mechanisms of diversity. In *Advances in Pharmacology* (Vol. 58, pp. 231–255). https://doi.org/10.1016/S1054-3589(10)58010-4

Platt, R. J., Chen, S., Zhou, Y., Yim, M. J., Swiech, L., Kempton, H. R., … Zhang, F. (2014). CRISPR-Cas9 knockin mice for genome editing and cancer modeling. *Cell*, *159*(2), 440–455. https://doi.org/10.1016/j.cell.2014.09.014

Plebani, J. G., Lynch, K. G., Rennert, L., Pettinati, H. M., O'Brien, C. P., & Kampman, K. M. (2013). Results from a pilot clinical trial of varenicline for the treatment of alcohol dependence. *Drug and Alcohol Dependence*, *133*(2), 754–758. https://doi.org/10.1016/j.drugalcdep.2013.06.019

Pleim, E. T., Matochik, J. A., Barfield, R. J., & Auerbach, S. B. (1990). Correlation of dopamine release in the nucleus accumbens with masculine sexual behavior in rats. *Brain Research*, *524*(1), 160–163. https://doi.org/10.1016/0006-8993(90)90507-8

Pontieri, F. E., Tanda, G., & Di Chiara, G. (1995). Intravenous cocaine, morphine, and amphetamine preferentially increase extracellular dopamine in the "shell" as compared with the "core" of the rat nucleus accumbens. *Proceedings of the National Academy of Sciences of the United States of America*, *92*(26), 12304–12308. https://doi.org/10.1073/pnas.92.26.12304

Posokhova, E., Wydeven, N., Allen, K. L., Wickman, K., & Martemyanov, K. A. (2010). RGS6/Gβ5 complex accelerates IKACh gating kinetics in atrial myocytes and modulates parasympathetic regulation of heart rate. *Circulation Research*, *107*(11), 1350–1354. https://doi.org/10.1161/CIRCRESAHA.110.224212

Powers, M. S., Broderick, H. J., Drenan, R. M., & Chester, J. A. (2013). Nicotinic acetylcholine receptors containing α6 subunits contribute to alcohol reward-related behaviours. *Genes, Brain and Behavior*, *12*(5), 543–553. https://doi.org/10.1111/gbb.12042

Pravetoni, M., & Wickman, K. (2008). Behavioral characterization of mice lacking GIRK/Kir3 channel subunits. *Genes, Brain and Behavior*, *7*(5), 523–531. https://doi.org/10.1111/j.1601-183X.2008.00388.x

Qato, D. M., Zhang, C., Gandhi, A. B., Simoni-Wastila, L., & Coleman-Cowger, V. H. (2020). Co-use of alcohol, tobacco, and licit and illicit controlled substances among pregnant and non-pregnant women in the United States: Findings from 2006 to 2014 National Survey on Drug Use and Health (NSDUH) data. *Drug and Alcohol Dependence*, *206*. https://doi.org/10.1016/j.drugalcdep.2019.107729

Rahman, S., & McBride, W. J. (2000). Feedback control of mesolimbic somatodendritic dopamine release in rat brain. *Journal of Neurochemistry*, *74*(2), 684–692. https://doi.org/10.1046/j.1471-4159.2000.740684.x

Rahman, S., & McBride, W. J. (2001). D1-D2 dopamine receptor interaction within the nucleus accumbens mediates long-loop negative feedback to the ventral tegmental area (VTA). *Journal of Neurochemistry*, *77*(5), 1248–1255. https://doi.org/10.1046/j.1471-4159.2001.00326.x

Rahman, Z., Schwarz, J., Gold, S. J., Zachariou, V., Wein, M. N., Choi, K. H., … Nestler, E. J. (2003). RGS9 modulates dopamine signaling in the basal ganglia. *Neuron*, *38*(6), 941–952. https://doi.org/10.1016/S0896-6273(03)00321-0

Rhodes, J. S., Best, K., Belknap, J. K., Finn, D. A., & Crabbe, J. C. (2005). Evaluation of a simple model of ethanol drinking to intoxication in C57BL/6J mice. *Physiology and Behavior*, *84*(1), 53–63. https://doi.org/10.1016/j.physbeh.2004.10.007

Rollema, H., Shrikhande, A., Ward, K. M., Tingley, F. D., Coe, J. W., O'Neill, B. T., … Bertrand, D. (2010). Pre-clinical properties of the α4β2 nicotinic acetylcholine receptor partial agonists varenicline, cytisine and dianicline translate to clinical efficacy for nicotine dependence. *British Journal of Pharmacology*, *160*(2), 334–345. https://doi.org/10.1111/j.1476-5381.2010.00682.x

Rose, T. R., & Wickman, K. (2022). Mechanisms and Regulation of Neuronal GABAB Receptor-Dependent Signaling. In *Current Topics in Behavioral Neurosciences* (Vol. 52, pp. 39–79). https://doi.org/10.1007/7854_2020_129

Runegaard, A. H., Sørensen, A. T., Fitzpatrick, C. M., Jørgensen, S. H., Petersen, A. V, Hansen, N. W., … Gether, U. (2018). Locomotor- and reward-enhancing effects of cocaine are differentially regulated by chemogenetic stimulation of Gi-signaling in dopaminergic neurons. *ENeuro*, *5*(3). https://doi.org/10.1523/ENEURO.0345-17.2018

SAMHSA. (2012). Treatment Episode Data Set (TEDS): 2000-2010. National Admissions to Substance Abuse Treatment Services. Retrieved February 25, 2022, from http://www.samhsa.gov/data/2k12/TEDS2010N/TEDS2010NWeb.pdf

Sanchez-Catalan, M. J., Kaufling, J., Georges, F., Veinante, P., & Barrot, M. (2014, December). The antero-posterior heterogeneity of the ventral tegmental area. *Neuroscience*. https://doi.org/10.1016/j.neuroscience.2014.09.025

Sarvet, A. L., & Hasin, D. (2016). The natural history of substance use disorders. *Current Opinion in Psychiatry*, *29*(4), 250–257. https://doi.org/10.1097/YCO.0000000000000257

Saunders, B. T., Richard, J. M., Margolis, E. B., & Janak, P. H. (2018). Dopamine neurons create Pavlovian conditioned stimuli with circuit-defined motivational properties. *Nature Neuroscience*, *21*(8), 1072–1083. https://doi.org/10.1038/s41593-018-0191-4

Schultz, W. (1998). Predictive reward signal of dopamine neurons. *Journal of Neurophysiology*. American Physiological Society. https://doi.org/10.1152/jn.1998.80.1.1

Schultz, W. (2007). Behavioral dopamine signals. *Trends in Neurosciences*. https://doi.org/10.1016/j.tins.2007.03.007
Schultz, W. (2010). Dopamine signals for reward value and risk: Basic and recent data. *Behavioral and Brain Functions*. https://doi.org/10.1186/1744-9081-6-24
Schultz, W. (2015). Neuronal reward and decision signals: From theories to data. *Physiological Reviews*, *95*(3), 853–951. https://doi.org/10.1152/physrev.00023.2014
Schultz, W. (2016). Dopamine reward prediction-error signalling: A two-component response. *Nature Reviews Neuroscience*. https://doi.org/10.1038/nrn.2015.26
Sharpe, A. L., Varela, E., Bettinger, L., & Beckstead, M. J. (2015). Methamphetamine self-Administration in mice decreases GIRK channel-mediated currents in midbrain dopamine neurons. *International Journal of Neuropsychopharmacology*, *18*(5), 1–10. https://doi.org/10.1093/ijnp/pyu073
Simms, J. A., Steensland, P., Medina, B., Abernathy, K. E., Chandler, L. J., Wise, R., & Bartlett, S. E. (2008). Intermittent access to 20% ethanol induces high ethanol consumption in Long-Evans and Wistar rats. *Alcoholism: Clinical and Experimental Research*, *32*(10), 1816–1823. https://doi.org/10.1111/j.1530-0277.2008.00753.x
Smith, A. M., Kelly, R. B., & Chen, W. J. A. (2002). Chronic Continuous Nicotine Exposure During Periadolescence Does Not Increase Ethanol Intake During Adulthood in Rats. *Alcoholism: Clinical and Experimental Research*, *26*(7), 976–979. https://doi.org/10.1111/J.1530-0277.2002.TB02630.X
Sneddon, E. A., White, R. D., & Radke, A. K. (2018). Sex differences in binge-like and aversion-resistant alcohol drinking in C57BL/6J mice. *Alcoholism: Clinical and Experimental Research*, acer.13923. https://doi.org/10.1111/acer.13923
Solecki, W., Wilczkowski, M., Pradel, K., Karwowska, K., Kielbinski, M., Drwięga, G., … Przewłocki, R. (2020). Effects of brief inhibition of the ventral tegmental area dopamine neurons on the cocaine seeking during abstinence. *Addiction Biology*, *25*(6), e12826. https://doi.org/10.1111/adb.12826
Spanagel, R., Zieglgänsberger, W., & Hundt, W. (1996). Acamprosate and alcohol: III. Effects on alcohol discrimination in the rat. *European Journal of Pharmacology*, *305*(1–3), 51–56. https://doi.org/10.1016/0014-2999(96)00176-8
Spielewoy, C., Gonon, F., Roubert, C., Fauchey, V., Jaber, M., Caron, M. G., … Giros, B. (2000). Increased rewarding properties of morphine in dopamine-transporter knockout mice. *European Journal of Neuroscience*, *12*(5), 1827–1837. https://doi.org/10.1046/j.1460-9568.2000.00063.x
Squeglia, L. M., Boissoneault, J., Van Skike, C. E., Nixon, S. J., & Matthews, D. B. (2014). Age-Related Effects of Alcohol from Adolescent, Adult, and Aged Populations Using Human and Animal Models. *Alcoholism: Clinical and Experimental Research*, *38*(10), 2509–2516. https://doi.org/10.1111/acer.12531
Stefani, M. R., & Moghaddam, B. (2006). Rule learning and reward contingency are associated with dissociable patterns of dopamine activation in the rat prefrontal cortex, nucleus accumbens, and dorsal striatum. *Journal of Neuroscience*, *26*(34), 8810–8818. https://doi.org/10.1523/JNEUROSCI.1656-06.2006
Steketee, J. D., & Kalivas, P. W. (1990). Sensitization to cocaine produced by injection of pertussis toxin into the A10 dopamine region. *NIDA Research Monograph*, *105*, 545–546. Retrieved from http://www.ncbi.nlm.nih.gov/pubmed/1908559
Steketee, J. D., & Kalivas, P. W. (1991). Sensitization to psychostimulants and stress after injection of pertussis toxin into the A10 dopamine region. *Journal of Pharmacology and Experimental Therapeutics*, *259*(2), 916–924.
Steketee, J. D., Striplin, C. D., Murray, T. F., & Kalivas, P. W. (1992). Pertussis Toxin in the A10 Region Increases Dopamine Synthesis and Metabolism. *Journal of*

Neurochemistry, *58*(3), 811–816. https://doi.org/10.1111/j.1471-4159.1992.tb09329.x
Stevens, K. E., Mickley, G. A., & McDermott, L. J. (1986). Brain areas involved in production of morphine-induced locomotor hyperactivity of the C57Bl/6J mouse. *Pharmacology, Biochemistry and Behavior*, *24*(6), 1739–1747. https://doi.org/10.1016/0091-3057(86)90514-9
Stewart, A., Maity, B., Anderegg, S. P., Allamargot, C., Yang, J., & Fisher, R. A. (2015). Regulator of G protein signaling 6 is a critical mediator of both reward-related behavioral and pathological responses to alcohol. *Proceedings of the National Academy of Sciences*, *112*(7), E786–E795. https://doi.org/10.1073/pnas.1418795112
Stewart, A., Maity, B., Wunsch, A. M., Meng, F., Wu, Q., Wemmie, J. A., & Fisher, R. A. (2014). Regulator of G-protein signaling 6 (RGS6) promotes anxiety and depression by attenuating serotonin-mediated activation of the 5-HT1A receptor-adenylyl cyclase axis. *FASEB Journal*, *28*(4), 1735–1744. https://doi.org/10.1096/fj.13-235648
Stirling, D. R., Swain-Bowden, M. J., Lucas, A. M., Carpenter, A. E., Cimini, B. A., & Goodman, A. (2021). CellProfiler 4: improvements in speed, utility and usability. *BMC Bioinformatics*, *22*(1). https://doi.org/10.1186/S12859-021-04344-9
Su, M., Li, L., Wang, J., Sun, H., Zhang, L., Zhao, C., … Zhang, H. (2019). Kv7.4 Channel Contribute to Projection-Specific Auto-Inhibition of Dopamine Neurons in the Ventral Tegmental Area. *Frontiers in Cellular Neuroscience*, *13*. https://doi.org/10.3389/fncel.2019.00557
Sun, H., Calipari, E. S., Beveridge, T. J. R., Jones, S. R., & Chen, R. (2015). The brain gene expression profile of dopamine D2/D3 receptors and associated signaling proteins following amphetamine self-administration. *Neuroscience*, *307*, 253–261. https://doi.org/10.1016/j.neuroscience.2015.08.053
Sutton, L. P., Khalatyan, N., Savas, J. N., & Martemyanov, K. A. (2021). Striatal rgs7 regulates depression-related behaviors and stress-induced reinstatement of cocaine conditioned place preference. *ENeuro*, *8*(2), 1–11. https://doi.org/10.1523/ENEURO.0365-20.2020
Swan, G. E., Carmelli, D., & Cardon, L. R. (1996). The consumption of tobacco, alcohol, and coffee in caucasian male twins: A multivariate genetic analysis. *Journal of Substance Abuse*, *8*(1), 19–31. https://doi.org/10.1016/S0899-3289(96)90055-3
Swan, G. E., Carmelli, D., & Cardon, L. R. (1997). Heavy consumption of cigarettes, alcohol and coffee in male twins. *Journal of Studies on Alcohol*, *58*(2), 182–190. https://doi.org/10.15288/jsa.1997.58.182
Syrovatkina, V., Alegre, K. O., Dey, R., & Huang, X. Y. (2016, September 25). Regulation, Signaling, and Physiological Functions of G-Proteins. *Journal of Molecular Biology*. NIH Public Access. https://doi.org/10.1016/j.jmb.2016.08.002
Tanabe, L. M., Suto, N., Creekmore, E., Steinmiller, C. L., & Vezina, P. (2004). Blockade of D2 dopamine receptors in the VTA induces a long-lasting enhancement of the locomotor activating effects of amphetamine. *Behavioural Pharmacology*, *15*(5–6), 387–395. https://doi.org/10.1097/00008877-200409000-00013
Tarren, J. R., & Bartlett, S. E. (2017). Alcohol and nicotine interactions: pre-clinical models of dependence. *American Journal of Drug and Alcohol Abuse*. https://doi.org/10.1080/00952990.2016.1197232
Thiele, T. E., & Navarro, M. (2014, May). “Drinking in the dark” (DID) procedures: A model of binge-like ethanol drinking in non-dependent mice. *Alcohol*. NIH Public Access. https://doi.org/10.1016/j.alcohol.2013.08.005

Toll, B. A., Cummings, K. M., O'Malley, S. S., Carlin-Menter, S., McKee, S. A., Hyland, A., … Celestino, P. (2012). Tobacco Quitlines Need to Assess and Intervene with Callers' Hazardous Drinking. *Alcoholism: Clinical and Experimental Research*, *36*(9), 1653–1658. https://doi.org/10.1111/j.1530-0277.2012.01767.x

Toll, B. A., White, M., Wu, R., Meandzija, B., Jatlow, P., Makuch, R., & O'Malley, S. S. (2010). Low-dose naltrexone augmentation of nicotine replacement for smoking cessation with reduced weight gain: A randomized trial. *Drug and Alcohol Dependence*, *111*(3), 200–206. https://doi.org/10.1016/j.drugalcdep.2010.04.015

Touchette, J. C., Maertens, J. J., Mason, M. M., O'Rourke, K. Y., & Lee, A. M. (2018). The nicotinic receptor drug sazetidine-A reduces alcohol consumption in mice without affecting concurrent nicotine consumption. *Neuropharmacology*, *133*, 63–74. https://doi.org/10.1016/j.neuropharm.2018.01.019

True, W. R., Xian, H., Scherrer, J. F., Madden, P. A. F., Bucholz, K. K., Heath, A. C., … Tsuang, M. (1999). Common genetic vulnerability for nicotine and alcohol dependence in men. *Archives of General Psychiatry*, *56*(7), 655–661. https://doi.org/10.1001/archpsyc.56.7.655

Truitt, W. A., Hauser, S. R., Deehan, G. A., Toalston, J. E., Wilden, J. A., Bell, R. L., … Rodd, Z. A. (2015). Ethanol and nicotine interaction within the posterior ventral tegmental area in male and female alcohol-preferring rats: Evidence of synergy and differential gene activation in the nucleus accumbens shell. *Psychopharmacology*, *232*(3), 639–649. https://doi.org/10.1007/s00213-014-3702-3

Tupala, E., Hall, H., Bergström, K., Särkioja, T., Räsänen, P., Mantere, T., … Tiihonen, J. (2001). Dopamine D2/D3-receptor and transporter densities in nucleus accumbens and amygdala of type 1 and 2 alcoholics. *Molecular Psychiatry*, *6*(3), 261–267. https://doi.org/10.1038/sj.mp.4000859

Tye, K. M., Mirzabekov, J. J., Warden, M. R., Ferenczi, E. A., Tsai, H. C., Finkelstein, J., … Deisseroth, K. (2013). Dopamine neurons modulate neural encoding and expression of depression-related behaviour. *Nature*, *493*(7433), 537–541. https://doi.org/10.1038/nature11740

Uhl, G. R., Koob, G. F., & Cable, J. (2019). The neurobiology of addiction. *Annals of the New York Academy of Sciences*. https://doi.org/10.1111/nyas.13989

Valyear, M. D., Glovaci, I., Zaari, A., Lahlou, S., Trujillo-Pisanty, I., Andrew Chapman, C., & Chaudhri, N. (2020). Dissociable mesolimbic dopamine circuits control responding triggered by alcohol-predictive discrete cues and contexts. *Nature Communications*, *11*(1). https://doi.org/10.1038/s41467-020-17543-4

van Rossum, J. M., van der Schoot, J. B., & Hurkmans, J. A. T. M. (1962). Mechanism of action of cocaine and amphetamine in the brain. *Experientia*, *18*(5), 229–231. https://doi.org/10.1007/BF02148316

Van Skike, C. E., Maggio, S. E., Reynolds, A. R., Casey, E. M., Bardo, M. T., Dwoskin, L. P., … Nixon, K. (2016). Critical needs in drug discovery for cessation of alcohol and nicotine polysubstance abuse. *Progress in Neuro-Psychopharmacology and Biological Psychiatry*, *65*, 269–287. https://doi.org/10.1016/j.pnpbp.2015.11.004

Vander Weele, C. M., Porter-Stransky, K. A., Mabrouk, O. S., Lovic, V., Singer, B. F., Kennedy, R. T., & Aragona, B. J. (2014). Rapid dopamine transmission within the nucleus accumbens: Dramatic difference between morphine and oxycodone delivery. *European Journal of Neuroscience*, *40*(7), 3041–3054. https://doi.org/10.1111/ejn.12709

Verplaetse, T. L., & McKee, S. A. (2017). An overview of alcohol and tobacco/nicotine interactions in the human laboratory. *American Journal of Drug and Alcohol Abuse*. NIH Public Access. https://doi.org/10.1080/00952990.2016.1189927

Vezina, P., Kalivas, P. W., & Stewart, J. (1987). Sensitization occurs to the locomotor effects of morphine and the specific μ opioid receptor agonist, DAGO, administered repeatedly to the ventral tegmental area but not to the nucleus accumbens. *Brain Research*, *417*(1), 51–58. https://doi.org/10.1016/0006-8993(87)90178-8

Vlachou, S., & Markou, A. (2010). GABA B receptors in reward processes. In *Advances in Pharmacology* (Vol. 58, pp. 315–371). https://doi.org/10.1016/S1054-3589(10)58013-X

Volkow, N. D., Fowler, J. S., Wang, G. J., Baler, R., & Telang, F. (2009). Imaging dopamine's role in drug abuse and addiction. *Neuropharmacology*, *56*(Suppl 1), 3. https://doi.org/10.1016/J.NEUROPHARM.2008.05.022

Volkow, Nora D., & Morales, M. (2015, August 13). The Brain on Drugs: From Reward to Addiction. *Cell*. Elsevier. https://doi.org/10.1016/j.cell.2015.07.046

Volkow, Nora D., Wang, G. -J, Fowler, J. S., Logan, J., Schlyer, D., Hitzemann, R., … Wolf, A. P. (1994). Imaging endogenous dopamine competition with [11C]raclopride in the human brain. *Synapse*, *16*(4), 255–262. https://doi.org/10.1002/syn.890160402

Volkow, Nora D., Wang, G. J., Fowler, J. S., Tomasi, D., & Telang, F. (2011, September 13). Addiction: Beyond dopamine reward circuitry. *Proceedings of the National Academy of Sciences of the United States of America*. National Academy of Sciences. https://doi.org/10.1073/pnas.1010654108

Waeiss, R. A., Knight, C. P., Hauser, S. R., Pratt, L. A., McBride, W. J., & Rodd, Z. A. (2019). Therapeutic challenges for concurrent ethanol and nicotine consumption: naltrexone and varenicline fail to alter simultaneous ethanol and nicotine intake by female alcohol-preferring (P) rats. *Psychopharmacology*, 1–14. https://doi.org/10.1007/s00213-019-5174-y

Walker, Q. D., Ray, R., & Kuhn, C. M. (2006). Sex differences in neurochemical effects of dopaminergic drugs in rat striatum. *Neuropsychopharmacology*, *31*(6), 1193–1202. https://doi.org/10.1038/sj.npp.1300915

Wang, R. Y. (1981). Dopaminergic neurons in the rat ventral tegmental area. I. Identification and characterization. *Brain Research Reviews*. https://doi.org/10.1016/0165-0173(81)90002-3

Watabe-Uchida, M., Zhu, L., Ogawa, S. K., Vamanrao, A., & Uchida, N. (2012). Whole-Brain Mapping of Direct Inputs to Midbrain Dopamine Neurons. *Neuron*, *74*(5), 858–873. https://doi.org/10.1016/j.neuron.2012.03.017

Wise, R. A. (2002, October 10). Brain reward circuitry: Insights from unsensed incentives. *Neuron*. Elsevier. https://doi.org/10.1016/S0896-6273(02)00965-0

Wise, R. A. (2004). Dopamine and food reward: Back to the elements. *American Journal of Physiology - Regulatory Integrative and Comparative Physiology*, *286*(1 55-1), 21224. https://doi.org/10.1152/ajpregu.00590.2003

Wise, R. A., & Koob, G. F. (2014). The development and maintenance of drug addiction. *Neuropsychopharmacology*, *39*(2), 254–262. https://doi.org/10.1038/npp.2013.261

Wise, R. A., & Rompre, P. P. (1989). Brain dopamine and reward. *Annual Review of Psychology*. https://doi.org/10.1146/annurev.ps.40.020189.001203

Witkiewitz, K, Litten, R. Z., & Leggio, L. (2019). Advances in the science and treatment of alcohol use disorder. *Science Advances*, *5*(9), eaax4043. https://doi.org/10.1126/sciadv.aax4043

Witkiewitz, Katie, Pfund, R. A., & Tucker, J. A. (2022). Mechanisms of behavior change in substance use disorders with and without formal treatment. *Annual Review of Clinical Psychology*, (in press). https://doi.org/10.1146/annurev-clinpsy-072720

Woodard, G. E., Jardín, I., Berna-Erro, A., Salido, G. M., & Rosado, J. A. (2015).

Regulators of G-Protein-Signaling Proteins: Negative Modulators of G-Protein-Coupled Receptor Signaling. *International Review of Cell and Molecular Biology*, *317*, 97–183. https://doi.org/10.1016/bs.ircmb.2015.02.001

Wydeven, N., Posokhova, E., Xia, Z., Martemyanov, K. A., & Wickman, K. (2014). RGS6, but not RGS4, is the dominant regulator of G protein signaling (RGS) modulator of the parasympathetic regulation of mouse heart rate. *The Journal of Biological Chemistry*, *289*(4), 2440–2449. https://doi.org/10.1074/jbc.M113.520742

Xi, Z. X., & Stein, E. A. (1999). Baclofen inhibits heroin self-administration behavior and mesolimbic dopamine release. *Journal of Pharmacology and Experimental Therapeutics*, *290*(3), 1369–1374. Retrieved from http://www.jpet.org

Xie, K., Allen, K. L., Kourrich, S., Colón-Saez, J., Thomas, M. J., Wickman, K., & Martemyanov, K. A. (2010). GB5 recruits R7 RGS proteins to GIRK channels to regulate the timing of neuronal inhibitory signaling. *Nature Neuroscience*, *13*(6), 661–663. https://doi.org/10.1038/nn.2549

Xue, Y., Steketee, J. D., Rebec, G. V, & Sun, W. (2011). Activation of D2-like receptors in rat ventral tegmental area inhibits cocaine-reinstated drug-seeking behavior. *European Journal of Neuroscience*, *33*(7), 1291–1298. https://doi.org/10.1111/j.1460-9568.2010.07591.x

Yang, L., Chen, M., Ma, Q., Sheng, H., Cui, D., Shao, D., … Zheng, P. (2020). Morphine selectively disinhibits glutamatergic input from mPFC onto dopamine neurons of VTA, inducing reward. *Neuropharmacology*, *176*, 108217. https://doi.org/10.1016/j.neuropharm.2020.108217

Yoneyama, N., Crabbe, J. C., Ford, M. M., Murillo, A., & Finn, D. A. (2008). Voluntary ethanol consumption in 22 inbred mouse strains. *Alcohol*, *42*(3), 149–160. https://doi.org/10.1016/j.alcohol.2007.12.006

Zachariou, V., Georgescu, D., Sanchez, N., Rahman, Z., DiLeone, R., Berton, O., … Nestler, E. J. (2003). Essential role for RGS9 in opiate action. *Proceedings of the National Academy of Sciences of the United States of America*, *100*(23), 13656–13661. https://doi.org/10.1073/pnas.2232594100

Zachry, J. E., Nolan, S. O., Brady, L. J., Kelly, S. J., Siciliano, C. A., & Calipari, E. S. (2021, December 14). Sex differences in dopamine release regulation in the striatum. *Neuropsychopharmacology*. Nature Publishing Group. https://doi.org/10.1038/s41386-020-00915-1